MESOSCOPIC EFFECTS AND LOCAL NEGATIVE SUPERFLUID DENSITIES

by

STEPHEN LING

A thesis submitted to
The University of Birmingham
for the degree of
DOCTOR OF PHILOSOPHY

School of Physics and Astronomy
The University of Birmingham

Sept 2010

Abstract

In this thesis we will discuss the effects of Weak Localisation, Aharonov-Bohm oscillations and sample-to-sample fluctuations in the context of Mesoscopic systems and also introduce an interesting concept indicating the possibility of local regions of negative superfluid densities. These normal state phenomena will be rigorously calculated using Green's functions and Diagrammatic techniques to help understand their underlying properties. The AC sample-to-sample fluctuations will be evaluated using an original diagrammatic calculation and will be used to show that there are an interesting set of cancellations when taking the DC limit, known as the wrong-sign cancellations.

The second half of this thesis will deal with these mesoscopic effects in the superconducting limit. This will help to understand and develop the useful diagrammatic techniques needed in the superconducting limit. In the final section we will derive the superconducting mesoscopic fluctuations in an original calculation which will help to understand whether or not there is the possibility of regions of local negative superfluid density as suggested in 1991 by Spivak and Kivelson [3].

Acknowledgements

I would like to thank my whole family especially my Father who encouraged me to pursue a PhD and whom I would like to dedicate this thesis to. Also a huge thanks goes to my Mum for her invaluable laundry and ironing services and, of course, her wonderful cakes which helped me through my frequent late nights of study and many thanks to my Brother too.

A very special thank you also goes to Ray who helped and supported me throughout my Undergraduate years.

Also I would like to mention all the students (past and present) for the weekly football matches and the office 'activities'. Especially Jo who was always there for a coffee and a good laugh (I'm sure the University Starbucks are struggling now we have left). Also the many great memories including the funny antics on the Ambleside and Warwick conferences, Matt's sporadic need to jump and throw things and Dom's strange obsession with two celebrity sisters on Youtube.

And thanks to my supervisor, Rob, for our frequent meetings and guidance.

In Loving Memory of my Father

Contents

Chapter 1

INTRODUCTION

This Thesis is based upon the properties of Mesoscopic systems and, more importantly, the effects on such systems around the Superconductor to Insulator Transition (SIT). The main characteristics of a Mesoscopic system, with respect to Macroscopic and Microscopic systems, will be explained in the next section before a motivation of this thesis is explained together with a general overview of what is contained.

1.1 Introduction to Mesoscopic Physics

The phenomenology of solid state physics is often considered through the nearly-free electron theory of metals in which the electrons interact weakly with an ordered crystalline lattice potential. And in a non-ideal lattice, with lattice defects and doped impurities, the electrons experience an irregular lattice potential. For systems larger than the coherence length, L_ϕ, the transport properties can be understood by Kinetic or Boltzmann theory but at length scales smaller than L_ϕ the dynamics of the system is greatly influenced by quantum phase coherence. At this *Mesoscopic scale*, that lies between microscopic and macroscopic, the influ-

ence of quantum phase coherence effects cause many observed phenomena such as conductance fluctuations and weak localisation. Contrary to intuition, these observable properties are often quite substantial and will be evaluated in further chapters within this Thesis.

Measurable physical properties for systems smaller than L_ϕ depend upon the specific realisation of the disorder. However, for systems greater than L_ϕ the phase coherence is lost and the system is observed to be independent upon the realisations of the disorder. Examples such as superconductivity, superfluidity, free electron gas at zero temperature are systems which maintain phase coherence up to the macroscopic scale.

The phase coherence length, L_ϕ, can be thought of more physically as the length scale with which the phase coherence is lost due to irreversible processes. Such suppression can be linked to phonon interactions, interactions with other electrons. In metals, L_ϕ will increase with temperature and is of the order of a few micrometers for temperatures less than one Kelvin. It must be noted that the phase coherence length is essentially independent upon static disorder such as static impurities or vacancies as these do not destroy the phase coherence of the system. However, the processes which do destroy coherence may depend upon the disorder. The length scale that includes such static disorder is the elastic mean free length l_e, which is the average length between two scattering events with no energy change.

The phase coherence length, L_ϕ, and the elastic mean free length, l_e, are fundamentally different which implies that the loss of coherence is not due to random potentials. At low temperatures, l_e may differ by a number of magnitudes from L_ϕ.

The interest in such mesoscopic systems has increased due to the development of modern fabrication methods and have resulted in many publications. This has lead to the motivation of this Thesis.

1.2 Motivation of Thesis

To understand the physical properties of any system the first step is to understand the system in the context of the free-electron gas. This approximation ignores such effects as electron interactions and the effects of the lattice and does not reproduce many of the interesting phenomena observed in most sample. In the case of a non-periodic lattice the next step is to introduce the effects of the lattice which introduces a scattering time, τ, which represents the average time taken for an electron to interact and scatter off a lattice point. This classical model is known as the Drude conductivity and is given as

$$\frac{\pi e^2 \tau}{m} \tag{1.2.1}$$

which is the basis of calculating the conductance in a given sample, and is derived in chapter 3.3.

Now that the lattice has been included in the calculation the next problem is to consider disordered systems which will also affect the conductance. The disorder will reduce the conductivity by a small amount, comparable to the background noise of the sample but distinctive by its tendency to vanish as a magnetic field is induced. This is known as Weak Localisation and was was interpreted as being the self-crossing of an electrons trajectory, and is discussed in chapter 2.1 and derived in chapter 3.4. It must also be noted that increasing the disorder can

induce an insulator transition known as Strong Localisation. To understand the effects of disorder the scaling theory of localisation, as shown in chapter 2.2, is used which describes a system as being constructed of 2^d cubes which are combined via perturbation theory. The change in the conductance of the sample, β, as more cubes are combined is only dependent upon the conductance, g, of the sample. This scaling theory determines the effect of localisation for a sample of any size, L, by scaling up from any size, l.

The effects of weak localisation is a mesoscopic property but can also be observed in macroscopic systems. which can be seen via the effects in small Au rings and metallic cylinders. Small mesoscopic Au rings with a flux, ϕ, through the centre shows an observable Aharonov-Bohm oscillation of h/e as described in chapter 2.3. A purely mesoscopic effect will vanish in the macroscopic regime, but when the mesoscopic rings are added together to construct a macroscopic cylinder the weak localisation effects are still present. However, in these metallic cylinders the weak localisation effect causes a new Aharonov-Bohm oscillation of $h/2e$. This will be discussed in chapter 2.3 and 2.4.

The next effect to conductivity is described via the sample to sample fluctuations which are purely mesoscopic. This means that the specific conductance of a sample cannot be sufficiently described by the average but is instead dependent upon the exact configuration of that specific sample. This effect is known as Mesoscopic conductance fluctuations or Universal conductance fluctuations and emphasises that there is a variance in observable properties for Mesoscopic samples with different realisations, see figure (1.1). These sample specific fluctuations are described in chapter 2.6 and derived in chapter 5.1.

All these effects on the conductivity are well known and described in chapter

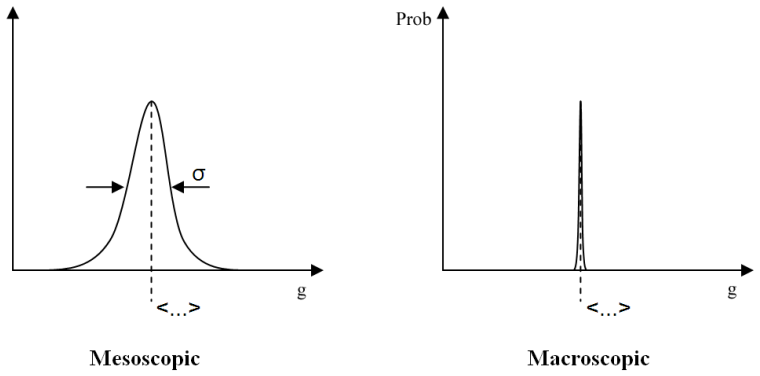

Figure 1.1 – A plot to show that the properties of a macroscopic system is well defined by its average properties. However, the properties of a mesoscopic system has a large variance and cannot simply be descibed by its average but instead must include the specific realisation.

2 and calculated in the normal state regime in chapter 3. Chapter 4 will introduce the ideas of superconductivity and will calculate the properties of Drude conductivity and Weak localisation in the superconducting state.

In 1991 Spivak and Kivelson produced a paper [3] describing the idea of a local negative superfluid density and many papers have been published on the Supeconductor-Insulator transition in thin films. A given system is believed to split up into regions, or islands, of differing physical properties (for example islands of higher conductivity). To try and understand this transition more and to answer the original question of Spivak and Kivelson the fluctuations in the superconducting regime will be calculated to see if these islands may have a local negative superfluid density. As the superfluid density can be related to the Josephson current, a negative superfluid density will cause a Glass state where the phase looks disordered but will have an underlining order. To find if the superfluid density becomes negative it is necessary to compare whether the variance exceeds the average, see figure 1.2. This will then be calculated by deriving the

Mesoscopic Conductance Fluctuations in the superconducting regime, which will be investigated in chapter 6. This will then be evaluated to see if it can exceed the average conductance which will result in a possibility of a local negative superfluid density.

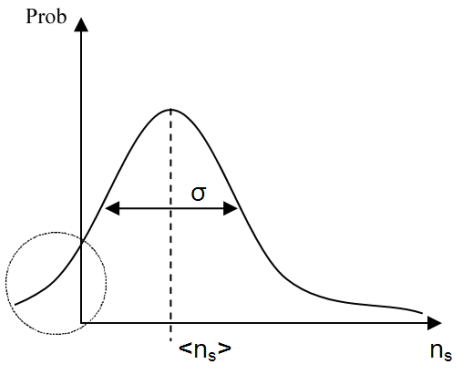

Figure 1.2 – A plot to show that when the variance, σ, exceeds the average, $\langle n_s \rangle$, then the superfluid density will become negative.

Chapter 2

INTRODUCTION TO PHENOMENA

As described in the main introduction, the transport properties of mesoscopic samples display some interesting phenomena. The classical regime is described by the Drude conductivity but in the quantum regime there are interference effects due to self-crossings of propagating paths. This is described by Weak Localisation and causes a decrease in the correction to conductivity compared to the Drude conductivity. As the disorder is increased the system may enter a insulator transition described by Strong Localisation which can be evaluated using the Scaling theory. This chapter will discuss the ideas of Weak Localisation and the Scaling argument and how disorder can affect the state of a system. The Aharonov-Bohm (AB) oscillations will also be discussed in Au rings, first experimented by Webb et. al. [31], and also in metallic cylinders, first experimented by Sharvin and Sharvin [10], and will be used to understand the underlying property in the Mesoscopic fluctuations. Each of these systems will give a different order of oscillation although the metallic cylinders were originally believed to be an ensemble average which would destroy these AB oscillations.

The SIT is then discussed and the idea of local negative superfluid densities at this transition is investigated. Before any calculations can be made, the sample

specific fluctuations must be understood as these fluctuations must be shown to exceed the average superfluid density to show that there exists regions of negative superfluid densities (or alternatively disprove this theory).

2.1 Weak-Localisation

The conductivity in dirty metals can be evaluated by the product of two complex amplitudes, A_i related to the probability of quantum diffusion. This describes the probability of a particle scattering from r to r' and is given by

$$P(r, r') \propto \sum_{i,j} A_i^* A_j \tag{2.1.1}$$

where A_i denotes the amplitude of a propagating trajectory from r to r' following a path described by i [37]. This indicates that the probability is dependent upon a pair of separate trajectories i and j each with an amplitude and phase. With this in mind, the probability can now be split into two parts. The first is when the pair of trajectories take the same path ($i = j$) which is described by the classical Drude conductivity, and the second term is when the two trajectories are independent ($i \neq j$) and describes the quantum term. This gives the probability the form [11]

$$P(r, r') \propto \underbrace{\sum_{i} |A_i|^2}_{\text{Classical Drude}} + \underbrace{\sum_{i \neq j} A_i^* A_j}_{\text{Quantum correction}} \tag{2.1.2}$$

The second term is non-zero when considering interference effects where the two trajectories follow the same scatterings but cross paths [1]. The case where the paths cross once is known as weak localisation as is shown in figure 2.1.

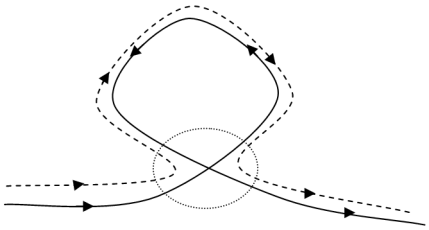

Figure 2.1 – The quantum correction to the classical Drude conductivity. The dashed circle emphasises the crossing of trajectories i and j and can be calculated by the weak localisation correction.

In a d-dimensional system this will give a correction to conductivity as

$$\begin{aligned} \delta\sigma &= -\frac{2e^2}{\pi}\left[L_\phi - l\right] \qquad \text{for} \qquad d = 1 \\ \delta\sigma &= -\frac{2e^2}{\pi}\ln\left(\frac{l}{L_\phi}\right) \qquad \text{for} \qquad d = 2 \\ \delta\sigma &= -\frac{2e^2}{\pi}\left[\frac{1}{l} - \frac{1}{L_\phi}\right] \qquad \text{for} \qquad d = 3 \end{aligned} \tag{2.1.3}$$

which will be derived in a later chapter using diagrammatic techniques. The correction for all dimension is negative which indicates that taking these self-crossing loops into account will reduce the overall conductance [37] - this is the main property of weak localisation. Furthermore, if the system is time reversal invariant then the two opposing paths will have the same amplitude, A, which will imply that their product is equal to that of two trajectories in the same direction. This suggests that a breaking of time reversal symmetry will cause the effects of weak localisation to vanish. Weak localisation is not the only interference effect correction which reduces the conductivity, there is also Anderson localisation which will be described in the next section using a scaling argument.

2.2 Scaling Theory of Localisation

When the mean free path, L_ϕ is short and comparable to the Fermi wavelength, λ_F, multiple scattering becomes important and the electron wavefunction becomes spatially localised. In the localised states, the wavefunction decays exponentially away from a localised centre as

$$\psi(r) \approx \exp\left(\frac{-r}{\xi}\right) \tag{2.2.1}$$

where ξ is the localisation length and r is the distance from the localised centre. These localised states cause a metal-insulator transition dependent upon the degree of disorder in the given system which is known as Anderson Localisation. This effect causes different properties for systems of different dimensions, d, as the system size increases. This dependence upon the dimensionality of the system can be derived via the scaling argument, originally proposed by Edwards and Thouless [24]. Consider a d-dimensional system of size L. The wavefunction and electronic properties of a system of size $2L$ can be derived by combining 2^d cubes via perturbation theory. Combining 2 cubes will cause a mixing of energy levels where the closest energy levels will couple to each other. This mixing will be governed by the ratio of the overlap integral between states in different blocks, t, to the average level spacing, W. This will give the mixing parameter as t/W and this parameter at one length scale will determine the same parameter at a different length scale. The dimensionless conductance, g $(= G/(e^2/\hbar))$ can be determined from t/W and thus $g(L)$ is the appropriate measure of disorder and is the only measure of disorder at length scale L [37]. If the system size is increased from L to $L + \delta L$ and we define the relevant change in conductance, $\beta(g(L), L)$, which

must only depend upon $g(L)$ as

$$\beta(g(L), L) = \frac{L}{g(L)} \frac{dg(L)}{dL} = \frac{d \ln g(L)}{d \ln L} \tag{2.2.2}$$

The function $\beta(g(L), L)$ needs to be evaluated in the limits of a good and poor conductor which implies that we need to understand the values of g in these limits. It must be realised that the dimensionless conductance, g, is a measure of the number of channels available for electron flow. Thus a good conductor will have many channels which will be described as $g >> 1$ and a poor conductor will have a small number of available channels $g << 1$. In the limit of a good conductor g will be described by the usual Ohmic formula

$$g = \frac{G}{e^2/\hbar} = \frac{\sigma L^{d-2}}{e^2/\hbar} \tag{2.2.3}$$

By substituting this into (2.2.2) we can see that in the limit $g >> 1$ then $\beta(g) = d - 2$. In the limit of the poor conductor the states will be localised and the only way for an electron to move across the sample is to hop between states. As described at the start of this section, this will lead to an exponential dependence of conductance with respect to the localisation length ξ as

$$g(L) \approx \exp\left(-L/\xi\right) \tag{2.2.4}$$

which will lead to $\beta(g) = \ln(g)$ [37]. Also note that in the weak disorder regime, weak localisation will add a correction to $\beta(g)$ of $-a/g$. This correction together with the values of $\beta(g)$ in both limiting cases, and connecting them with a smooth monotonic curve, will give the final form of $\beta(g)$ as shown in figure 2.2. The

plot shows that $\beta(g)$ increases with g and has no singularities. In summary we

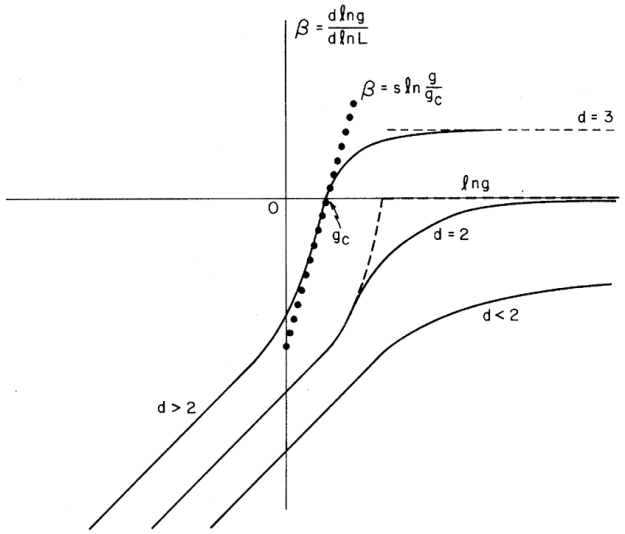

Figure 2.2 – A plot of the relevant change in conductance, $\beta(g)$, versus the log of the dimensionless conductance, $\ln g$, for $d = 1, 2, 3$. This plot shows that when $d = 1, 2$ then g decreases as the system size, L, increases and will always be in the localised regime.

start with a sample of size l with dimensionless conductance $g_0 = g(l)$ and use the form $\beta(g)$, given in equation(2.2.2), to scale up to size L. The plot therefore shows that $g < 0$ for systems of dimensions less than or equal to 2 irrespective of the initial value of g_0. This means that 1D and 2D systems will always be in the localised regime as it can be seen that $g(L)$ decreases as L increases. For systems of dimensions greater than 2 ($d > 2$) there is an unstable fixed point at a critical value g_c. This means that if the system begins with $g_0 > g_c$ then $\beta(g)$ is positive which means that as L increases we will scale into the conducting regime. However, if the system begins with $g_0 < g_c$ then $\beta(g)$ will be negative which means that as L increases we will scale into the localised regime. This shows that for

$d > 2$ there is a conductor-to-insulator transition at the critical level of disorder given by $g(l) = g_c$.

2.3 Aharonov-Bohm oscillations in Au Rings

In 1985, Webb et al studied the Aharonov-Bohm (AB) effect in small metallic Au rings of the order of a micrometer [31].

Figure 2.3 shows the original results published by Webb et al which shows that the rings have an AB oscillation of $\frac{h}{e}$ which will be derived using the amplitudes of the two paths with which the electron can propagate.

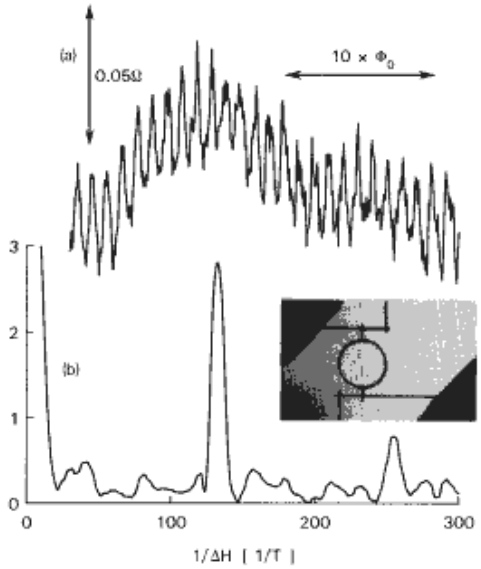

Figure 2.3 – (a) The magnetoresistance of a gold ring with an inside diameter $\approx 400\mathring{A}$ and width $\approx 400\mathring{A}$ at $T = 0.01K$ (b) Fourier spectrum showing peaks at h/e and $h/2e$.

For the trajectories within the ring, the corresponding amplitudes for each path 1 and 2 will be

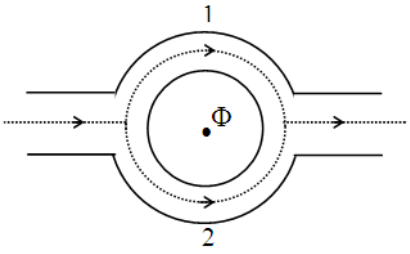

Figure 2.4 – An Aharonov-Bohm interferometer with trajectories 1 and 2 and a flux ϕ.

$$a_{1,2} = |a_{1,2}| \exp i\delta_{1,2} \tag{2.3.1}$$

where the electron propagator within a magnetic field, $\mathbf{B} = \nabla \times \mathbf{A}$, will pick up an additional Quantum mechanical phase and is given by

$$\begin{aligned} \delta_1 &= \delta_1^0 - \frac{e}{\hbar} \int_1 \mathbf{A} \cdot \mathbf{dl} \\ \delta_2 &= \delta_2^0 - \frac{e}{\hbar} \int_2 \mathbf{A} \cdot \mathbf{dl} \end{aligned} \tag{2.3.2}$$

The corresponding integrals are line integrals of the vector potential $\mathbf{A}$ along the two trajectories and $\delta_{1,2}^0$ are the phases with zero magnetic flux [6]. Therefore, the conductance in the presence of the magnetic flux can be represented as a combination of the two amplitudes, given as

$$G(\phi) = |a_1 + a_2|^2 = |a_1|^2 + |a_2|^2 + 2|a_1 a_2| \cos(\delta_1 + \delta_1) \tag{2.3.3}$$

When the trajectories split above and below the enclosing flux, the phase difference between the upper and lower paths will become $e\phi/\hbar$ and is now modulated by

the magnetic flux as

$$\Delta\delta(\phi) = \delta_1 - \delta_2 = \delta_1^0 - \delta_2^0 + \frac{e}{\hbar}\oint \mathbf{A}\cdot\mathbf{dl} \tag{2.3.4}$$

This shows that the total conductance of the ring is a periodic function of the flux

$$G(\phi) = G_0 + \delta G\cos(\delta^0 + 2\pi\phi/\phi_0) \tag{2.3.5}$$

where $\phi_0 = h/e$ is the quantum of the magnetic flux, this is the Aharonov-Bohm effect. On increasing the temperature or the diameter of the ring then this effect disappears due to decoherence effects as L_ϕ decreases [2]. The system size at which the AB effect disappears signifies the temperature dependent coherence length, L_ϕ.

Before this experiment it was believed that coherence effects were only observable within the single scattering regime, where the level of disorder is low. A high level of disorder would, intuitively, be equivalent to a system of N thin, single scattering films, with each film corresponding to a different and independent realisation. The resulting conductance would be an average over all these thin films and would cause the AB effect to vanish. However, the Webb et al experiment showed that the multiple scattering regime did not correspond to an ensemble average and that the coherence effect did remain. This proved that the classical approach is invalid in such mesoscopic systems and this is why the coherence effects of such systems have increased in interest since the 1980s.

This shows that the effect of weak localisation in mesoscopic samples is an oscillation of $\frac{h}{e}$ however, weak localisation effects are also present in macroscopic cylinders and will be described in the next section.

2.4 Aharonov-Bohm oscillations in Metallic Cylinders

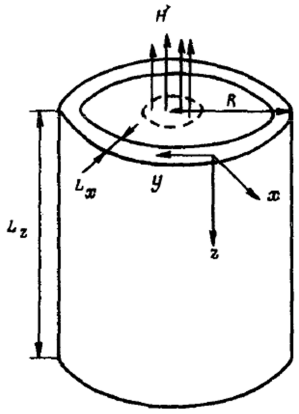

Figure 2.5 – This shows the cylindrical magnesium film with a flux threaded through the centre, as used by Sharvin and Sharvin.

The original motivation for the research of Webb et al was due to the experimental results obtained by Sharvin and Sharvin 4 years earlier, in 1981 [10]. They observed a conductance oscillation of order $h/2e = \phi_0/2$ in cylindrical magnesium films, see figure (2.5). As soon as the publication of Sharvin and Sharvin many theoretical papers were written to discuss the possible oscillations in metallic rings and discussed the possibility of difference oscillations in such systems. The experiment by Webb et al was the first to observe the oscillations in metallic rings and [36].

Intuitively, it would seem sensible to believe that a cylinder with a length larger than the phase coherence length, L_ϕ, would be equivalent to $N(= L/L_\phi)$ independent metallic rings. This would suggest that a metallic cylinder would be a ensemble average and that the coherent effects would disappear and destroy

the oscillations. This is untrue and, although the ϕ_0 oscillations disappear as the length of the ring becomes larger than L_ϕ, the $\phi_0/2$ conductance oscillations exist both in the metallic rings ($L < L_\phi$) and in metallic cylinders ($L > L_\phi$). The existence of these oscillations is due to the self-crossing paths of electrons which causes a larger backscattering amplitude, known as weak localisation. Because the wavefunction is periodic then the electron path must go around a full circle for a contribution and if the electron path only followed a half circle then they will cancel due to the scatterings in the cylinder.

These two research papers show that although weak localisation is a mesoscopic effect it is also present in macroscopic samples. The mesoscopic rings, experimented by Webb, show that this effect can be observed by an AB oscillation of $\frac{h}{e}$ whereas in macroscopic cylinders, experimented by Sharvin and Sharvin, the observable property is an oscillation of $\frac{h}{2e}$. This shows that although weak localisation is described as a mesoscopic effect it is also observable on the macroscopic level.

These AB oscillations will be observed when investigating the mesoscopic conductance fluctuations and will result in an underlying oscillation in the fluctuations. Also the AB oscillations may be a method to investigate the existence of regions of negative superfluid densities, which will be discussed in the next section.

2.5 Local Negative Superfluid Density

There has been long extensive research into the superconductor-insulator transition through the years [23] [5] [30]. In 1991 the question of negative superfluid density arose due to research by Spivak and Kivelson [3] [33]. The idea was that

when approaching the superconductor-insulator transition in a disordered superconductor the value of the average superfluid density, $\langle n_s \rangle$, (where $\langle ... \rangle$ denotes the impurity average) will become smaller than the fluctuations in the local superfluid density, δn_s [7]. If this is true then it will be possible for the local superfluid density to become negative [3] [33].

The possibility of a negative n_s will cause an array of many observable phenomena [15] [14]. It will result in slow relaxation times in resistances and other properties, a half natural period of the Aharonov-Bohm effect (which will be observed to be a period of $h/4e$) and a negative magnetoresistance at weak fields in the normal state near to the superconducting transition [13] [9]. The model will correspond to a system of superconducting grains, labelled by the index j, each with an order parameter and a fluctuating phase θ_j. Such a system will be described by the Hamiltonian

$$H = -2e^2 \sum_{i,j} n_i (C^{-1}) n_j + \sum_j \mu_j n_j - \sum_{i,j} J_{ij} \cos\left(\theta_i - \theta_j + \frac{A_{ij}}{\Phi_0}\right) \qquad (2.5.1)$$

where n_j is the number of Cooper pairs, C_{ij} is the capacitance matrix, μ_j is the chemical potential, J_{ij} is the Josephson Coupling between grains i and j, Φ_0 is the superconductor flux quantum ($h/2e$) and A_{ij} is the vector potential from grain i to j [3]. J_{ij} can be considered as the lattice version of the superfluid density, n_s. The phase of the grain, θ_j, is canonically conjugate to n_j. This means that the transformations $n_j \rightarrow S_j^z$ and $\exp(\pm i\theta_j \rightarrow S_j^{\pm})$ can be used to transform the Hamiltonian into the quantum Heisenberg-Ising model

$$H = -2e^2 \sum_{ij} S_i^z (C_{-1}) S_j^z + \sum_j \mu_j S_j^z - \sum_{ij} \frac{J_{ij}}{2} \left(S_i^+ S_j^- + S_i^- S_j^+\right) \qquad (2.5.2)$$

J_{ij} will act like the XY part of the exchange interaction, $(C^{-1})_{ij}$ is Ising part and μ_j will be a random magnetic field term introduced to the Hamiltonian [33]. Therefore a negative superfluid density is equivalent to a negative J_{ij} which implies that it has the same universality class as a spin-glass [18]. This shows that a negative superfluid density will cause shifts in the phase with a complicated ordering.

The idea of a local negative superfluid density has been debated through the years and to be thorough one must also consider the arguments against this phenomena. In the next subsection I will outline a research paper which disagrees with the idea of a negative superfluid density before disgussing the physical properties which would be observable if this phenomena did exist.

2.5.1 Counter Arguments

In 2001 Titov et. al. investigated the idea of a negative superfluid density by calculating the Josephson coupling energy, U_j, and showing that U_j cannot have a maximum for zero phase difference [34], ϕ, of the superconductor parameter - indicating that a negative superfluid density cannot exist. This paper investigated the relative magnitude of mesoscopic fluctuations of the supercurrent in a disordered SNS junction. The SNS contacts have N propagating modes at the Fermi Energy so that the $2N \times 2N$ scattering matrix, $S(\varepsilon)$, can be determined via the Josephson Coupling energy as [30]

$$U_j = -2k_BT \sum_{n=0}^{\infty} \ln \det \left[1 - S_A(i\omega_n)S_N(i\omega_n)\right] \tag{2.5.3}$$

where $\omega_n = (2n+1)\pi k_B T$ is the Matsubara frequency.

By using the identity $\ln \det ... = \mathrm{Tr} \ln ...$ the first and second derivatives can be

calculated as

$$\frac{dU_j}{d\phi} = 2k_BT\sum_{n=0}^{\infty}\mathrm{Im}\mathrm{Tr}\left[h_{11}(\omega_n) - h_{22}(\omega_n)\right] \tag{2.5.4}$$

and

$$\frac{d^2U_j}{d\phi^2} = 4k_BT\sum_{n=0}^{\infty}\mathrm{Re}\mathrm{Tr}\left[f_{12}(\omega_n)f_{21}*(\omega_n) - h_{12}*(\omega_n)h_{21}(\omega_n)\right] \tag{2.5.5}$$

where

$$\begin{pmatrix} h_{11} & h_{12} \\ h_{21} & h_{22} \end{pmatrix} = Z^*Z(1+Z^*Z)^{-1}; \qquad \begin{pmatrix} f_{11} & f_{12} \\ f_{21} & f_{22} \end{pmatrix} = Z(1+Z^*Z)^{-1} \tag{2.5.6}$$

where

$$Z(\omega_n) = \left(\sqrt{1+\omega^2/\Delta^2} - \omega/\Delta\right)e^{-i\Lambda\phi/2}S(i\omega) \tag{2.5.7}$$

At $\phi = 0$ the symmetry of S implies $F = F^T$ and $H = H^T$ so that $f_{21} = f_{12}$ and $h_{21} = h_{12}^*$. This implies that every term in the sum of the second derivative is positive and the first derivative is equal to the supercurrent and vanishes at $\phi = 0$. Therefore,

$$\frac{dU_j}{d\phi}\Big|_{\phi=0} = 0 \qquad \text{and} \qquad \frac{d^2U_j}{d\phi^2}\Big|_{\phi=0} > 0 \tag{2.5.8}$$

This indicates that mesoscopic fluctuations cannot invert the stability of the SNS junction at zero phase.

The next step is to investigate the physical interpretation of Negative super-

fuid densities and whether experimentally this phenomena could be proved or disproved.

2.5.2 A physical interpretation

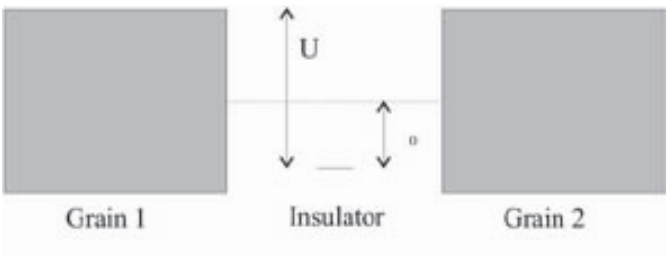

Figure 2.6 – A diagram of the two grain model considered by Spivak and Kivelson with Josephson coupling J_{ij} between the grains.

Spivak and Kivelson theoretically considered the model of two grains with a Josephson coupling, J_{ij}, between them. With only direct single-electron tunneling the Josephson coupling term will be positive in the absence of spin-orbit coupling. If an intermediate state is introduced between grains and we assume that the tunneling can occur indirectly through this localised state then the model becomes more interesting. Consider the Hamiltonian of the form

$$H = H_0 + H_t \tag{2.5.9}$$

where

$$H_0 = H_1 + H_2 + \varepsilon_0 n_0 + U n_0(n_0 - 1) + V_1 m_1 n_0 + V_2 m_2 n_0 \tag{2.5.10}$$

and

$$H_t = \sum_{k,q,s} t_{kq}(c^\dagger_{1ks}c_{2qs} + h.c) + \sum_{j=1}^{2}\sum_{ks} T_{jk}(c^\dagger_{jks}c_{0s} + h.c) \tag{2.5.11}$$

H_t is the contribution due to tunneling, the grains are labelled by the index $j = 1, 2$, c_{jks} annihilates an electron with spin s on grain j, c_{0s} annihilates an electron in the localised state and n_0 denotes the number of electrons in the localised state. The energy to put a single electron into the localised state is given by ε_0 and the energy to put two electrons into the insulating state is $\varepsilon_0 + U$.

The explanation for the negative sign in the superfluid density is due to the permutations of the electrons once they have indirectly tunneled through the localised state. To understand this one must consider the BCS wave function for one of the grains

$$|\psi_j\rangle = \prod_q (u_q + e^{i\theta_j} v_q c^\dagger_{jq\uparrow} c^\dagger_{j-q\downarrow}|0\rangle \tag{2.5.12}$$

A phase convention must be arbitrarily introduced but must be maintained throughout all the calculations. The order will be that the spin-up electrons will always be to the left of the spin-down electrons. This canonical ordering is what will introduce the negative value of n_s as direct tunneling between each grain will maintain this order but indirect tunneling does not. For example consider the following case, shown in figure 2.7.

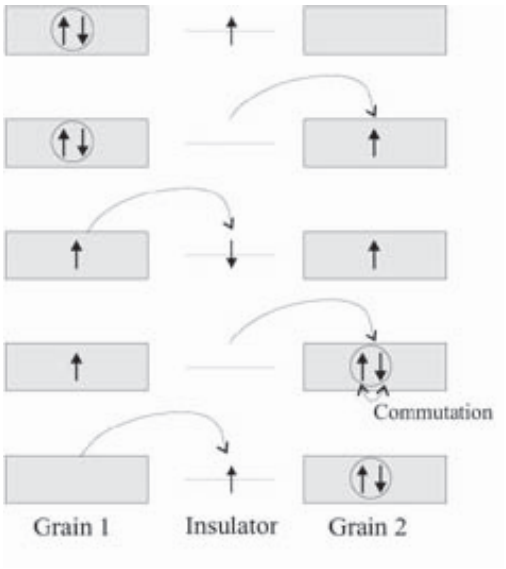

Figure 2.7 – A diagram showing how indirect tunneling can cause a negative n_s due to canonical ordering.

2.5.3 Mathematical interpretation

The research of Spivak and Kivelson [3] in 1991 was motivated by the work of Spivak and Zyuzin in 1988 [7] which deduced that

$$\left\langle \left(\frac{\delta n_s}{n_s} \right)^2 \right\rangle \approx \left\langle \left(\frac{\delta G}{\langle G \rangle} \right)^2 \right\rangle \approx \left(\zeta(0) \frac{l p_F}{\hbar^2} \right)^{-2} \tag{2.5.13}$$

where n_s is the superfluid density, G is the conductance of normal metal cube $\zeta(0)$ in size, p_F is the Fermi momentum and $\delta G = G - \langle G \rangle$. This was not an exact calculation as it assumes the relations of G and n_s. Spivak and Kivelson used this result to show that

$$\left\langle \left(\frac{\delta n_s}{n_s} \right)^2 \right\rangle \propto \frac{e^4}{\hbar \langle G \rangle^2} \left[1 + \mathcal{O}\left(\frac{1}{k_F l} \right) \right] \tag{2.5.14}$$

and explained that as a function of increasing disorder, when $k_F l$ gets to become of order 1, this equation breaks down and the fluctuations of n_s become comparable in magnitude to the mean. In this case it was argued that there could be a substantial probability of a negative n_s. Although this has not been shown in the BCS superconductor, it has been shown in the previous subsection that for Josephson-coupled superconducting grains, spin-exchange scattering of the tunneling electron by a localised spin can produce $J_{ij} < 0$ [20]. One result of a negative n_s will be observed via the altering of the Arahonov-Bohm oscillations [34].

2.5.4 Arahonov-Bohm oscillations

As stated the previous subsection, local negative superfluid densities will cause an AB oscillation of $\frac{h}{4e}$ which will now be explained in this subsection. Consider a dirty superconductor with an array of holes which we pass a flux, ϕ. The properties of such a system will be controlled by the configuration average of a single hole. To calculate the Aharonov-Bohm period one must evaluate the configuration average of the free energy

$$\langle F \rangle = -kT \langle \ln[\mathrm{Tr}\{\exp(-H/kT)\}] \rangle \tag{2.5.15}$$

which can be expanded in the limit $T \gg T_c$

$$\langle F \rangle = \langle \mathrm{Tr}\{H\} \rangle + \frac{\langle [\mathrm{Tr}\{H^2\} - \mathrm{Tr}\{H\}^2] \rangle}{2kT} + ... \tag{2.5.16}$$

where the trace and the configuration average, $\langle ... \rangle$, is taken over all quantum states. The contributions will come from the shortest closed paths which, in Aharonov-Bohm geometry, correspond to the shortest path enclosing the flux, ϕ

[26]. Intuitively, the shortest path will come from the closed trajectory which encloses the flux once. But on taking the configuration average, $\langle F \rangle$, this will give a zero contribution due to the random sign of J_{ij} [25]. This means that the leading term in the expansion will come from the paths which enclose the flux twice. This will lead to an Aharonov-Bohm period of $h/4e$ and all thermodynamic properties will be observed to have oscillations with such a period.

The last subsection showed that the possibility of a local negative superfluid density is based on an assumption and to prove (or disprove) this theory it is essential to produce an exact result for $\delta n_s/n_s$. An exact solution for δn_s will be derived for a 2 dimensional thin film in chapter 6 of this thesis. The method of calculating this term will be via Green's functions and, for completeness, the results in the normal state will be derived.

2.6 Mesoscopic Conductance Fluctuations

2.6.1 Universal Conductance Fluctuations

Quantum interference effects can be observed in the transport of solids through the universal conductance fluctuations, which were discovered in 1985 [29]. Altshuler [4], Lee and Stone [29] predicted that small metallic wires at low temperatures revealed 'random-like' conductance fluctuations as a function of magnetic field [12]. At a similar time Webb experimented on 3 samples (a) 0.8 μm gold ring, (b) quasi-1D silicon MOSFET, figure 2.8 is a plot of the fluctuations in 3 samples. It was also noted that the fluctuations remain order unity whilst the background conductance varied.

Although these fluctuations seemed random, they showed a remarkable repro-

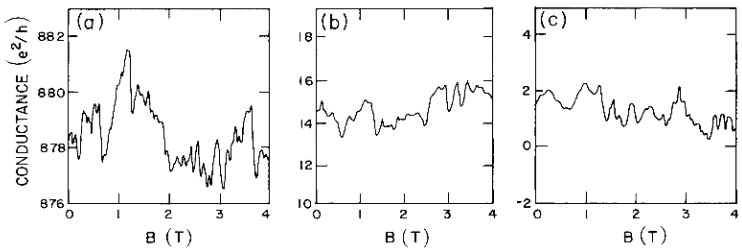

Figure 2.8 – A plot of the conductance fluctuations as a function of magnetic field for (a) 0.8 μm gold ring, (b) quasi-1D silicon MOSFET and (c) Numerical calculation for Anderson model.

ducibility at a given temperature, and were experimentally observed as having a 97% cross-correlation in superconducting $Au_{0.7}In_{0.3}$ cylinders [16]. Literature in this area often call these fluctuations *Magnetic Fingerprints* due to the individuality of these fluctuations, although one must note that these fluctuations do have a universal amplitude of order $\frac{e^2}{\hbar}$ at zero temperature [16]. These size independent fluctuations were unexpected from the usual Ohms conductance, $g = \sigma L^{d-2}$ (where σ is the conductivity) as the fluctuation of the conductance is given as

$$\delta g = \sqrt{\langle (g - \langle g \rangle)^2 \rangle} \tag{2.6.1}$$

This implies that $\delta g^2 / \langle g \rangle^2 \sim O(L^{-d})$ which will give the fluctuations in the conductance as $\delta g^2 = L^{d-4}$. However, with quantum effects the fluctuations in a d-dimensional system is given by

$$\begin{aligned} \sqrt{\delta g^2} &= 0.733 \text{ for } d = 1 \\ &= 0.867 \text{ for } d = 2 \\ &= 0.953 \text{ for } d = 3 \end{aligned} \tag{2.6.2}$$

and will be derived in chapter 5. This shows that quantum interference has dramatic effects on observable transport properties of solids and that the amplitude of the conductance fluctuations are size independent, hence 'Universal'.

A physical interpretation of these fluctuations is in the energy level statistics of a metal. For a normal metal the conductance is dependent upon the number of single electron levels, N, inside an energy band of width E_T centered at the Fermi surface, where E_T is the Thouless energy [24]. The conductance is calculated as

$$G = \frac{e^2}{\hbar} N \tag{2.6.3}$$

and although N is dependent upon the dimensionality of the system, the fluctuations in the number of single electron levels within this band is universally of order unity.

These random-like fluctuations are fully reproducible for a given sample but are different when the impurity configuration of a sample is changed. This shows a physical breakdown of *Transport theory*, which states that any observables can be expressed in terms of the average properties of the sample. In experiments, large changes in the Fermi energy or magnetic field will be used to simulate a change in the impurity configuration in a given sample.

A temperature of $0.27K$ was found to destroy the fluctuations in superconducting $Au_{0.7}In_{0.3}$ cylinders and a small increase in magnetic field was also found to have the same effect (with a critical field $H*$), shown in figure 2.9.

The conductance fluctuations are also found experimentally in metallic rings [31] where a periodic structure of $\frac{h}{e}$ is superimposed over these magnetic fingerprints due to *Aharonov-Bohm oscillations*.

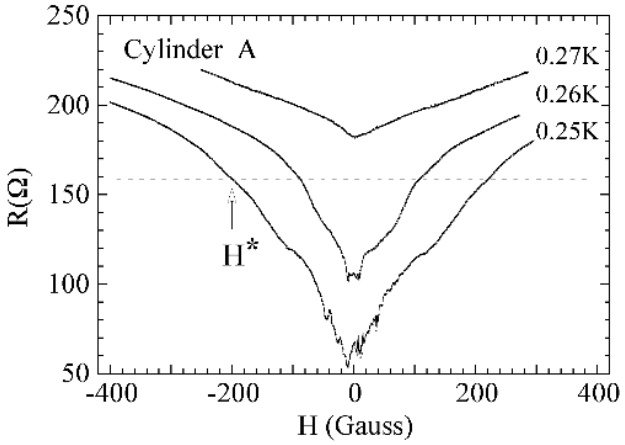

Figure 2.9 – A plot on a superconducting $Au_{0.7}In_{0.3}$ cylinder to show that a critical field $H*$ will destroy the fluctuations

Chapter 3

THEORY OF THE NORMAL STATE

To investigate the phenomena described in chapter 2 one must construct a mathematical means to calculate the mesoscopic properties. The most useful method is to use Green's Functions and Diagrammatic techniques which are essential tools in representing long and complicated equations in a more simplified form.

To construct the Green's Function one must first introduce the Schrodinger (and Heisenberg) representation where the operators are independent (dependent) upon time and the wavefunctions are dependent (independent) upon time. This will help to construct the Interaction representation which is the fundamental starting point for deriving the Green's functions. The Hamiltonian for this representation is split into two parts

$$H = H_0 + V \tag{3.0.1}$$

where H_0 is the Hamiltonian which can be solved exactly and V is the remaining part. The wavefunctions and operators in the interaction representation are both dependent upon time with respect to the full Hamiltonian, H, and the exactly

solvable part, H_0, and is given as

$$O_{int}(t) = e^{iH_0 t} O e^{-iH_0 t}, \quad \text{and} \quad \psi_{int}(t) = e^{iH_0 t} e^{-iHt} \psi(0) \tag{3.0.2}$$

It will also be shown that the matrix elements in any of these 3 representations are consistent and will give the same answer. To investigate the properties of an interacting system one must construct an operator which evolves the wavefunction from time t' to t given by

$$\psi_{int}(t) = S(t, t')\psi_{int}(t') \tag{3.0.3}$$

where $S(t, t')$ is known as the scattering matrix. Calculating this S-matrix will give an insight into the system and it will be constructed of many creation and annihilation operators c_k and $c_k^\dagger$. These operators can be grouped together to give a Green's function which is represented mathematically as [17]

$$G(k, t - t') = -i\langle c_k(t) c_k^\dagger(t')\rangle \quad \text{if} \quad t > t' \tag{3.0.4}$$

This corresponds to an excitation being created at time t' and then being destroyed at the later time t. During the interval $t - t'$ the excitation can be scattered and changed. The measurement at time t can then give an insight into the system [22]. Equivalently

$$G(k, t - t') = +i\langle c_k^\dagger(t') c_k(t)\rangle \quad \text{if} \quad t < t' \tag{3.0.5}$$

where the change in the sign is due to the anti-commutation of one fermionic operator with the other. This corresponds to an electron being destroyed at time

t and then being recreated at a later time t'. When the electron is destroyed it produces a hole which interacts in the interval $t - t'$. This will give information about the hole excitation [22].

When constructing the S-matrix it can be observed that there will be many creation and annihilation operators which can be grouped in several ways to construct different Green's functions, this grouping is known as Wick's theorem [22]. This is where the diagrammatic techniques become useful as each diagram represents a single Green's function as a solid line and each point is a given time.

The following chapter will first describe these different representations before deriving the Green's functions and S-matrix before calculating the results of Drude conductivity and Weak Localisation which were stated in the previous chapter.

3.1 S-Matrix expansions

3.1.1 Introduction to the Interaction Representation

To proceed with any calculations we must define the interaction representation where the Hamiltonian is split into two parts

$$H = H_0 + V \tag{3.1.1}$$

where H_0 is the Hamiltonian which can be solved exactly and V denotes the remaining parts. H_0 and V are chosen in such a way that V is small and that the system with only H_0 is described and V is introduced to see how the system changes. In this brief introduction, 3 representations of the wavefunctions and operators must be introduced and the annotations must be shown as to not incur

any confusion. It must be noted that each of the three representation will give exactly the same results but will use different methods, as will be shown in equations (3.1.4), (3.1.6) and (3.1.10).

The first is the Schrödinger representation where the wavefunction, ψ and operator H are denoted as

$$i\frac{\partial}{\partial t}\psi(t) = H\psi(t) \tag{3.1.2}$$

and

$$\psi(t) = e^{-iHt}\psi(0) \tag{3.1.3}$$

The main property of the Schrödinger representation is that the wavefunction is dependent upon time whereas the operators are independent upon time. Evaluating the matrix elements of the operator O between 2 states in this representation will be give by

$$\langle\psi_1^\dagger(t)O(0)\psi_2(t)\rangle = \langle\psi_1^\dagger(0)e^{iHt}O(0)e^{-iHt}\psi_2(0)\rangle \tag{3.1.4}$$

This result will be compared with the other representations to shown that they all give the same result.

The second is the Heisenberg representation where the operators O are time dependent and the wavefunctions are independent upon time. The operator in this representation is given by

$$O(t) = e^{iHt}O(0)e^{-iHt} \tag{3.1.5}$$

Initially this looks like the time dependences of the Schrödinger and Heisenberg representations will give different results when used, but the following argument shows that they do give the same results. Using the Heisenberg representation the matrix element will be evaluated as

$$\langle\psi_1^\dagger(0)O(t)\psi_2(0)\rangle = \langle\psi_1^\dagger(0)e^{iHt}O(0)e^{-iHt}\psi_2(0)\rangle \tag{3.1.6}$$

This gives the exact same result as in the Schrödinger representation (3.1.4).

The final representation is the interaction representation where the operators and wavefunctions will be labeled as $O_{int}(t)$ and $\psi_{int}(t)$ to distinguish from the previous 2 representations. Operators in the interaction representation are defined as

$$O_{int}(t) = e^{iH_0t}Oe^{-iH_0t} \tag{3.1.7}$$

and the wave functions

$$\psi_{int}(t) = e^{iH_0t}e^{-iHt}\psi(0) = U(t)\psi(0) \tag{3.1.8}$$

where it is conventient to define $U(t)$ as

$$U(t) = e^{iH_0t}e^{-iHt} \tag{3.1.9}$$

As in the previous representations the matrix element must be evaluated to show that this representation gives the same result. This is evaluated as

$$\langle\psi_1^\dagger(t)O(t)\psi_2(t)\rangle \;=\; \langle\psi_1^\dagger(0)e^{iHt}e^{-iH_0t}e^{iH_0t}O(0)e^{-iH_0t}e^{iH_0t}e^{-iHt}\psi_2(0)\rangle$$

$$= \langle \psi_1^\dagger(0) e^{iHt} O(0) e^{-iHt} \psi_2(0) \rangle \tag{3.1.10}$$

which is exactly the same result as the Schrödinger representation (3.1.4) and the Heisenberg representation (3.1.6) which shows that they are all equivalent.

3.1.2 Introduction to the S-Matrix

If we define the S-Matrix as the operator $S(t,t')$ which scatters the wave function from $\psi_{int}(t')$ to $\psi_{int}(t)$ and is written as

$$\psi_{int}(t) = S(t,t')\psi_{int}(t') \tag{3.1.11}$$

Now that the terms have been defined, the next step is to derive a more suitable form of the S-Matrix which can be used to create the diagrammatic expansions.

Using the relation (3.1.8)

$$\psi_{int}(t) = U(t)\psi(0) = S(t,t')U(t')\psi(0) \tag{3.1.12}$$

and given that $U(t)U^\dagger(t) = 1$ this gives

$$S(t,t') = U(t)U^\dagger(t') \tag{3.1.13}$$

Finally, the S-Matrix can be constructed into a more suitable form by showing that

$$\begin{aligned} \frac{\partial}{\partial t} S(t,t') &= \frac{\partial}{\partial t} U(t) U^\dagger(t') \\ &= \left[\frac{\partial}{\partial t} e^{iH_0 t} e^{-iHt} \right] U^\dagger(t') \end{aligned}$$

$$\begin{aligned} &= i(H_0 - H)U(t)U^\dagger(t') \\ &= -iV_{int}(t)S(t,t') \end{aligned} \tag{3.1.14}$$

This equation can be solved by integrating both sides with respect to time as

$$S(t,t') - S(0,t') = -i\int_0^t dt_1 V_{int}(t_1)S(t_1,t') \tag{3.1.15}$$

Which, rearranged, gives

$$S(t,t') = 1 - i\int_0^t dt_1 V_{int}(t_1)S(t_1,t') \tag{3.1.16}$$

Repeating this integration will give the full solution as

$$\begin{aligned} S(t,t') &= 1 - i\int_t^{t'} V_{int}(t_1)dt_1 \\ &\quad +(-i)^2\int_t^{t'} dt_1\int_t^{t_1} dt_2 V_{int}(t_1)V_{int}(t_2) + ... \end{aligned} \tag{3.1.17}$$

In this derivation of the S-matrix it has never been enforced that the times are ordered in any way and $t' < t_1 < t_2 < ... < t$ is not necessarily true. To resolve this problem we can rewrite the third term in (3.1.17) as

$$\begin{aligned} \int_t^{t'} dt_1\int_t^{t'} dt_2 V_{int}(t_1)V_{int}(t_2) &= \frac{1}{2}\int_t^{t'} dt_1\int_t^{t_1} dt_2 V_{int}(t_1)V_{int}(t_2) \\ &\quad +\frac{1}{2}\int_t^{t'} dt_2\int_t^{t_2} dt_1 V_{int}(t_2)V_{int}(t_1) \end{aligned}$$

where the second term is just a change of indices. This can be rewritten using the

Heaviside function Θ to give

$$\frac{1}{2}\int_t^{t'} dt_1 \int_t^{t'} dt_2 \left(\Theta(t_1 - t_2)V_{int}(t_1)V_{int}(t_2) + \Theta(t_2 - t_1)V_{int}(t_2)V_{int}(t_1)\right) \tag{3.1.18}$$

This will now be denoted as the time-ordering operator defined as

$$T[V_{int}(t_1)V_{int}(t_2)] = \Theta(t_1 - t_2)V_{int}(t_1)V_{int}(t_2) + \Theta(t_2 - t_1)V_{int}(t_2)V_{int}(t_1) \tag{3.1.19}$$

which acts upon a group of time-dependent operators and arranges them so that the earliest time is to the right

$$T[V_{int}(t_1)V_{int}(t_2)V_{int}(t_3)] = V_{int}(t_2)V_{int}(t_3)V_{int}(t_1) \quad \text{if} \quad t_2 > t_3 > t_1 \tag{3.1.20}$$

The same method can be used to rewrite

$$\begin{aligned}\int_t^{t'} dt_1 \int_t^{t_1} dt_2 \int_t^{t_2} dt_3 V_{int}(t_1)V_{int}(t_2)V_{int}(t_3) \\ = \frac{1}{3!}\int_t^{t'} dt_1 \int_t^{t'} dt_2 \int_t^{t'} dt_3 T[V_{int}(t_1)V_{int}(t_2)V_{int}(t_3)]\end{aligned} \tag{3.1.21}$$

Therefore the S-Matrix can be written in an abbreviated form as

$$\begin{aligned} S(t,t') &= 1 - iT\int_t^{t'} V_{int}(t_1)dt_1 + \frac{(-i)^2}{2!}T\int_t^{t'} dt_1 \int_t^{t'} dt_2 V_{int}(t_1)V_{int}(t_2) + ... \\ &= T\mathrm{e}^{-i\int_t^{t'} V_{int}(t_1)dt_1} \end{aligned} \tag{3.1.22}$$

3.1.3 Introduction to the Green's Function

The problem with the interaction representation is that the groundstate wave function, which is the basis for the calculation, is unknown for the whole Hamiltonian. In the previous subsection the Hamiltonian in the interaction representation was defined as $H = H_0 + V$ where the eigenvalues and eigenstates are known for the H_0 term. Therefore it maybe possible to determine the unknown groundstate wavefunction, $\psi(0)$, in terms of the known wavefunction, ϕ_0. In 1951 Gell-Mann and Low found the relation between these two wavefunctions as

$$\psi(0) = S(0, -\infty)\phi_0 \tag{3.1.23}$$

and also recall the relation

$$\psi_{int}(0) = S(0, t)\psi(t) \tag{3.1.24}$$

The main assumption is that at time $t = -\infty$ the wavefunction does not contain any terms from the interaction, V, so that $\psi_{int}(-\infty)$ is equal to the known wavefunction ϕ_0. The system is brought adiabatically to the present time, $t = 0$, where the wavefunction now contains the interaction term via the operator $S(0, -\infty)$. By symmetry, it should be deduced that at $t = +\infty$ the wavefunction must also be related to ϕ_0 and is in fact only different via an additional phase factor. To show this, we must manipulate the unknown wavefunction at $t = \infty$ as

$$\begin{aligned} \psi_{int}(\infty) &= S(\infty, 0)\psi(0) = S(\infty, 0)S(0, -\infty)\phi_0 \\ &= S(\infty, -\infty)\phi_0 \end{aligned} \tag{3.1.25}$$

This shows that the additional phase factor is $S(\infty, -\infty)$. At zero temperature the Green's function is represented as

$$G(k, t - t') = -i\langle|Tc_k(t')c_k^\dagger(t)|\rangle \tag{3.1.26}$$

where $|\rangle$ is the groundstate of the Hamiltonian, H. This can be derived in the interaction representation by using

$$c(t) = e^{iHt}e^{-iH_0t}c_{int}(t)e^{iH_0t}e^{-iHt} = S(0,t)c_{int}(t)S(t,0) \tag{3.1.27}$$

and the relation $|\rangle = S(0, -\infty)|\rangle_0$ where $|\rangle_0$ is the groundstate of H_0. Combining and simplifying will give the interaction representation of the Green's function as

$$G(k, t - t') = -i\frac{{}_0\langle|c_{int}(t')c_{int}^\dagger(t)|\rangle_0}{{}_0\langle|S(\infty, -\infty)|\rangle_0} \tag{3.1.28}$$

where $|\rangle_0$ is the groundstate of the Hamiltonian H_0, previously defined as ϕ_0.

3.1.4 Diagrammatic Expansion

Recall that the S-matrix is represented as

$$\begin{aligned} S(t,t') &= T\mathrm{e}^{-i\int_t^{t'}V(t_1)dt_1} \\ &= 1 - iT\int_t^{t'}V(t_1)dt_1 + \frac{(-i)^2}{2!}T\int_t^{t'}dt_1\int_t^{t'}dt_2V(t_1)V(t_2) + ... \end{aligned}$$

Consider a two particle interaction defined by the operator

$$V(t_1) = \sum_{k,k',q} U_q c_k^\dagger(t_1)c_{k'}^\dagger(t_1)c_{k'+q}(t_1)c_{k-q}(t_1) \tag{3.1.29}$$

where the interaction is illustrated in figure 3.1. Substituting the interaction

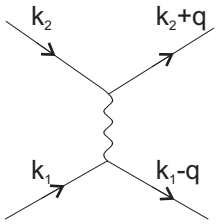

Figure 3.1 – A typical 2 particle interaction where 2 particles with momentum k_1 and k_2 interact and exchange a momenta q at a time t_1 which is represented by (3.1.29).

Hamiltonian into the expansion will give

$$S(t,t') = 1 - iT \int_t^{t'} dt_1 \sum_{k,k',q} U_q c_k^\dagger(t_1) c_{k'}^\dagger(t_1) c_{k'+q}(t_1) c_{k-q}(t_1) + ...$$

Wick's theorem can now be used to group each creation and annihilation operator together in every possible combination. Then each term can be related to the fundamental Green's function and used to construct a diagrammatic expansion to a given order. Wick's theorem is the method used to evaluate such terms in

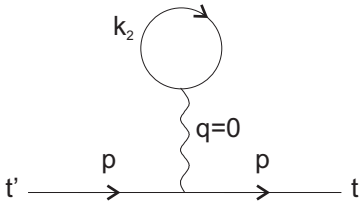

Figure 3.2 – A first order contribution to the Green's function with a 2 particle interaction. This contribution gives an interaction with no exchange of momentum, $q = 0$.

the S-matrix expansion by grouping certain creation and annihilation operators. A term $\langle|...|\rangle$, where $\langle|$ denotes the groundstate, will only be non-zero when each creation operator matches with an annihilation operator so that we return to the groundstate. For example the term

$$\langle T c_\alpha(t) c^\dagger_\beta(t')\rangle \tag{3.1.30}$$

is only non-zero if $\alpha = \beta$. Likewise, the term

$$\langle T c_\alpha(t) c^\dagger_\beta(t_1) c_\gamma(t_2) c^\dagger_\delta(t')\rangle \tag{3.1.31}$$

is only non-zero if $\alpha = \beta$ and $\gamma = \delta$ or $\alpha = \delta$ and $\gamma = \beta$. Given Wick's theorem states then the term in the integral can be grouped in 6 ways, of which only 4 are distinct diagrams. One of the contributions will be of the form

$$\langle c_p(t) c^\dagger_k(t_1)\rangle \langle c^\dagger_{k'}(t_1) c_{k'+q}(t_1)\rangle \langle c_{k-q}(t_1) c^\dagger_p(t')\rangle = \\ (-i)^3 \delta_{p,k} G_0(p, t_1 - t) \delta_{q=0} G_0(k', t_1 - t_1) \delta_{k-q,p} G_0(p, t' - t_1)$$

which is diagrammatically represented in figure 3.2.

The next distinct diagram comes from the grouping

$$\langle c_p(t) c^\dagger_k(t_1)\rangle \langle c^\dagger_{k'}(t_1) c_{k-q}(t_1)\rangle \langle c_{k'+q}(t_1) c^\dagger_p(t')\rangle = \\ (-i)^3 \delta_{p,k} G_0(p, t_1 - t) \delta_{k',k-q} G_0(k', t_1 - t_1) \delta_{k'+q,p} G_0(p, t' - t_1)$$

This term must contain a finite value of q which causes this diagram to be different from the previous one; this diagram is represented in figure 3.3. All 4 distinct

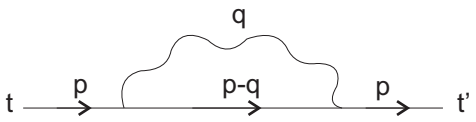

Figure 3.3 – This is a contribution to the S-matrix with a 2 particle interaction. This diagram will be used in a later chapter to derive the superconducting contribution.

diagrams are shown in figure 3.4. Diagram 3.4(a) corresponds to an interaction

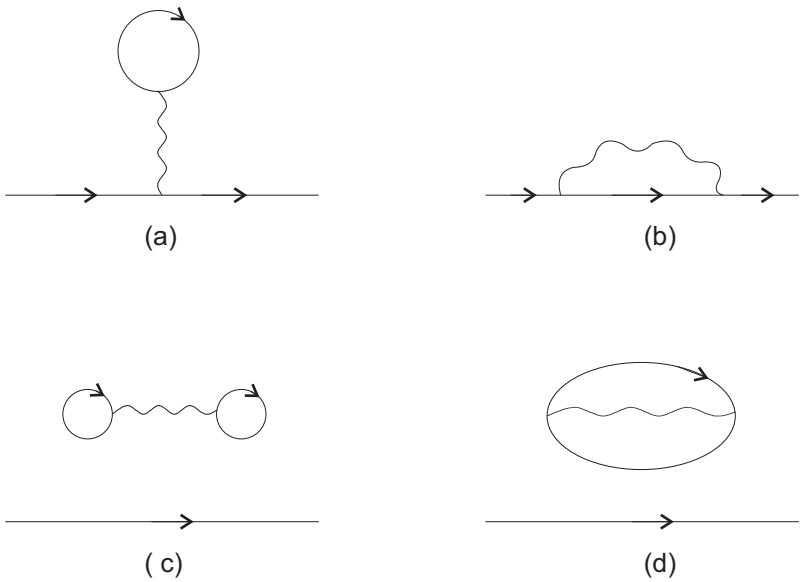

Figure 3.4 – The diagrammatic expansion for a 2 particle interaction. (a) corresponds to an interaction with no momenta $q = 0$. (c) and (d) are disconnected and (b) can be calculated to construct the superconducting Green's functions.

with no momentum $q = 0$ which implies that its contribution can be ignored. Diagrams 3.4(c) and 3.4(d) are disconnected diagrams which will only contribute a constant to the final solution and can also be ignored. This cancellation is because one has to divide by $\langle|S(\infty, -\infty)|\rangle$ in the Green's function. The only first order contribution to the S-matrix of the 2-particle interaction is given by diagram 3.4(b); which will be used later in this report in the *Nambu-Gorkov* calculation of

superconductivity.

3.1.5 Matsubara Green's Function

One can calculate diagrams with zero temperature Green's functions, and one would expect that this would be a simpler task than solving them for finite-temperature; this is untrue. Zero temperature Green's functions cause difficulties in constructing the contour integrals and, in general, are more difficult to solve than the finite-temperature Green's functions. This is due to the introduction of an *imaginary-time evolution* and the simplification of the *Matsubara Summation*, which will be discussed in the next subsection.

The Green's function is defined as

$$G(k, t - t') = -i\langle T c_k(t') c_k^\dagger(t)\rangle \tag{3.1.32}$$

where T is the time ordering operator and in the finite-temperature Green's function $\langle ...\rangle$ denotes a quantum and thermodynamic averaging. The thermodynamic average is defined by

$$\langle \hat{A}\rangle = \frac{\sum_n \mathrm{e}^{-\beta E_n}\langle n|A_{int}|n\rangle}{\sum_n \mathrm{e}^{-\beta E_n}} = \frac{\mathrm{Tr}\{\mathrm{e}^{-\beta H}A_{int}\}}{\mathrm{Tr}\{\mathrm{e}^{-\beta H}\}} \tag{3.1.33}$$

Recalling the time-evolution operator $U(t) = \exp\{-i\hat{H}t\}$, one can rewrite the thermodynamic averaging as

$$\langle A_{int}\rangle = \frac{\sum_n U(-i\beta)\langle n|A_{int}|n\rangle}{\sum_n U(-i\beta)} = \frac{\mathrm{Tr}\{\mathrm{e}^{-\beta H}A_{int}\}}{\mathrm{Tr}\{\mathrm{e}^{-\beta H}\}} \tag{3.1.34}$$

and the introduction of $U(-i\beta)$ is like evolving in imaginary time. The Green's

function can now be written in imaginary time, τ as

$$G(k,\tau,\tau') = -\langle T_\tau c_k(\tau) c_k^\dagger(\tau')\rangle \tag{3.1.35}$$

where

$$c_k(\tau) = \mathrm{e}^{\tau\hat{H}} c_k \mathrm{e}^{-\tau\hat{H}} \qquad \text{and} \qquad c_k^\dagger(\tau) = \mathrm{e}^{\tau\hat{H}} c_k^\dagger \mathrm{e}^{-\tau\hat{H}} \tag{3.1.36}$$

One must note that the operators $c_k(\tau)$ and $c_k^\dagger(\tau)$ are no longer hermitian conjugates of each other.

Using the formula above together with the definition of the thermodynamic averaging, recalling that the partition function is represented as $\mathcal{Z} = \sum_n \mathrm{e}^{-\beta E_n}$, one can write the Green's function as

$$\begin{aligned} G(k,\tau,\tau') &= \frac{1}{\mathcal{Z}}\big[-\Theta(\tau-\tau')\mathrm{Tr}\{\mathrm{e}^{-\beta\hat{H}}\mathrm{e}^{\tau\hat{H}} c_k \mathrm{e}^{-\tau\hat{H}}\mathrm{e}^{\tau'\hat{H}} c_k^\dagger \mathrm{e}^{-\tau'\hat{H}}\} \\ &\quad +\Theta(\tau'-\tau)\mathrm{Tr}\{\mathrm{e}^{-\beta\hat{H}}\mathrm{e}^{\tau'\hat{H}} c_k^\dagger \mathrm{e}^{-\tau'\hat{H}}\mathrm{e}^{\tau\hat{H}} c_k \mathrm{e}^{-\tau\hat{H}}\}\big] \end{aligned} \tag{3.1.37}$$

The properties of a trace is that any cyclic permutation leaves the trace invariant $\mathrm{Tr}\{ABC\} = \mathrm{Tr}\{CAB\} = \mathrm{Tr}\{BCA\}$. This property can be used to cyclically permute the operators into the form

$$\begin{aligned} G(k,\tau,\tau') &= \frac{1}{\mathcal{Z}}\big[-\Theta(\tau-\tau')\mathrm{Tr}\{\mathrm{e}^{-\beta\hat{H}}\mathrm{e}^{(\tau-\tau')\hat{H}} c_k \mathrm{e}^{-(\tau-\tau')\hat{H}} c_k^\dagger\} \\ &\quad +\Theta(\tau'-\tau)\mathrm{Tr}\{\mathrm{e}^{-\beta\hat{H}}\mathrm{e}^{(\tau'-\tau)\hat{H}} c_k^\dagger \mathrm{e}^{-(\tau'-\tau)\hat{H}} c_k\}\big] \end{aligned} \tag{3.1.38}$$

This reveals that the Green's function is only a function of the difference between the two imaginary times $\tau - \tau'$, with $-\beta < \tau < \beta$ and $-\beta < \tau' < \beta$. Denoting

$\tilde{\tau} = \tau - \tau'$ and by shifting by β in imaginary time one can write

$$\begin{aligned} G(k, \tilde{\tau} + \beta) &= \frac{-1}{\mathcal{Z}} \mathrm{Tr}\{\mathrm{e}^{-\beta\hat{H}} \mathrm{e}^{(\tau+\beta)\hat{H}} c_k \mathrm{e}^{-(\tau+\beta)\hat{H}} c_k^\dagger\} \\ &= \frac{-1}{\mathcal{Z}} \mathrm{Tr}\{\mathrm{e}^{-\beta\hat{H}} c_k^\dagger \mathrm{e}^{\tau\hat{H}} c_k \mathrm{e}^{-\tau\hat{H}}\} \\ &= -G(k, \tau) \end{aligned} \tag{3.1.39}$$

Note that this result holds for fermions only; bosons will give $G(k, \tau+\beta) = G(k, \tau)$ due to commutation rules. Taking the Fourier transformation one can write

$$G(k, i\omega_n) = \int_0^\beta d\tau G(k, \tau) \mathrm{e}^{i\tau\omega_n} \tag{3.1.40}$$

where

$$\omega_n = \frac{(2n+1)\pi}{\beta} \tag{3.1.41}$$

This differs for bosons due to the anticommutation relations and we will define the bosonic representation as

$$\Omega_n = \frac{2n\pi}{\beta} \tag{3.1.42}$$

3.1.6 Free-particle Green's function

The Matsubara frequency have been represented in the previous subsection but here the free-particle Green's function will be derived with respect to these momenta. As in the previous subsection, the Green's function can be represented

as

$$G(k,\tau) = \frac{-1}{\mathcal{Z}}\mathrm{Tr}\{\mathrm{e}^{-\beta\hat{H}}\mathrm{e}^{\tau\hat{H}}c_k\mathrm{e}^{-\tau\hat{H}}c_k^\dagger\} \tag{3.1.43}$$

where

$$c_k(\tau) = \mathrm{e}^{-\xi_k\tau}c_k \qquad \text{and} \qquad c_k^\dagger(\tau) = \mathrm{e}^{\xi_k\tau}c_k^\dagger \tag{3.1.44}$$

with the energy being $\xi_k = \varepsilon_k - \mu$.

So the free-particle Green's function can be written as

$$\begin{aligned} G_0(k,\tau) &= -\langle c_k(\tau)c_k^\dagger(0)\rangle \\ &= -\mathrm{e}^{-\xi_k\tau}\frac{\mathrm{Tr}\{\mathrm{e}^{-\beta\hat{H}}c_kc_k^\dagger\}}{\mathrm{Tr}\{\mathrm{e}^{-\beta\hat{H}}\}} \end{aligned} \tag{3.1.45}$$

By commuting the operators, using the Fermionic commutation rules, one can rewrite the terms in the fraction as $1 - n_F(\xi_k)$, where $n_F(\xi_k)$ is the distribution function. Fourier transforming this into momenta space one is given

$$\begin{aligned} G_0(k,i\omega) &= -[1-n_F(\xi_k)]\int_0^\beta \mathrm{e}^{-\xi_k\tau}\mathrm{e}^{i\omega_n\tau}\mathrm{d}\tau \\ &= -[1-n_F(\xi_k)]\frac{\mathrm{e}^{(i\omega_n-\xi_k)\beta}-1}{i\omega_n-\xi_k} \end{aligned} \tag{3.1.46}$$

Recalling $\omega_n = (2n+1)\pi/\beta$ one is left with the free-particle Green's function as

$$G_0(k,i\omega_n) = \frac{1}{i\omega_n - \xi_k} \tag{3.1.47}$$

This is the finite-temperature Green's function that will be used throughout this

thesis.

3.2 Impurity Greens Function

The Greens function for a particle scattered off an impurity can be written diagrammatically as figure 3.5.

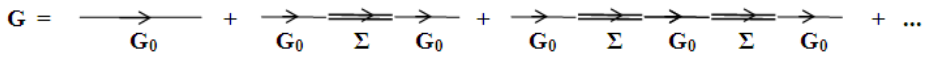

Figure 3.5 – Diagrammatic representation of Dyson's equation

Dyson's equation is represented as

$$G^{-1} = G_0^{-1} - \Sigma \tag{3.2.1}$$

If one only considers a potential scattering where there is no change in the overall state of the system then the only effect is to inflict a scattering time given by Fermi's Golden Rule

$$\tau^{-1} = 2\pi N(\varepsilon_F) n_i |u|^2 \tag{3.2.2}$$

which, when rearranged, gives

$$n_i |u|^2 = [2\pi N(\varepsilon_F)\tau]^{-1} \tag{3.2.3}$$

The impurity Greens function therefore becomes

$$G = \frac{1}{2\pi N(\varepsilon_F)\tau} \sum_k \frac{1}{i\omega - \xi_k} \tag{3.2.4}$$

Once again, the summation substitution can be performed $\sum_k \to N(\varepsilon_F) \int d\xi$ and by multiplying the numerator and denominator by $i\omega + \xi_k$ gives

$$G = \frac{1}{2\pi\tau} \int_{-\infty}^{\infty} \frac{i\omega + \xi_k}{\omega^2 + \xi^2} = \frac{i\omega}{2\pi\tau} \frac{\pi}{|\omega|} \tag{3.2.5}$$

This means that the self energy becomes

$$\Sigma = \frac{i}{2\tau} \text{sign}\omega \tag{3.2.6}$$

Therefore the rule for changing from a clean to dirty sample is by merely changing the Matsubara frequencies

$$\begin{array}{ccc} \omega & \to & \frac{i}{2\tau}\text{sign}\omega \\ \text{Clean} & & \text{Dirty} \end{array} \tag{3.2.7}$$

3.3 Drude conductivity

This Thesis is mainly concerned with *mesoscopic conductance fluctuations* and so the natural starting point is to reproduce the Drude conductivity. The simplest contribution to conductivity is the particle-hole propagator, given by the diagram shown in figure 3.6, which can be found in the second order contribution of the phonon-propagated S-matrix expansion.

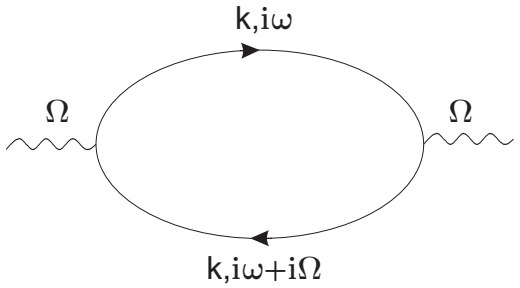

Figure 3.6 – The second order contribution of the phonon-propagated S-matrix expansion which represents the diagrammatic interpretation of the Drude conductivity

The electromagnetic response function then becomes

$$\begin{aligned} K_{\alpha\beta}(i\Omega) &= T\sum_{\omega}\sum_{k}\frac{ek_\alpha}{m}\frac{ek_\beta}{m}G(k,i\omega)G(k,i\omega+i\Omega) \qquad (3.3.1)\\ &= T\sum_{\omega}\sum_{k}\frac{ek_\alpha}{m}\frac{ek_\beta}{m}\frac{1}{i\omega-\xi_k+\frac{i}{2\tau}sign(\omega)}\frac{1}{i\omega+i\Omega-\xi_k+\frac{i}{2\tau}sign(\omega)} \end{aligned}$$

The major contribution to the k-sum is due to the electrons near the Fermi surface. Therefore, one can substitute $\sum_k \rightarrow N(0)\int d\xi$ with an additional factor contributing to the angular integral in d-dimensions. This factor can be calculated by writing

$$\sum_k k_\alpha k_\beta = Ck_F^2\delta_{\alpha\beta} \qquad (3.3.2)$$

where C is a constant that needs to be calculated. Contracting on α and β and realising that the number of diagonal components of the δ-function is represented by the dimension of the system d, one can write

$$CdK_F^2\delta_{\alpha\beta} = Cdk_F^2 \qquad (3.3.3)$$

Therefore, $C = d^{-1}$ which means that the angular integral contribution to the k-summation will give, in d-dimensions,

$$\sum_k k_\alpha k_\beta = \frac{k_F^2}{d}\delta_{\alpha\beta} \tag{3.3.4}$$

Using this relation, the response function now becomes

$$K_{\alpha\beta}(i\Omega) = T\frac{e^2k_F^2N(0)}{dm^2}\sum_\omega \int_{-\infty}^{\infty} d\xi \frac{1}{i\omega - \xi_k + \frac{i}{2\tau}sign(\omega)}\frac{1}{i\omega + i\Omega - \xi_k + \frac{i}{2\tau}sign(\omega)}$$

The only contribution to this integral is when either $\omega > 0$ and $\omega + \Omega < 0$ or $\omega < 0$ and $\omega + \Omega > 0$ otherwise the two poles will be in the same half-plane and so the contour integral can be performed on the other half-plane to give zero. Arbitrarily choose $\omega < 0$ and $\omega + \Omega > 0$. The pole is $\xi_k = i\omega - \frac{i}{2\tau}$ and by using Cauchy's Residue theorem,

$$\int_{-\infty}^{\infty} d\xi \frac{1}{i\omega - \xi_k + \frac{i}{2\tau}sign(\omega)}\frac{1}{i\omega + i\Omega - \xi_k + \frac{i}{2\tau}sign(\omega)} = \frac{2\pi i}{i\Omega + \frac{i}{\tau}} \tag{3.3.5}$$

Substituting the limits $\omega < 0$ and $\omega + \Omega > 0$ as Heaviside functions then the electromagnetic response function becomes,

$$K_{\alpha\beta}(i\Omega) = \frac{2\pi e^2k_F^2\tau N(0)}{dm^2(1+\Omega\tau)}T\sum_\omega \Theta(-\omega)\Theta(\omega+\Omega) \tag{3.3.6}$$

The sum can be calculated as $\frac{\Omega}{2\pi T}$ which will give the final answer as

$$K_{\alpha\beta}(i\Omega) = \frac{e^2k_F^2\tau N(0)\Omega}{dm^2(1+\Omega\tau)} \tag{3.3.7}$$

Using the substitution $N(0) = \frac{3n}{4\omega_F}$ together with $\sigma(i\omega) = \frac{K(i\Omega)}{\Omega}$ this gives,

$$\sigma(i\omega) = \frac{\pi e^2 \tau}{m} \frac{1}{1 + \Omega\tau} \tag{3.3.8}$$

and upon changing to real frequency gives,

$$\sigma(i\omega) = \frac{\pi e^2 \tau}{m} \frac{1}{1 - i\Omega\tau} \tag{3.3.9}$$

In the limit $\Omega = 0$ this will give

$$\sigma(i\omega) = \frac{\pi e^2 \tau}{m} \tag{3.3.10}$$

which is the Drude conductivity term stated in the introduction. The next step is to derive the weak localisation correction will be shown in the next section.

3.4 Weak-localisation

Different experimental phenomena was found in dirty metals which must now be investigated to determine the change in the system's conductivity. The main contribution is due to the intersection of various paths that the electron can propagate along. If one considers the probability of propagating from point A to point B being the modulus squared of the amplitudes as

$$P = |\sum_i A_i|^2 = \sum_i |A_i|^2 + \sum_{i \neq j} A_i^* A_j \tag{3.4.1}$$

If two paths, one the time-reversed path of the other, is scattered off the same impurity then, as long as the system is time-reversal symmetric, the phases of these

two paths will cancel. This will result in a contribution only from a set of closed loops. Intuitively, this will cause the conductivity to decrease due to the electrons decreased probability of propagating from points A to B and instead propagating through these closed loops. It is well known that the introduction of a magnetic field would destroy time-reversal symmetry and will therefore destroy these interference effects. Therefore an applied magnetic field will cause the conductivity to increase and is known as negative magnetoresistance.

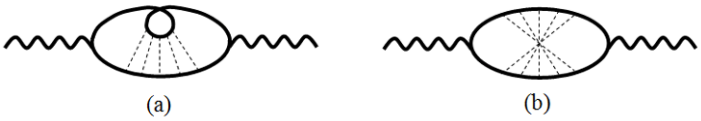

Figure 3.7 – (a)The diagrammatics of the effect of weak localisation due to the self-intersecting paths. This diagram can be 'uncoiled' to give the diagrammatic representation shown in (b).

To calculate such interference effects diagrammatically one must include these self-intersecting paths into the Drude conductivity diagram. The initial diagram is shown in figure 3.7(a) but the loop can be represented using a more convenient diagram shown in figure 3.7(b). The latter is described as the particle-particle ladder or the Cooperon, denoted hereafter as $\mathcal{C}$. There is a similar diagram, known as the Diffuson, which corresponds to a corelator in the particle-hole channel but is not needed here. The propagating ladder will be calculated before the Normal-State Weak-localistion diagram is solved.

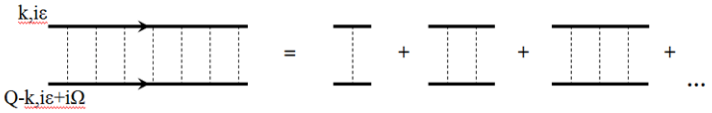

Figure 3.8 – This is the Cooperon together with the term-by-term expansion needed to calculate it.

3.4.1 Normal-State ladder calculation

To evaluate the Cooperon one must first make the expansion given diagrammatically in figure 3.8 which corresponds to to the following

$$\mathcal{C} = \Gamma^0 + \Gamma^0\Pi\Gamma^0 + \Gamma^0\Pi\Gamma^0\Pi\Gamma^0 + ... \tag{3.4.2}$$

where

$$\Gamma^0 = (2\pi N(0)\tau)^{-1} \tag{3.4.3}$$

$$\Pi = \sum_k G(k, i\omega)G(Q-k, i\omega + i\Omega) \tag{3.4.4}$$

with Γ^0 denoting the impurity scattering which enforces a scattering time given by Fermi's Golden Rule. As stated in the previous section, the Matsubara frequencies change from $\omega \to \omega \pm isign(\omega)/2\tau$ when going from the clean→dirty limit. The integral, that proceeds, will be a contour integral in the upper or lower half-plane (UHP/LHP). The $\pm$ in the Matsubara frequencies will result in four seperate solutions. Two of these solutions will result in both poles either in the LHP or UHP which will give zero contribution as one can close the contour on the half-plane with no poles. The other two solutions will cause the same result so the

following is the only contribution

$$\Pi = \sum_k \frac{1}{\xi - i\omega + i/2\tau} \frac{1}{\xi_Q - i\omega - i\Omega - i/2\tau} \tag{3.4.5}$$

where $\xi_Q = (Q-k)^2/2m$. In the presence of a magnetic field one must use minimal coupling $Q \to Q - pA; k \to k - pA$. These minimal coupling terms will cancel and cause no change to the result. Expanding out ξ_Q in the small Q-limit and using the angle-representation for the scalar product one is left with

$$\Pi = \sum_k \frac{1}{\xi - i\omega + i/2\tau} \frac{1}{\xi - Qv_F cos\theta - i\omega - i\Omega - i/2\tau} \tag{3.4.6}$$

Transforming the summation into integral form and closing the contour in the UHP one must solve

$$\Pi = N(0)2\pi i Res(f, \xi) = \frac{N(0)2\pi i}{Qv_F cos\theta + i\Omega + i/\tau} \tag{3.4.7}$$

One must now take the angular average by rearranging into a geometric summation form

$$\begin{aligned} \Pi &= \left\langle \frac{N(0)2\pi i}{Qv_F cos\theta + i\Omega + i/\tau} \right\rangle_\theta & (3.4.8) \\ &= 2\pi N(0)\tau \left\langle \frac{1}{1 + \Omega\tau - i\tau Q v_F \cos\theta} \right\rangle_\theta & (3.4.9) \end{aligned}$$

and by using the geometric series formula one can expand the brackets to become

$$\begin{aligned} \Pi &= 2\pi N(0)\tau \left[\frac{1}{1+\Omega\tau} + \frac{i\tau Q v_F}{(1+\Omega\tau)^2} \langle \cos\theta \rangle + \frac{(\tau Q v_F)^2}{(1+\Omega\tau)^3} \langle \cos^2\theta \rangle + ... \right] \\ &= 2\pi N(0)\tau \left[\frac{1}{1+\Omega\tau} + \frac{(\tau Q v_F)^2}{3(\Omega+1)^3} \right] \end{aligned} \tag{3.4.10}$$

Taking the diffusion limit $\Omega\tau << 1$ and by introducing the *Diffusion coefficient* $D = v_F^2\tau/3$ one can now obtain the final equation as

$$\Pi = 2\pi N(0)\tau \left[1 - (DQ^2 + \Omega)\tau\right] \tag{3.4.11}$$

By using figure 3.8 together with the equations for Π and Γ^0 one can calculate the Cooperon as

$$\Gamma = \frac{1}{2\pi N\tau} + \left(\frac{1}{2\pi N\tau}\right) 2\pi N(0)\tau \left[1 - (DQ^2 + \Omega)\tau\right] + ... \tag{3.4.12}$$

This is simply a geometric series with an extra factor of $1/2\pi N\tau$. Using the geometric summation equation one has

$$\begin{aligned}
\Gamma &= \frac{1}{2\pi N\tau} \cdot \frac{1}{1 - \frac{1}{2\pi N\tau} \cdot 2\pi N\tau[1 - (DQ^2 + \Omega)\tau]} && (3.4.13)\\
&= \frac{1}{2\pi N\tau} \cdot \frac{1}{1 - 1 + (DQ^2 + \Omega)\tau} && (3.4.14)\\
&= \frac{1}{2\pi N\tau} \cdot \frac{1}{(DQ^2 + \Omega)\tau} && (3.4.15)\\
&= \frac{1}{2\pi N\tau^2} \cdot \frac{1}{DQ^2 + |\Omega|} && (3.4.16)
\end{aligned}$$

This solution is incomplete and must also include the heaviside function, Θ, due to the contour integral that was taken. Therefore the full solution is given by

$$\Gamma = \frac{1}{2\pi N\tau^2} \cdot \frac{1}{DQ^2 + |\Omega|} \Theta(-\varepsilon(\varepsilon + \Omega)) \tag{3.4.17}$$

3.4.2 Normal-State Weak-localisation calculation

One must now use the value of Γ to construct and solve the response function to find what the correction to the conductivity becomes.

The response function is given as

$$K_{\alpha\beta}(0,i\Omega) = T\sum_{\omega}\sum_{k,Q} k_\alpha k_\beta G(k,i\omega)G(k,i\omega{+}i\Omega)G(Q{-}k,i\omega)G(Q{-}k,i\omega{+}i\Omega)\Gamma(Q,i\omega,i\Omega) \tag{3.4.18}$$

The main contribution comes from $Q \to 0$ so that one now has two 'double' Green's functions. Also the angular integral sets $k_\alpha k_\beta \to k_F^2/d$. Using the two statements above together with the fact that the two poles must be on seperate half-planes, as in previous calculations, one must now solve

$$\sum_k G(k,i\omega)^2 G(k,i\omega{+}i\Omega)^2 = N(0)\int d\xi \frac{1}{(\xi - i\omega + i/2\tau)^2(\xi - i\omega - i\Omega - i/2\tau)^2} \tag{3.4.19}$$

Closing the contour in the UHP the integral now becomes

$$\begin{aligned}\sum_k G(k,i\omega)^2 G(k,i\omega+i\Omega)^2 &= 2\pi i N(0)\frac{-2}{(i\omega + i\Omega + i/2\tau - i\omega + i/2\tau)^3} \\ &= \frac{4\pi N(0)\tau^3}{(1+\Omega\tau)^3}\end{aligned} \tag{3.4.20}$$

Substituting this into the response function gives

$$K = T\sum_{\varepsilon}\sum_{Q}\frac{-k_F^2}{d}\frac{4\pi N(0)\tau^3}{(1+\Omega\tau)^3}\frac{1}{2\pi N\tau^2}\cdot\frac{1}{DQ^2+|\Omega|} \tag{3.4.21}$$

The only consideration here will be the limit $\Omega\tau << 1$ and $\sum_\varepsilon \to \Omega/2\pi$ which finnaly leads us to

$$K = -\frac{2De^2\Omega}{\pi}\sum_Q \frac{1}{DQ^2 + |\Omega|} \tag{3.4.22}$$

This will give us the correction to the conductivity due to quantum interference effects as

$$\delta\sigma = \frac{K}{\sigma} = -\frac{2De^2}{\pi}\sum_Q \frac{1}{DQ^2 + |\Omega|} \tag{3.4.23}$$

The Q-summation can now be performed to find the correction to the conductivity in d-dimensions. The upper limit of the Q integral is $1/l$ which is the elastic mean free path . The lower limit of the Q integral is $1/L_\phi$ which is the length with which the electron is still phase coherent. Therefore, the correction to the conductivity can be found by evaluating

$$\delta\sigma = \frac{-2De^2}{\pi}\int_{1/L_\phi}^{1/l} \frac{1}{DQ^2} d^dQ \tag{3.4.24}$$

In one-dimension this can be calculated as

$$\delta\sigma = -\frac{2e^2}{\pi}\left[L_\phi - l\right] \tag{3.4.25}$$

In two-dimensions this will give

$$\delta\sigma = -\frac{2e^2}{\pi}\ln\left(\frac{l}{L_\phi}\right) \tag{3.4.26}$$

and in three-dimensions this gives

$$\delta\sigma = -\frac{2e^2}{\pi}\left[\frac{1}{l} - \frac{1}{L_\phi}\right] \tag{3.4.27}$$

Chapter 4

THEORY OF THE SUPERCONDUCTING STATE

Superconductivity was first discovered in 1911 by Kamerlingh Onnes [28] and later experiments by Quinn and Ittner [8] sufficiently showed that at a transition temperature, T_c, the resistance of certain systems can diminish to zero [27]. This transition temperature is given by

$$T_c = 1.14\omega_D \exp\left[-1/N(0)V\right] \tag{4.0.1}$$

and will be derived in section (4.1) using the previoulsy derived Green's functions. It will be shown that there exists a divergence in the electron-electron propagator at this critical temperature due to correlation between electrons which have not been taken into account [32]. This correlation was first proposed by Fröhlich in 1950 [19] and was later understood by Cooper in 1956, which was the signature idea behind the BCS theory of superconductivity [21]. This was named as the Cooper pairing of electrons and to reduce the energy to a minimum then the paired electrons must have opposite spin and momenta $(k_\uparrow, -k_\downarrow)$ [27]. This correlation

leads to a correction the Green's functions in the superconducting regime $T < T_c$ [22]. The superconducting Green's functions will be derived via the Nambu-Gorkov approach in section (4.2) by introducting the term $\langle\psi_\uparrow\psi_\downarrow\rangle$ and its complex conjugate, both denoted as Δ. This will result in a matrix representation of the superconducting Green's functions, which will be derived in section (4.3), given by

$$G = \frac{1}{i\omega\tau_0 - \xi_k\tau_3 - \Delta\tau_1} \tag{4.0.2}$$

where τ_0, τ_1, τ_2 and τ_3 are the Pauli matrices, ω is the Matsubara frequency and ξ_k is the energy of the particle. Using the superconducting Green's function the Drude conductivity and Weak Localisation results will be calculated in the superconducting regime together with the superconducting ladder propagator in sections (4.4)-(4.6). The superconducting ladder propagator will be a fundamental tool in calculating the superconducting mesoscopic fluctuations in chapter 6.

4.1 The Cooper Instability

Consider an electron gas with an attractive interaction, $V_{k,k'} = -V$, within the energy range $\pm\omega_D$ about the Fermi surface. To investigate the effects of this interaction, the electron-electron propagator, shown in figure 4.1, must be evaluated. This propagator is a simple geometric series with the self-interaction term $\Pi(Q, i\Omega)$ and is given as

$$t(Q, i\Omega) = \frac{-V}{1 + V\Pi(Q, i\Omega)} \tag{4.1.1}$$

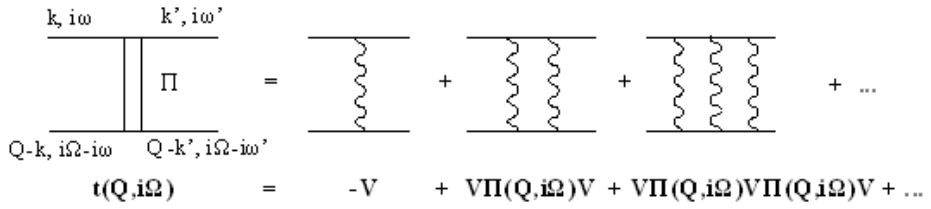

Figure 4.1 – The diagrammatic representation of the electron-electron propagator to investigate the effects of an attractive interaction between particles. The geometric series of this diagram is given below and is with repect to the self-interaction Π.

where

$$\begin{aligned}\Pi(Q,i\Omega) &= T\sum_{k,\omega} G(k,i\omega)G(Q-k,i\Omega-i\omega) \\ &= T\sum_{k,\omega}\frac{1}{i\omega-\xi_k}\frac{1}{i\Omega-i\omega-\xi_{Q-k}} \end{aligned} \tag{4.1.2}$$

Transforming $\sum_k = \int d\xi \int_{-1}^{1} dx/2$ and making the substitution $\xi_{Q-k} \approx \xi_k - Qv_F\cos\theta$ then

$$\Pi(Q,i\Omega) = T\sum_{\omega}\int_{-1}^{1}\frac{dx}{2}\frac{1}{i\omega-\xi_k}\frac{1}{i\Omega-i\omega-Qv_Fx} \tag{4.1.3}$$

must be evaluated. To proceed with the ξ integral we must constrain the poles to be either side of the real axis. This can be achieved by the inequalities $\omega > 0, \Omega-\omega < 0$ and $\omega < 0, \Omega-\omega > 0$ and by performing the integrals, with $\Omega > 0$, will give

$$T\sum_{\omega}\int_{-1}^{1}\frac{dx}{2}2\pi i\frac{-1}{2i\omega-i\Omega-Qv_Fx}\Big|_{\omega>\Omega} + \frac{1}{2i\omega-i\Omega-Qv_Fx}\Big|_{\omega<0} \tag{4.1.4}$$

By making the transformation $\omega \to \Omega - \omega$ in the second term it can be seen that the two terms are the same, with only a sign difference with the x term that can be ignored since the x integral will only keep the even terms. Extending the summation and also evalauting the integral with $\Omega < 0$ will give

$$\Pi(Q, i\Omega) = T \sum_{\omega} \int_{-1}^{1} \frac{dx}{2} \frac{2\pi}{2|\omega| + |\Omega| + iQv_F x} \tag{4.1.5}$$

In the limit $Q \to 0$ and $\Omega \to 0$ this can be expanded out as

$$\frac{1}{2|\omega| + |\Omega| + iQv_F x} \to \frac{1}{2|\omega|} + \frac{|\Omega|}{4|\omega|^2} - \frac{Q^2 v_F^2 x^2}{8|\omega|^3} \tag{4.1.6}$$

The integral over x can now be taken to give

$$\Pi(Q, i\Omega) = T \sum_{\omega} \frac{1}{2|\omega|} + \frac{|\Omega|}{4|\omega|^2} - \frac{Q^2 v_F^2}{24|\omega|^3} \tag{4.1.7}$$

Each summation can be taken individually, recalling that $\omega = 2\pi T(2n+1)$ together with the Riemann Zeta function

$$\zeta(s) = \sum_{x=1}^{\infty} \frac{1}{x^s} \tag{4.1.8}$$

Therefore

$$\sum_{\omega} \frac{1}{|\omega|^2} = \frac{2}{(\pi T)^2} \sum_{n=0}^{\infty} \frac{1}{(2n+1)^2} = \frac{2}{(\pi T)^2} \left[\zeta(2) - \frac{1}{4}\zeta(2) \right] = \frac{1}{4T^2} \tag{4.1.9}$$

and

$$\sum_{\omega} \frac{1}{|\omega|^3} = \frac{2}{(\pi T)^3} \sum_{n=0}^{\infty} \frac{1}{(2n+1)^3} = \frac{2}{(\pi T)^3} \left[\zeta(3) - \frac{1}{8}\zeta(3) \right] = \frac{7}{4\pi^3 T^3}\zeta(3)$$

The summation over $1/|\omega|$ diverges and so must be cut off at the upper energy, given by the Debye frequency ω_D as

$$\sum_{\omega} \frac{1}{2|\omega|} = \frac{1}{2\pi T} \sum_{n=0}^{\omega_D/2\pi T} \frac{1}{2n+1} \tag{4.1.10}$$

The digamma function must now be introduced as

$$\psi(x) = -\gamma + H_{n-1} = -\gamma + \sum_{n=1}^{\infty} \left(\frac{1}{n} - \frac{1}{n+x} \right) \tag{4.1.11}$$

where H_n is the usual Harmonic numbers and γ is the Euler-Mascheroni constant. The digamma function will be used to transform the summation into a more manageable form

$$\sum_{n=0}^{\omega_D/2\pi T} \frac{1}{2n+1} = \frac{1}{2} \left[\sum_{n=0}^{\infty} \frac{1}{n+1/2} - \sum_{n=1}^{\infty} \frac{1}{n+\omega_D/2\pi T} \right] \tag{4.1.12}$$

and by adding and subtracting a factor of $\sum_1^{\infty} 1/n$ this will become

$$\begin{aligned} \sum_{n=0}^{\omega_D/2\pi T} \frac{1}{2n+1} &= \frac{1}{2} \sum_{n=1}^{\infty} \left[\frac{-1}{n} + \frac{1}{n+1/2} \right] - \frac{1}{2} \sum_{n=1}^{\infty} \left[\frac{1}{n} - \frac{1}{n+\omega_D/2\pi T} \right] \\ &= \frac{1}{2} \left[\psi\left(\frac{\omega_D}{2\pi T} \right) - \psi\left(\frac{1}{2} \right) \right] \end{aligned} \tag{4.1.13}$$

This will give the full summation as

$$\Pi(Q, i\Omega) = N(0) \left[\psi\left(\frac{\omega_D}{2\pi T} \right) - \psi\left(\frac{1}{2} \right) - \frac{\pi|\Omega|}{8T} - \frac{7Q^2 v_F^2 \zeta(3)}{48\pi^2 T^2} \right] \tag{4.1.14}$$

Using the substitution $\psi(1/2) = -\gamma - 2\log 2$, $\psi(x) \approx \log(x)$ for large x and $2e^{\gamma}/\pi = 1.14$ the self-interaction can be rewritten as

$$\Pi(Q, i\Omega) = N(0)\left[\log\left(\frac{1.14\omega_D}{T}\right) - \frac{\pi|\Omega|}{8T} - \frac{7Q^2 v_F^2 \zeta(3)}{48\pi^2 T^2}\right] \tag{4.1.15}$$

Now that the self-interaction has been calculated, the electron-electron propagator can be constructed and any properties can be extracted. In the limit $Q, \Omega = 0$ the propagator can be written as

$$t(Q, i\Omega) = \frac{1}{1/V + N(0)\log(1.14\omega_D/T)} \tag{4.1.16}$$

This contains a pole at

$$-\frac{1}{N(0)V} = \log(1.14\omega_D/T) \tag{4.1.17}$$

This gives rise to a divergence in the electron-electron propagator at a critical temperature given by

$$T_c = 1.14\omega_D \exp[-1/N(0)V] \tag{4.1.18}$$

and the electron-electron propagator is given as

$$t(Q, i\omega) = \frac{1}{N(0)\left[\log\left(\frac{T}{T_c}\right) - \frac{\pi|\Omega|}{8T} - \frac{7Q^2 v_F^2 \zeta(3)}{48\pi^2 T^2}\right]} \tag{4.1.19}$$

This divergence suggests that at temperatures $T < T_c$ there is a correlation between electrons that have not been taken into account. The limit $Q = 0$ shows that the correlation exists between electrons with opposite momenta and the lowest en-

ergy for an s-wave potential will be from a spin-singlet state where the electrons have opposite spins. This correlation is more commonly denoted as Cooper pairing and is the signature of superconductivity.

As this Thesis is mainly concerned with dirty systems with impurities it seems inadequate to just consider the clean regime. Due to Anderson's theorem, it should be suggested that the introduction of impurities will not affect T_c but this will now be shown implicitly.

In the dirty limit the diagrams to calculate will be of the same form but with impurity scattering ladders as shown in figure 4.2.

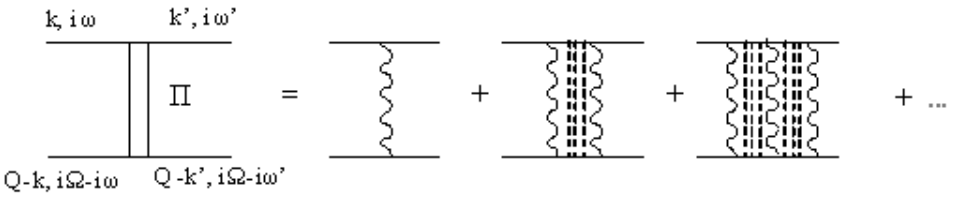

Figure 4.2 – The electron-electron propagator with an attractive interaction in the dirty limit.

The self interaction term is the impurity ladder which was calculated in chapter 3.4 which gives

$$\Pi(Q, i\Omega) = 2\pi N(0)T \sum_{\omega} \frac{1}{DQ^2 + |2\omega - \Omega|} \Theta(-\omega(\Omega - \omega)) \tag{4.1.20}$$

Imposing the constraints on ω and Ω this is given as

$$\Pi(Q, i\Omega) = 2\pi N(0)T \sum_{\omega} \frac{1}{DQ^2 + 2|\omega| + |\Omega|} \tag{4.1.21}$$

By substituting the matsubara frequency and by adding and subtracting a value

of $\sum 1/n + 1/2$ this can be written as

$$\Pi(Q, i\Omega) = N(0)\left[\sum_{n=0}^{\infty}\frac{1}{n+1/2} - \sum_{n=0}^{\infty}\frac{1}{n+1/2} + \sum_{n=0}^{\infty}\frac{1}{n+1/2+(DQ^2+|\Omega|)/4\pi T}\right]$$

As with the clean limit, the digamma function will be introduced and the following substitution will be used

$$\sum_{n=0}^{\infty}\left(\frac{1}{n+1/2+(DQ^2+|\Omega|)/4\pi T} - \frac{1}{n+1/2}\right) = \psi\left(\frac{1}{2}\right) - \psi\left(\frac{1}{2}+\frac{DQ^2+|\Omega|}{4\pi T}\right)$$

The remaining summation is divergent so the limits $\omega = 0 \to \omega_D/2\pi T$ will be imposed again. This will give the same contribution as the lowest order term in the clean case, and was derived above. This will give

$$\Pi(Q, i\Omega) = N(0)\left[\log\left(\frac{1.14\omega_D}{T}\right) + \psi\left(\frac{1}{2}\right) - \psi\left(\frac{1}{2}+\frac{DQ^2+|\Omega|}{4\pi T}\right)\right] \quad (4.1.22)$$

and the digamma functions can be simplified as

$$\begin{aligned}\psi\left(\frac{1}{2}\right) - \psi\left(\frac{1}{2}+A\right) &= \sum_{n=0}^{\infty}\left[\frac{1}{n} - \frac{1}{n+x+1/2}\right] - \sum_{n=0}^{\infty}\left[\frac{1}{n} - \frac{1}{n+1/2}\right] \\ &= \sum_{n=0}^{\infty}\left[\frac{1}{n+1/2} - \frac{1}{n+x+1/2}\right] \quad (4.1.23)\end{aligned}$$

In the limit $A \ll n$ this can be given as

$$\psi\left(\frac{1}{2}\right) - \psi\left(\frac{1}{2}+A\right) \approx \sum_{n=0}^{\infty}\frac{x}{(n+1/2)^2} = 3\zeta(3)A = \frac{\pi^2 x}{2} \quad (4.1.24)$$

Thus, the final result for the self interaction is

$$\Pi(Q, i\Omega) = N(0)\left[\log\left(\frac{T}{T_c}\right) + \frac{\pi^2(DQ^2 + |\Omega|)}{2}\right] \tag{4.1.25}$$

which gives the electron-electron propagator as

$$t(Q, i\omega) = \frac{1}{N(0)\left[\log\left(\frac{T}{T_c}\right) + \frac{\pi^2(DQ^2+|\Omega|)}{2}\right]} \tag{4.1.26}$$

As expected within the limits $Q, \omega = 0$ there is a divergence in the electron-electron propagator and this divergence is present at the same critical temperature as in the clean limit. The only difference in the clean to dirty limit is the coefficient of the Q^2 factor.

4.2 Superconducting Green's Functions

Superconductivity is described by an instability at the Fermi surface due to the creation of Cooper pairs which overcome the Coulomb repulsion [32]. Due to the Hamiltonian containing such terms as $c^\dagger_{k\uparrow}c^\dagger_{k\downarrow}$ and $c_{k\uparrow}c_{k\downarrow}$ one has to consider the off-diagonal terms $\langle\psi_\uparrow\psi_\downarrow\rangle$ and $\langle\psi^\dagger_\uparrow\psi^\dagger_\downarrow\rangle$ in the Green's function - producing the Nambu-Gorkov function [1] as

$$G = \left\langle (\psi_\uparrow, \psi^\dagger_\downarrow)\begin{pmatrix}\psi^\dagger_\uparrow \\ \psi_\downarrow\end{pmatrix}\right\rangle = \begin{pmatrix}\langle\psi_\uparrow\psi^\dagger_\uparrow\rangle & \langle\psi_\uparrow\psi\downarrow\rangle \\ \langle\psi^\dagger_\downarrow\psi^\dagger_\uparrow\rangle & \langle\psi^\dagger_\downarrow\psi_\downarrow\rangle\end{pmatrix} \tag{4.2.1}$$

The diagonal components are the usual Green's function and it's complex conjugate and the off-diagonal components are defined by the symbol Δ - which is

assumed to be real and the same for both off-diagonal components

$$G = \begin{pmatrix} \frac{1}{i\omega - \xi_k} & \Delta \\ \Delta & \frac{1}{i\omega + \xi_k} \end{pmatrix} \quad \text{if } T < T_c \tag{4.2.2}$$

$$= \begin{pmatrix} \frac{1}{i\omega - \xi_k} & 0 \\ 0 & \frac{1}{i\omega + \xi_k} \end{pmatrix} \quad \text{if } T < T_c \tag{4.2.3}$$

where ε corresponds to the Matsubara frequencies and ξ is the energy of the system $(\frac{k^2}{2m})$ [22]. Dyson's equation can be represented as

$$G = G_0 + G_0 \Sigma G \tag{4.2.4}$$

$$G^{-1} = G_0^{-1} - \Sigma \tag{4.2.5}$$

where G is the 'dressed' Green's function and G_0 is the bare Green's function - diagrammatically given in figure 4.3. Note that the matrices τ_0, τ_1, τ_3 correspond

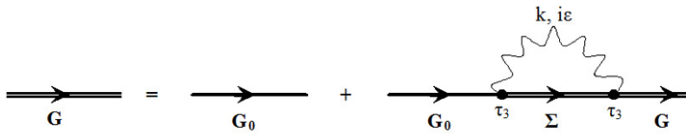

Figure 4.3 – This is the diagrammatic representation of the superconducting Green's function

to the 2x2 Pauli matrices

$$\tau_0 = \begin{pmatrix} 1 & 0 \\ 0 & 1 \end{pmatrix} \quad \tau_1 = \begin{pmatrix} 0 & 1 \\ 1 & 0 \end{pmatrix} \quad \tau_3 = \begin{pmatrix} 1 & 0 \\ 0 & -1 \end{pmatrix} \tag{4.2.6}$$

and can be used to construct the 2 by 2 Green's function. Using Dyson's equation and $\Sigma = \Delta\tau_1$ then:

$$G^{-1} = i\omega\tau_0 - \xi_k\tau_3 - \Delta\tau_1 \tag{4.2.7}$$

Diagrammatically one must determine the interaction vertex terms before proceeding any further. The interaction operator can be grouped as in two seperate ways

$$\psi_\uparrow^\dagger\psi_\uparrow + \psi_\downarrow^\dagger\psi_\downarrow = (\psi_\uparrow^\dagger, \psi_\downarrow) \begin{pmatrix} 1 & 0 \\ 0 & -1 \end{pmatrix} \begin{pmatrix} \psi_\uparrow \\ \psi_\downarrow^\dagger \end{pmatrix} \tag{4.2.8}$$

This means that each interaction vertex should be represented with the annotation of the pauli matrix τ_3. This and the diagrammatic rules determine that

$$\Sigma = -VT\sum_\omega\sum_k \tau_3 G(k, i\omega)\tau_3 \tag{4.2.9}$$

$$= -VT\sum_\omega\sum_k \frac{i\omega + \xi_k\tau_3 - \Delta\tau_1}{\xi_k^2 + \omega^2 + \Delta^2}; \tag{4.2.10}$$

note the change of signs due to the anti-commutation of the Pauli matricies. Using the usual substitution $\sum_k \to N(\omega_F)\int d\xi$ and by realising that the odd terms in ω and ξ will give a zero contribution one can write

$$\Sigma = VT\sum_\omega N(\omega_F)\int_{-\infty}^{\infty} d\xi \frac{\Delta\tau_1}{\xi_k^2 + \omega^2 + \Delta^2} \tag{4.2.11}$$

$$= VT\sum_\omega N(\omega_F)\frac{\pi\Delta\tau_1}{\sqrt{\omega^2 + \Delta^2}} \tag{4.2.12}$$

This proves that the ansatz $\Sigma = \Delta\tau_1$ was justified and can now be used to find the order parameter Δ. By equating the formula above with the ansatz and cancelling the $\Delta\tau_1$ terms one is left with

$$1 = VT\pi N(\omega_F) \sum_{\omega} \frac{1}{\sqrt{\omega^2 + \Delta^2}} \tag{4.2.13}$$

As usual one can write the summation as an integration at $T = 0$ with the Debye frequency as the limits of integration. Since the function is even then one can collapse the limits to $0 \rightarrow \omega_D$ and cancelling the factor of $1/2$ and by using simple trigonometry this integral can be performed to give

$$1 = N(0)V \sinh^{-1}\left(\frac{\omega_D}{\Delta}\right) \tag{4.2.14}$$

Rearranging and by realising that experimentally $1/N(0)V << 1$ one can equate the order parameter as

$$\Delta(T = 0) \approx 2\omega_D \exp\left(\frac{-1}{N(0)V}\right) \tag{4.2.15}$$

This correspond to the energy gap due to the superconducting transition. The Nambu-Gorkov operators have reproduced the same gap equation as that calculated via the *BCS Hamiltonian*. As in the Normal-State diagrams, the next step is to construct the superconducting Green's functions with impurities which induce a scattering time τ. This will be constructed in the next subsection before any diagrammatic calculations will be made.

4.3 Diagrams with impurities

To consider the Green's function for a superconductor with impurities one must use the same method as in the previous section but with an impurity scattering in addition to a phonon mediated interaction. To calculate such a Green's function one must use Dyson's equation with the diagrammatics shown in figure 4.4. The scattering potential V is assumed to be short ranged and gaussian. This means that $\langle V \rangle = 0$ and that the only contribution comes from pairs of scattering events with equal but oppsoite phase shifts. Using Pauli matrices one can deduce

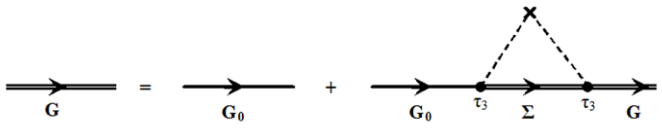

Figure 4.4 – Diagrammatic representation for the impurity scattered Green's function

$$G_0^{-1} = i\omega\tau_0 - \xi\tau_3 - \Delta\tau_1 \tag{4.3.1}$$

First one must make an ansatz for the self-energy Σ and check that it is consistent before calculating each term explicitly. The ansatz will be

$$\Sigma = i(\omega - \bar{\omega})\tau_0 - (\Delta - \bar{\Delta})\tau_1 \tag{4.3.2}$$

By using Dyson's equation $G^{-1} = G_0^{-1} - \Sigma$ and cancelling each term one is left with

$$G^{-1} = i\bar{\omega}\tau_0 - \xi\tau_3 - \bar{\Delta}\tau_1 \tag{4.3.3}$$

If one ignores any scattering that alters the state of the system, spin-flip scattering for example, then the only effect will be to inflict a scattering time τ given by Fermi's golden rule. Using this rule one can deduce that $n_i|u|^2 = \frac{1}{2\pi N(\omega_F)\tau}$ where u denotes the interaction potential. This causes the self-enegry term to become

$$\Sigma = \frac{1}{2\pi N(\omega_F)\tau}\sum_k \tau_3 G(k, i\omega)\tau_3 \tag{4.3.4}$$

$$= \frac{1}{2\pi\tau}\int d\xi \frac{i\bar{\omega}\tau_0 + \xi\tau_3 - \bar{\Delta}\tau_1}{-\bar{\omega}^2 - \xi^2 - \bar{\Delta}^2} \tag{4.3.5}$$

recalling that the τ_3 terms correspond to the interaction verticies. The second line is obtained by substituting in the dressed Green's function, multiplying by the denominator and commuting τ_3 - a similar calculation was performed rigorously in the previous section. The ξ-term in the numerator will give zero contribution due to the function being odd. The remaining terms can be solved using a *tanh* substitution. The integral can now be solved to give

$$\Sigma = -\frac{i\bar{\omega}\tau_0 - \bar{\Delta}\tau_1}{2\tau\sqrt{\bar{\omega}^2 + \bar{\Delta}^2}} \tag{4.3.6}$$

Substituting the ansatz for Σ one can compare the clean and dirty gap equation and Matsubara frequencies

$$\omega = \bar{\omega}\left(1 - \frac{1}{2\tau\sqrt{\bar{\omega}^2 + \bar{\Delta}^2}}\right) \tag{4.3.7}$$

$$\Delta = \bar{\Delta}\left(1 - \frac{1}{2\tau\sqrt{\bar{\omega}^2 + \bar{\Delta}^2}}\right) \tag{4.3.8}$$

This gives a very important result that

$$\frac{\bar{\omega}}{\bar{\Delta}} = \frac{\omega}{\Delta} \tag{4.3.9}$$

This implies that the critical temperature, T_c, and the gap equation, Δ, are the same for a dirty superconductor as a clean one - note that this is only true for impurities which do not effect the state of the system. This is known as Anderson's Theorem.

Now that the main properties of superconductivity have been reproduced using diagrammatics the next step is to construct the Drude conductivity and Weak localisation in the superconducting case. This will help to calculate the more complicated superconducting UCF diagrams and all the results will be used to construct a new, and more convenient, method to reproducing these calculations.

4.4 Drude Calculation

For full consistency, the electromagnetic response function for the Drude conductivity with impurities will be calculated. The current vertex is written as

$$\mathbf{k}\psi^{\dagger}_{k\uparrow}\psi_{k\uparrow} - \mathbf{k}\psi^{\dagger}_{-k\downarrow}\psi_{-k\downarrow} = \mathbf{k}\begin{pmatrix}\psi^{\dagger}_{k\uparrow} & \psi_{-k\downarrow}\end{pmatrix}\begin{pmatrix}1 & 0\\ 0 & 1\end{pmatrix}\begin{pmatrix}\psi_{k\uparrow}\\ \psi^{\dagger}_{-k\downarrow}\end{pmatrix} \tag{4.4.1}$$

so that each current vertex will contribute a matrix element τ_0. Perfoming the usual manipulations, the Drude conductivity diagram in the dirty limit becomes

$$K(Q = 0, i\Omega) = \frac{e^2 N(0) k_F}{3m^2} \int \mathrm{Tr}\Big[\frac{(i\bar{\omega} + \xi\tau_3 + \bar{\Delta}\tau_1)(i\bar{\omega} + i\Omega + \xi\tau_3 + \bar{\Delta}\tau_1)}{(\xi^2 + \overline{W}^2)(\xi^2 + \overline{W}_+^2)}\Big] \tag{4.4.2}$$

where $\overline{W}^2 = \bar{\Delta}^2 + \bar{\omega}^2$ and $\overline{W}_+^2 = \bar{\Delta}^2 + (\bar{\omega} + \Omega)^2$perfoming the integral will give

$$K(Q = 0, i\Omega) = \frac{e^2 N(0) k_F}{3m^2} T\Big[\frac{\pi(\overline{WW}_+ + \bar{\Delta}^2 - \bar{\omega}(\bar{\omega} + \Omega)}{\overline{WW}_+(\overline{W} + \overline{W}_+)}\Big] \tag{4.4.3}$$

Using the identities relating ω, $\Delta \to \bar{\omega}$, $\bar{\Delta}$ we can see that $(\overline{W} + \overline{W}_+) = 1/\tau$ which gives the final form of the response function as

$$K(Q = 0, i\Omega) = \frac{\pi e^2 N(0) k_F \tau}{m^2} T\Big[1 + \frac{\Delta^2 - \omega(\omega + \Omega)}{\sqrt{\Delta^2 + \omega^2}\sqrt{\Delta^2 + (\omega + \Omega)^2}}\Big] \tag{4.4.4}$$

The superconducting number density, n_s, can be calculated by taking the limit $\Omega = 0$

$$K(Q = 0, 0) = \frac{n_s e^2}{m} = \frac{2\pi n e^2 \tau}{m} T \sum_{\omega} \frac{\Delta^2}{\Delta^2 + \omega^2} \tag{4.4.5}$$

The summation over ω can be performed by transforming the contour as shown in figure 4.5. This will give

$$\sum_{\omega} \frac{\Delta^2}{\Delta^2 + \omega^2} = \int \frac{\Delta^2}{\Delta^2 - z^2} f(z) \frac{dz}{2\pi i} \tag{4.4.6}$$

The only contribution will come from the two poles either side of the imaginary axis, which can be calculated as

$$\int \frac{\Delta^2}{\Delta^2 - z^2} f(z) \frac{dz}{2\pi i} = \frac{\Delta}{2} \left[f(-\Delta/2T) - f(\Delta/2T)\right]$$

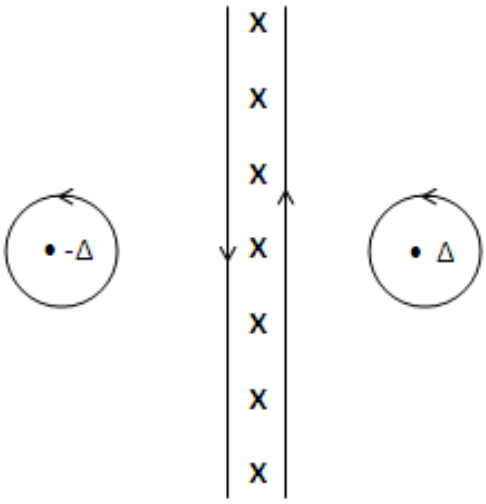

Figure 4.5 – A plot of the contour needed to calculate the superconducting Drude calculation. The poles are at $\pm\Delta$ and the Matsubara poles up the imaginary axis.

$$= \frac{\Delta}{2} \tanh\left(\Delta/2T\right) \tag{4.4.7}$$

This can now be used to calculate the n_s correction as

$$n_s = n\pi\Delta\tau \tanh\left(\Delta/2T\right) \tag{4.4.8}$$

4.5 Superconducting Ladder calculation

The superconducting ladder propagator is constructed as a direct product of two 2x2-matricies to give the 4x4-matrix $\Gamma_{\alpha\beta\gamma\delta}$. Using this together with figure 4.6 one

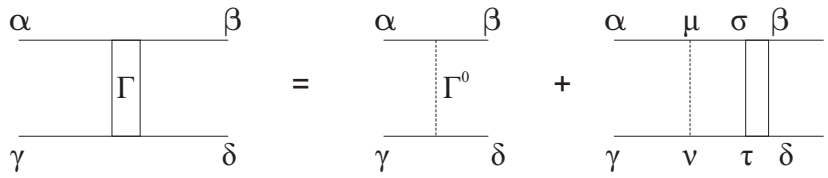

Figure 4.6 – The diagrammatic expansion of the superconducting ladder needed to calculate the correction due to weak localisation in the superconducting state.

can construct the superconducting Cooperon as

$$\Gamma_{\alpha\beta\gamma\delta} = \Gamma^0_{\alpha\beta\gamma\delta} + \Gamma_{\alpha\mu\gamma\nu}\Pi_{\mu\sigma\nu\tau}\Gamma_{\sigma\beta\tau\delta} \tag{4.5.1}$$

where

$$\Gamma^0_{\alpha\beta\gamma\delta} = \frac{1}{2\pi N(0)\tau}(\tau_3)_{\alpha\beta}(\tau_3)_{\gamma\delta} \tag{4.5.2}$$

and

$$\Pi_{\mu\sigma\nu\tau} = \sum_k G_{\mu\sigma}(k, i\bar{\omega})G_{\nu\tau}(Q-k, i\bar{\omega}' + i\Omega') \tag{4.5.3}$$

$$= N(0)\int \frac{(\bar{\omega}\tau_0 + \xi_k\tau_3 + \bar{\Delta}\tau_1)\otimes(\bar{\omega}'\tau_0 + \xi_{Q-k}\tau_3 + \bar{\Delta}'\tau_1)}{(\xi_k^2 + \overline{W}^2)(\xi_{Q-k}^2 + \overline{W}'^2)} \tag{4.5.4}$$

Note that $\otimes$ denotes the direct product given by

$$A\otimes B = \begin{pmatrix} A_{11} & A_{12} \\ A_{21} & A_{22} \end{pmatrix} \otimes \begin{pmatrix} B_{11} & B_{12} \\ B_{21} & B_{22} \end{pmatrix} = \begin{pmatrix} A_{11}B_{11} & A_{11}B_{12} & A_{12}B_{11} & A_{12}B_{12} \\ A_{11}B_{21} & A_{11}B_{22} & A_{12}B_{21} & A_{12}B_{22} \\ A_{21}B_{11} & A_{21}B_{12} & A_{22}B_{11} & A_{22}B_{12} \\ A_{21}B_{21} & A_{21}B_{22} & A_{22}B_{21} & A_{22}B_{22} \end{pmatrix}$$

Using the usual expansion $\xi_{Q-K} = \xi_k + Qv_F x = \xi_k + q$, together with the introduction of $\overline{W} = \sqrt{\bar{\Delta}^2 + \bar{\omega}^2}$ and $\overline{W}' = \sqrt{\bar{\Delta}'^2 + \bar{\omega}^2}$. The odd terms in ξ_k will give zero contribution when making the usual transformation $\sum_k \to N(0)\int d\xi_k$ giving

$$N(0)\int d\xi_k \frac{(\xi_k(\xi_k+q))\tau_3\otimes\tau_3 + (i\bar{\omega}+\bar{\Delta}\tau_1)\otimes(i\bar{\omega}'+\bar{\Delta}'\tau_1)}{(\xi_k^2+\overline{W}^2)(\xi_{Q-k}^2+\overline{W}'^2)} \tag{4.5.5}$$

as the only contribution. The integral can be performed by constructing the contour around two single order poles. The next step is to take the angular average by first performing partial fractions and then expanding to $\mathcal{O}(q^2)$, recalling that $\langle q\rangle = Qv_F\langle\cos\theta\rangle = 0$ and $\langle q^2\rangle = Q^2v_F^2/2$. This gives the final solution as

$$\Pi_{\mu\sigma\nu\tau} = 2\pi N(0)\tau I\left[\tau_3\otimes\tau_3 - \frac{(i\bar{\omega}+\bar{\Delta}\tau_1)\otimes(i\bar{\omega}'+\bar{\Delta}'\tau_1)}{\overline{W}\overline{W}'}\right] \tag{4.5.6}$$

where

$$I = \frac{1}{2\tau(\overline{W}+\overline{W}')}\left[1 - \frac{v_F^2\tau^2}{3(\overline{W}+\overline{W}')^2}\right] \tag{4.5.7}$$

Now that the self-energy has been calculated we must use this to construct the full superconducting ladder, given by

$$\Gamma = \Gamma^0 + \Gamma^0\Pi\Gamma^0 + \Gamma^0\Pi\Gamma^0\Pi\Gamma^0 + ... \tag{4.5.8}$$

The first term is simply given by

$$\Gamma^0 = \frac{1}{2\pi N(0)\tau}\tau_3\otimes\tau_3 \tag{4.5.9}$$

The second term is calculated as

$$\begin{aligned}\Gamma^0\Pi\Gamma^0 &= \frac{I}{2\pi N(0)\tau}\left[[\tau_3]\tau_3[\tau_3]\otimes[\tau_3]\tau_3[\tau_3]-\frac{[\tau_3](i\bar{\omega}+\bar{\Delta}\tau_1)[\tau_3]\otimes[\tau_3](i\bar{\omega}'+\bar{\Delta}'\tau_1)[\tau_3]}{\overline{WW}'}\right]\\ &= \frac{I}{2\pi N(0)\tau}\left[\tau_3\otimes\tau_3-\frac{(i\bar{\omega}-\bar{\Delta}\tau_1)\otimes(i\bar{\omega}'-\bar{\Delta}'\tau_1)}{\overline{WW}'}\right] \qquad (4.5.10)\end{aligned}$$

where the final step is constructed by commuting τ_3 and the minus sign is due to the anticommutation of τ_1 and τ_3. The next term in the expansion is $\Gamma^0\Pi\Gamma^0\Pi\Gamma^0$ and by using the result for $\Gamma^0\Pi\Gamma^0$ can be constructed as

$$\begin{aligned}\frac{I^2}{2\pi N(0)\tau}\Bigg[&\tau_3\tau_3\tau_3\otimes\tau_3\tau_3\tau_3-\frac{(i\bar{\omega}-\bar{\Delta}\tau_1)}{\overline{W}}\tau_3\tau_3\otimes\frac{(i\bar{\omega}'-\bar{\Delta}'\tau_1)}{\overline{W}'}\tau_3\tau_3\\ &-\tau_3\frac{(i\bar{\omega}+\bar{\Delta}\tau_1)}{\overline{W}}\tau_3\otimes\tau_3\frac{(i\bar{\omega}'+\bar{\Delta}'\tau_1)}{\overline{W}'}\tau_3\\ &+\frac{(i\bar{\omega}-\bar{\Delta}\tau_1)}{\overline{W}}\frac{(i\bar{\omega}+\bar{\Delta}\tau_1)}{\overline{W}}\tau_3\otimes\frac{(i\bar{\omega}-\bar{\Delta}\tau_1)}{\overline{W}}\frac{(i\bar{\omega}'+\bar{\Delta}'\tau_1)}{\overline{W}'}\tau_3\Bigg]\end{aligned}$$

Commuting and simplifying will give

$$\Gamma^0\Pi\Gamma^0\Pi\Gamma^0=\frac{2I^2}{2\pi N(0)\tau}\left[\tau_3\otimes\tau_3-\frac{(i\bar{\omega}-\bar{\Delta}\tau_1)\otimes(i\bar{\omega}'-\bar{\Delta}'\tau_1)}{\overline{WW}'}\right] \qquad (4.5.11)$$

The contribution from each term is the same except for the coefficient, which forms a geometric series. Due to the additional Γ^0 in the expansion of Γ the $\tau_3\otimes\tau_3$ coefficients become

$$1+I+2I^2+4I^3....=1+\frac{I}{1-2I}=\frac{1-I}{1-2I} \qquad (4.5.12)$$

and the coefficients of the term $(i\bar{\omega} - \bar{\Delta}\tau_1) \otimes (i\bar{\omega}' - \bar{\Delta}'\tau_1)$ becomes

$$I + 2I^2 + 4I^3.... = \frac{I}{1-2I} \tag{4.5.13}$$

These geometric series terms must be simplified in order to progress and to do so we must look back at the equations for $\bar{\omega}$ and $\bar{\Delta}$ in the dirty limit, and by squaring and adding them we have

$$\overline{W} + \overline{W}' = \sqrt{\omega^2 + \Delta^2} + \sqrt{\omega'^2 + \Delta'^2} + \frac{1}{\tau} = W + W' + \frac{1}{\tau} \tag{4.5.14}$$

Substituting this into the value for I and expanding to $\mathcal{O}(Q^2\tau)$ gives

$$I = \frac{1}{2}\Big[1 - (DQ^2 + \sqrt{\omega^2 + \Delta^2} + \sqrt{\omega'^2 + \Delta'^2})\tau\Big] \tag{4.5.15}$$

To first order this will give

$$I = \frac{1}{2} \tag{4.5.16}$$

and also

$$1 - 2I = (DQ^2 + \sqrt{\omega^2 + \Delta^2} + \sqrt{\omega'^2 + \Delta'^2})\tau \tag{4.5.17}$$

Combining these two equations will give

$$\frac{I}{1-2I} = \frac{1-I}{1-2I} = \frac{1}{2(DQ^2 + \sqrt{\omega^2 + \Delta^2} + \sqrt{\omega'^2 + \Delta'^2})\tau} \tag{4.5.18}$$

Gathering all terms together and simplifying will give the final superconducting ladder as

$$\Gamma \quad = \quad \frac{1}{4\pi N(0)\tau^2}\frac{1}{DQ^2+W+W_+}\left[\tau_3\otimes\tau_3-\frac{(i\omega\tau_0-\Delta\tau_1)\otimes(i\omega'\tau_0-\delta'\tau_1)}{\overline{WW}'}\right] \tag{4.5.19}$$

4.6 Weak Localisation calculation

We derived the 4×4-matrix superconducting ladder, $\Gamma_{\alpha\beta\gamma\delta}$, in a previous chapter and found that the infinite summation simplified down to a basic geometric series. This helped to construct the full superconducting ladder as

$$\Gamma=\frac{1}{4\pi N(0)\tau^2}\frac{1}{DQ^2+W+W_+}\left[\tau_3\otimes\tau_3-\frac{(i\bar{\omega}\tau_0-\bar{\Delta}\tau_1)\otimes(i(\bar{\omega}+\Omega)\tau_0-\bar{\Delta}\tau_1)}{\overline{WW}_+}\right] \tag{4.6.1}$$

This can be used to calulate the superconducting number density, n_s, correction to *weak localisation*, shown in figure 4.7. Once again, the main contribution outside of the superconducting ladder comes from $Q\to0$.

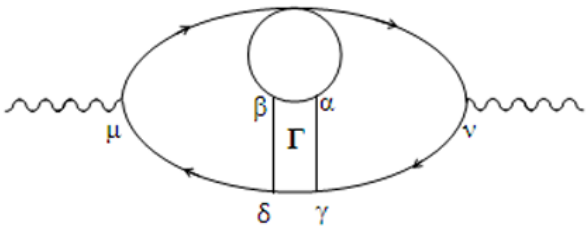

Figure 4.7 – The diagrammatic representation of weak localisation in the superconducting state together with the tensor form of the propagating ladder.

The electromagnetic response kernel is then written as

$$K(0,i\Omega) = \frac{-e^2k_F^2}{3m^2}T\sum_{\bar{\omega},Q}\sum_{k}(G_k)_{\mu\alpha}(G_k)_{\beta\nu}(G'_k)_{\nu\gamma}(G'_k)_{\delta\mu}\Gamma_{\alpha\beta\gamma\delta} \tag{4.6.2}$$

where $G_k = G(k, i\bar{\omega} + i\Omega)$ and $G'_k = G(k, i\bar{\omega})$. Substituting in the expression for Γ, making sure to operate the ladder verticies corectly, one is left to calculate

$$\begin{aligned} K(0,i\Omega) &= \frac{-e^2k_F^2}{3m^2}T\left[\frac{1}{4\pi N(0)\tau^2}\frac{1}{DQ^2 + W + W_+}\right] \\ &\times\sum_{\bar{\omega},Q}\sum_{k}\left[Tr\{G_k\tau_3G_kG'_k\tau_3G'_k\} - \frac{1}{\overline{WW}_+}Tr\{G_k(i\bar{\omega} - \bar{\Delta}\tau_1)G_kG'_k(\bar{\omega} - \bar{\Delta}\tau_1)G'_k\}\right] \end{aligned} \tag{4.6.3}$$

One must now perform the k-sums seperately

$$\sum_{k} Tr\{G_k\tau_3G_kG'_k\tau_3G'_k\} \tag{4.6.4}$$

This summation contains the two terms $G_k\tau_3G_k$ and $G'_k\tau_3G'_k$ for which τ_3 needs to commute. The Pauli commutation rule state that $\tau_\alpha\tau_\beta = i\epsilon_{\alpha\beta\gamma}\tau_\gamma$ suggesting that if two τ_3s were present in each term in the summation, then the commutation will give back the same Pauli matrix (with only a possible minus sign difference). This will simplify the calculations and will cause the summation to remain the same, to a possible prefactor of -1. One can now commute τ_3 through each term in this summation

$$\begin{aligned} G_k\tau_3G_k &= \frac{i\bar{\omega} + \xi_k\tau_3 + \bar{\Delta}\tau_1}{\xi_k^2 + \bar{\omega}^2 + \bar{\Delta}^2}\tau_3\frac{i\bar{\omega} + \xi_k\tau_3 + \bar{\Delta}\tau_1}{\xi_k^2 + \bar{\omega}^2 + \bar{\Delta}^2} \\ &= \tau_3\frac{(i\bar{\omega} + \xi_k\tau_3 - \bar{\Delta}\tau_1)(i\bar{\omega} + \xi_k\tau_3 + \bar{\Delta}\tau_1)}{(\xi_k^2 + \overline{W}^2)^2} \\ &= \tau_3\frac{(-\omega^2 + \xi^2 - \Delta^2) + 2i\omega\xi_k\tau_3 + 2i\Delta\xi_k\tau_2}{(\xi_k^2 + \overline{W}^2)^2} \end{aligned}$$

$$= \tau_3 \frac{(\xi^2 - \overline{W}^2) + 2i\Delta\xi_k\tau_2 + 2i\omega\xi_k\tau_3}{(\xi_k^2 + \overline{W}^2)^2}$$

and

$$G'_k\tau_3 G'_k = \tau_3 \frac{(\xi^2 - \overline{W}'^2) + 2i\Delta'\xi_k\tau_2 + 2i\omega'\xi_k\tau_3}{(\xi_k^2 + \overline{W}'^2)^2}$$

The original summation is a product of these two terms, and by commuting the τ_3 term through, can be written as

$$\begin{aligned} &\tau_3 \frac{(\xi^2 - \overline{W}^2) + 2i\Delta\xi_k\tau_2 + 2i\omega\xi_k\tau_3}{(\xi_k^2 + \overline{W}^2)^2} \tau_3 \frac{(\xi^2 - \overline{W}'^2) + 2i\Delta'\xi_k\tau_2 + 2i\omega'\xi_k\tau_3}{(\xi_k^2 + \overline{W}'^2)^2} \\ &= \frac{(\xi^2 - \overline{W}^2) - 2i\Delta\xi_k\tau_2 + 2i\omega\xi_k\tau_3}{(\xi_k^2 + \overline{W}^2)^2} \frac{(\xi^2 - \overline{W}'^2) + 2i\Delta'\xi_k\tau_2 + 2i\omega'\xi_k\tau_3}{(\xi_k^2 + \overline{W}'^2)^2} \end{aligned} \quad (4.6.5)$$

The trace will be taken and the usual substitution $\sum_k \to 2N(0)\int d\xi$ will be taken. The only contribution will come from terms even in ξ which gives

$$\begin{aligned} \sum_k \mathrm{Tr}\{G_k\tau_3 G_k G'_k\tau_3 G'_k\} &= 2N(0)\int d\xi \frac{(\xi^2 - \overline{W}^2)(\xi^2 - \overline{W}'^2)}{(\xi^2 + X^2)^2(\xi^2 + X'^2)^2} - \frac{4\xi_k^2(\bar{\Delta}\bar{\Delta}' - \bar{\omega}\bar{\omega}')}{(\xi^2 + \overline{W}^2)^2(\xi^2 + \overline{W}'^2)^2} \\ &= 2N(0)\int d\xi \frac{1}{(\xi^2 + X^2)(\xi^2 + X'^2)} - \frac{2\xi_k^2(2\bar{\Delta}\bar{\Delta}' - 2\bar{\omega}\bar{\omega}' + \overline{W}^2 + \overline{W}'^2)}{(\xi^2 + \overline{W}^2)^2(\xi^2 + \overline{W}'^2)^2} \end{aligned}$$

where $\overline{W} = \sqrt{\bar{\omega}^2 + \bar{\Delta}^2}$, $\overline{W}' = \sqrt{\bar{\omega}'^2 + \bar{\Delta}'^2}$. The two integrals will now be taken separately. The second term can be simplified by differentiating under the integral sign, which will reduce the integral into a sum of two single order poles as oppose to two second order poles. The simplification is

$$\int d\xi \frac{2\xi_k^2(2\bar{\Delta}\bar{\Delta}' - 2\bar{\omega}\bar{\omega}' + \overline{W}^2 + \overline{W}'^2)}{(\xi^2 + \overline{W}^2)^2(\xi^2 + \overline{W}'^2)^2} = \frac{\partial}{\partial X'^2}\frac{\partial}{\partial X^2}\int d\xi \frac{2\xi_k^2(2\bar{\Delta}\bar{\Delta}' - 2\bar{\omega}\bar{\omega}' + \overline{W}^2 + \overline{W}'^2)}{(\xi^2 + \overline{W}^2)(\xi^2 + \overline{W}'^2)} \tag{4.6.6}$$

This can be solved using the residue theorem with the poles at $\xi = i\overline{W}$ and $\xi = i\overline{W}'$ which will give

$$\frac{\pi(2\bar{\Delta}\bar{\Delta}' - 2\bar{\omega}\bar{\omega}' + \overline{W}^2 + \overline{W}'^2)}{\overline{W} + \overline{W}'} \tag{4.6.7}$$

The second term will become,

$$\frac{\partial}{\partial X'^2}\frac{\partial}{\partial X^2}\frac{\pi 2\xi_k^2(2\bar{\Delta}\bar{\Delta}' - 2\bar{\omega}\bar{\omega}' + \overline{W}^2 + \overline{W}'^2)}{\overline{W} + \overline{W}'}$$

$$= \frac{1}{4\overline{W}\overline{W}'}\frac{\partial}{\partial \overline{W}'}\frac{\partial}{\partial \overline{W}}\frac{\pi 2\xi_k^2(2\bar{\Delta}\bar{\Delta}' - 2\bar{\omega}\bar{\omega}' + \overline{W}^2 + \overline{W}'^2)}{\overline{W} + \overline{W}'}$$

$$= -\frac{\pi 2\xi_k^2(2\bar{\Delta}\bar{\Delta}' - 2\bar{\omega}\bar{\omega}' + \overline{W}^2 + \overline{W}'^2)}{2\overline{W}\overline{W}'(\overline{W} + \overline{W}')^3}$$

The first term will now be evaluated using partial fractions

$$\int d\xi \frac{1}{(\xi^2 + \overline{W}^2)(\xi^2 + \overline{W}'^2)} = \int d\xi \frac{1}{(\overline{W}^2 - \overline{W}'^2)}\Big[\frac{1}{\xi^2 + \overline{W}'^2} - \frac{1}{\xi^2 + \overline{W}^2}\Big] \tag{4.6.8}$$

which can be solved in the UHP as

$$-\frac{\pi}{\overline{W}\overline{W}'(\overline{W} + \overline{W}')} \tag{4.6.9}$$

Next we must calculate the term

$$\sum_k Tr\{G(i\bar{\omega}-\bar{\Delta}\tau_1)GG'(i\bar{\omega}'-\bar{\Delta}'\tau_1)G'\} \tag{4.6.10}$$

The aim is to commute the $(i\bar{\omega}-\bar{\Delta}\tau_1)$ terms passed the Green's functions so that we can eliminate then from the summation, since they are independent on k. To do this we note that we must commute through the numerator of the Green's function. The first step is to recognise that $\tau_3\tau_1=-\tau_1\tau_3$ which gives

$$\begin{aligned}(i\bar{\omega}+\bar{\Delta}\tau_1+\xi\tau_3)(i\bar{\omega}-\bar{\Delta}\tau_1) &= (i\bar{\omega}+\bar{\Delta}\tau_1)(i\bar{\omega}-\bar{\Delta}\tau_1+\xi\tau_3)\\ &= (i\bar{\omega}+\bar{\Delta}\tau_1)\tau_3(i\bar{\omega}+\bar{\Delta}\tau_1+\xi\tau_3)\tau_3 \end{aligned}\tag{4.6.11}$$

which implies that

$$G(i\bar{\omega}-\bar{\Delta}\tau_1)=(i\bar{\omega}+\bar{\Delta}\tau_1)\tau_3G\tau_3 \tag{4.6.12}$$

Similarly

$$(i\bar{\omega}'-\bar{\Delta}'\tau_1)G'=\tau_3G'\tau_3(i\bar{\omega}'+\bar{\Delta}'\tau_1) \tag{4.6.13}$$

Hence $\sum_k G(i\omega-\Delta\tau_1)GG'(i\omega-\Delta'\tau_1)G'$ now becomes

$$\begin{aligned}&(i\bar{\omega}+\bar{\Delta}\tau_1)\Big[\sum_k G_k\tau_3G_kG'_k\tau_3G'_k\Big](i\bar{\omega}'+\bar{\Delta}'\tau_1)\\ &=\frac{-2\pi}{\overline{WW'}(\overline{W}+\overline{W}')^3}\Big[(\bar{\omega}\bar{\omega}'-\bar{\Delta}\bar{\Delta}')-\overline{WW'}+i(\bar{\omega}\bar{\Delta}'+\bar{\omega}'\bar{\Delta})\tau_1\Big]\Big[(\bar{\Delta}\bar{\Delta}'-\bar{\omega}\bar{\omega}')+i(\bar{\omega}\bar{\Delta}'+\bar{\omega}'\bar{\Delta})\tau_1\Big]\end{aligned}$$

And so

$$\sum_k Tr\{G(i\bar{\omega}-\bar{\Delta}\tau_1)GG'(i\bar{\omega}-\bar{\Delta}'\tau_1)G'\} = \frac{-4\pi}{(\overline{W}+\overline{W}')^3}\Big(\overline{WW}'+\bar{\omega}\bar{\omega}'-\bar{\Delta}\bar{\Delta}'\Big) \tag{4.6.14}$$

Therefore the full electromagnetic response function becomes,

$$K(0,i\Omega) = \frac{-e^2k_F^2}{3m^2}T\left[\frac{1}{4\pi N(0)\tau^2}\frac{1}{DQ^2+W+W'}\right]$$
$$\times\sum_{\bar{\omega},Q} -\frac{4\pi N(0)}{\overline{WW}'(\overline{W}+\overline{W}')^3}\Big[-\overline{WW}'+(\bar{\omega}\bar{\omega}'-\bar{\Delta}\bar{\Delta}')\Big]-\frac{1}{\overline{WW}'}\frac{-4\pi N(0)}{(\overline{W}+\overline{W}')^3}\Big(-\overline{WW}'+\bar{\omega}\bar{\omega}'-\bar{\Delta}\bar{\Delta}'\Big) \tag{4.6.15}$$

These two terms give the same contribution, and setting $\overline{W}+\overline{W}'=1/\tau$ we get

$$\begin{aligned} K(0,i\Omega) &= \frac{-e^2k_F^2}{3m^2}T\sum_{\bar{\omega},Q}\left[\frac{1}{4\pi N(0)\tau^2}\frac{1}{DQ^2+W+W'}\right] \\ &\qquad\times\Big(\frac{-8\pi N(0)}{\overline{WW}'(\overline{W}+\overline{W}')^3}(-\overline{WW}'+\bar{\omega}\bar{\omega}'-\bar{\Delta}\bar{\Delta}')\Big) \\ &= \frac{-2e^2k_F^2\tau^3}{3m^2}T\sum_{\bar{\omega},Q}\frac{1}{DQ^2+W+W'}\Big[1+\frac{\bar{\Delta}\bar{\Delta}'-\bar{\omega}\bar{\omega}'}{\overline{WW}'}\Big] \end{aligned}$$

Using the diffusion constant $D=\frac{k_F^2\tau^3}{3m^2}$ and $\bar{\omega}'=\bar{\omega}+\Omega$ gives the final solution as

$$K(0,i\Omega) = -2De^2T\sum_{\bar{\omega},Q}\frac{1}{DQ^2+W+W'}\Big(1+\frac{\bar{\Delta}^2-\bar{\omega}(\bar{\omega}+\Omega)}{\overline{WW}'}\Big) \tag{4.6.16}$$

Chapter 5

NORMAL-STATE UCF

5.1 AC UCF calculation

In this section we will derive the first ,second and third order contributions to the conductance fluctuation calculations; which corresponds to the presence of two, three and four propagating ladders respectively. Before proceeding with any calculations, one must construct the leading diagrams corresponding to these conductance fluctuations together with any multiplicity factors. The variance is the physical property concerned here and is defined by

$$\mathrm{Var}(G) = \langle G - \langle G \rangle \rangle^2 \tag{5.1.1}$$

where G is the conductance which, diagrammatically, corresponds a single conduction bubble with the non-averaged impurity scatterings, shown in figure 5.1. The diagram to calculate the variance will consist of the combination of two conduction bubbles shown in figure 5.2 The only non-zero contribution to the variance will be when the impurity averaging causes the impurity lines to connect both conduction bubbles (due to the subtraction of the square of the average conductance).

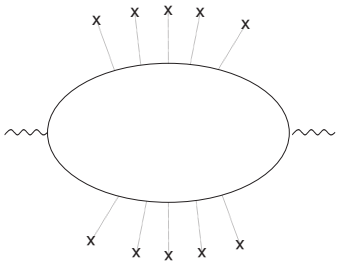

Figure 5.1 – The non impurity averaged Drude conductivity bubble in the dirty regime.

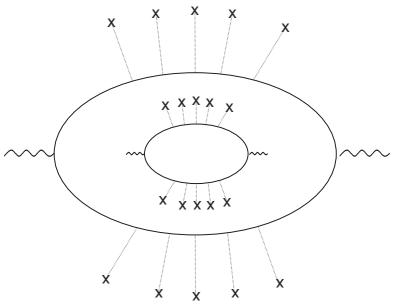

Figure 5.2 – An example of the term which is present in calculating the variance.

Recalling that the overall contribution will reduce by a factor of at least $(k_F l)^{-1}$ if the impurity lines cross which means that they can can be ignored. The diagrams together with their Hikami representation and multiplicity [29] are shown in figure 5.3 The first two diagrams have only a small contribution and do not need to be evaluated. The remaining diagrams will be calculated individually in the following subsections to find both the Normal-state and Superconducting-state contributions to the mesoscopic conductance fluctuations.

5.1.1 2 ladder calculation

The electomagnetic response function for two propagating ladders will be of the form

$$K = \left(\frac{e}{2m}\right)^4 T \sum_{\omega,\omega'} \sum_{k,k'} \sum_{Q} k_\alpha k_\beta [G^+(k)G^-(k-Q)]^2 [G^+(k')G^-(k'+Q)]^2 \Gamma(\omega'+\Omega', \omega)\Gamma(\omega+\Omega, \omega') \tag{5.1.2}$$

where the propagating ladders are defined as

$$\Gamma = \frac{1}{2\pi N(0)\tau^2} \frac{1}{DQ^2 + |\Omega|} \Theta(-\omega(\omega + \Omega)) \tag{5.1.3}$$

The next step is to calculate the contribution from the momentum summations, k, together with the coefficients from the diffusion terms. For ease, the two diffusion diagrams can be re-written in Hikami representation, shown in figure 5.4. Assuming the largest contribution comes when $Q \to 0$ outside of the propagating ladders then the electromagnetic response function will be of the form

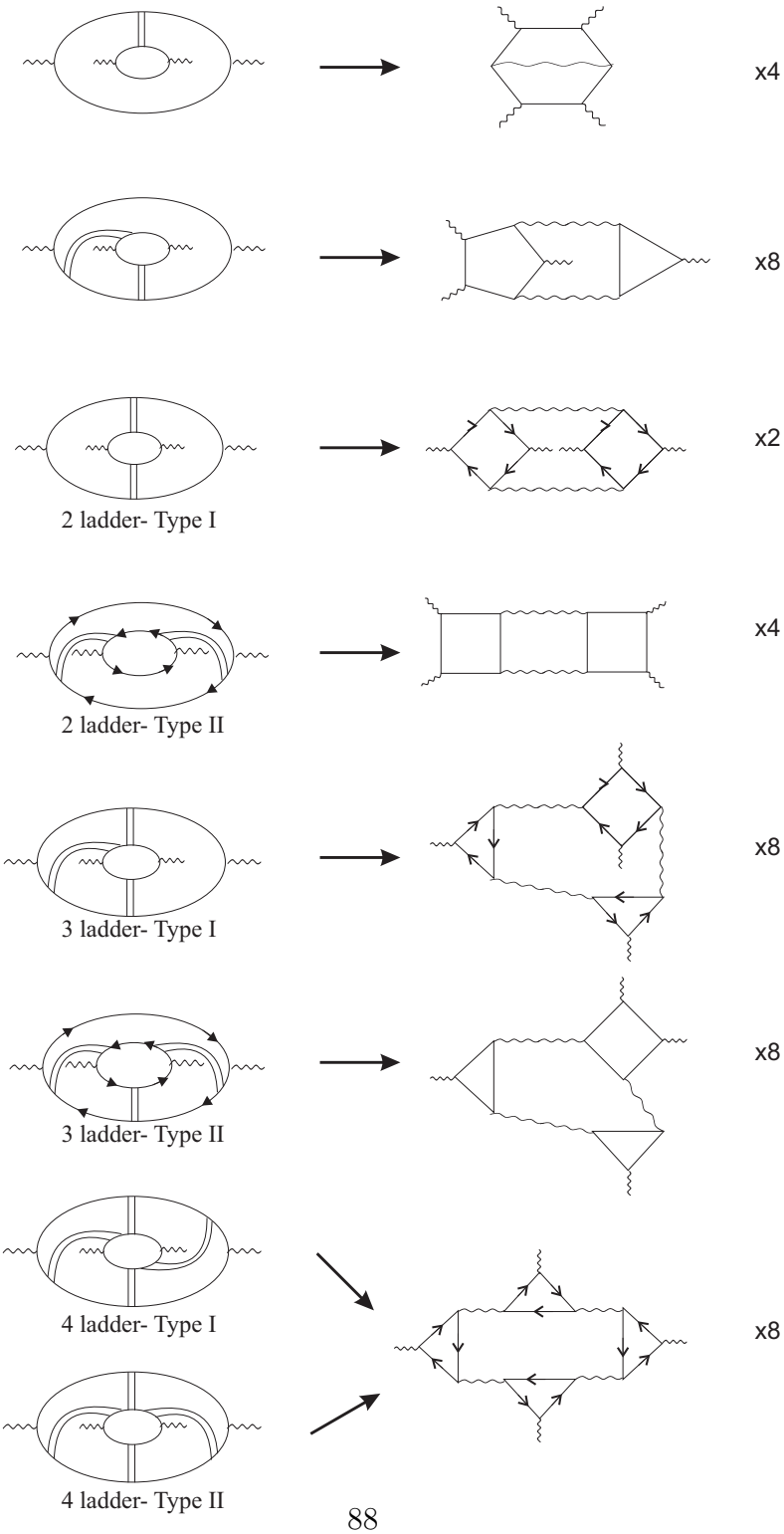
x4
x8
x2
2 ladder- Type I
x4
2 ladder- Type II
x8
3 ladder- Type I
x8
3 ladder- Type II
x8
4 ladder- Type I
4 ladder- Type II

Figure 5.3

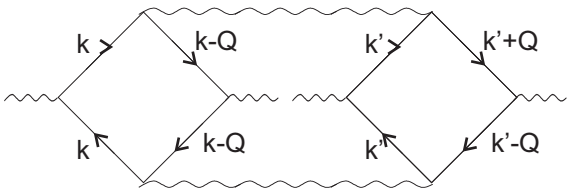

Figure 5.4 – The Hikami box representation of the 2 ladder UCF calculation.

$$K = 2^2 \sum_{kk'} T \sum_{\omega} T \sum_{\omega'} \sum_{Q} \left(\frac{ek_\alpha}{m}\right)\left(\frac{ek'_\beta}{m}\right)\left(\frac{ek_\gamma}{m}\right)\left(\frac{ek'_\delta}{m}\right)$$
$$\times G^2_+(k,\omega+\Omega)G^2_-(k,\omega)G^2_+(k',\omega'+\Omega')G^2_-(k',\omega')\Gamma(\omega',\omega+\Omega)\Gamma(\omega'+\Omega',\omega)$$

Contracting on the current indicies and integrating out the Green's function as

$$N(0)\int d\xi [G^-]^m[G^+]^n = 2\pi N(0)\tau \begin{pmatrix} m+n-2 \\ m-1 \end{pmatrix} (-i\tau)^{m-1}(i\tau)^{n-1} \qquad (5.1.4)$$

which is proved in Appendix (A) this takes the form

$$K \;=\; 4\left(\frac{e^4 v_F^4}{d^2}\right)\delta_{\alpha\gamma}\delta_{\beta\delta}(4\pi N(0)\tau^3)^2 \sum_{Q} T \sum_{\omega} T \sum_{\omega'} \Gamma(\omega',\omega+\Omega)\Gamma(\omega'+\Omega',\omega) \qquad (5.1.5)$$

The heaviside functions in each of the ladder propagators causes a set of four different inequalities for the Fermion and Boson frequencies given by

$$\omega > 0 \quad \omega+\Omega > 0 \quad \omega' < 0 \quad \omega'+\Omega' < 0 \qquad (5.1.6)$$

$$\omega > 0 \quad \omega+\Omega < 0 \quad \omega' > 0 \quad \omega'+\Omega' < 0 \qquad (5.1.7)$$

$$\omega < 0 \quad \omega + \Omega > 0 \quad \omega' < 0 \quad \omega' + \Omega' > 0 \tag{5.1.8}$$

$$\omega < 0 \quad \omega + \Omega < 0 \quad \omega' > 0 \quad \omega' + \Omega' > 0 \tag{5.1.9}$$

Equation (5.1.7), in this case, can be ignored as it corresponds to negative Boson frequencys Ω and Ω' which means that the inequalities (5.1.6),(5.1.8) and (5.1.9) need only be considered. Given the inequality (5.1.6) this will give

$$\Gamma(\omega', \omega+\Omega)\Gamma(\omega'+\Omega', \omega) \propto T\sum_{\omega>0} T \sum_{\omega'<-\Omega'} \frac{1}{DQ^2 + \omega + \Omega - \omega'} \frac{1}{DQ^2 + \omega - \omega' - \Omega'} \tag{5.1.10}$$

For consistency the limits on the summations should be transformed using the substitution $\omega' \to -(\omega' + \Omega')$ to give the final solution as

$$\Gamma(\omega', \omega+\Omega)\Gamma(\omega'+\Omega', \omega) \propto T\sum_{\omega>0} T \sum_{\omega'>0} \frac{1}{DQ^2 + \omega + \omega'} \frac{1}{DQ^2 + \omega + \Omega' + \omega' + \Omega'} \tag{5.1.11}$$

The inequality (5.1.9) will give the same contribution as (5.1.6) but the contribution from inequality (5.1.8) is more complicated and will be shown rigorously.

$$\begin{aligned}\Gamma(\omega', \omega+\Omega)\Gamma(\omega'+\Omega', \omega) &\propto T \sum_{0>\omega>\Omega} T \sum_{0>\omega'>\Omega'} \frac{1}{DQ^2 + \omega + \Omega - \omega'} \frac{1}{DQ^2 - \omega + \omega' + \Omega'} \\ &\propto T \sum_{0<\omega<\Omega} T \sum_{0<\omega'<\Omega'} \frac{1}{DQ^2 - \omega + \Omega + \omega'} \frac{1}{DQ^2 + \omega - \omega' + \Omega'}\end{aligned}$$

Using partial fractions this can be written as

$$\frac{1}{2DQ^2 + \Omega + \Omega'} T \sum_{0<\omega<\Omega} T \sum_{0<\omega'<\Omega'} \Big[\frac{1}{DQ^2 - \omega + \Omega + \omega'} + \frac{1}{DQ^2 + \omega - \omega' + \Omega'}\Big]$$

Making the substitution $\Omega - \omega \to \omega$ and $\Omega' - \omega' \to \omega'$ and equating will give

$$\frac{2}{2DQ^2+\Omega+\Omega'} T \sum_{0<\omega<\Omega} T \sum_{0<\omega'<\Omega'} \frac{1}{DQ^2+\omega+\omega'} \tag{5.1.12}$$

For consistency the limits of the summation need to be transformed which will generate

$$\frac{2}{2DQ^2+\Omega+\Omega'} T \sum_{\omega>0} T \sum_{\omega'>0} \Big[\frac{1}{DQ^2+\omega+\omega'} - \frac{1}{DQ^2+\omega+\Omega+\omega'} - \frac{1}{DQ^2+\omega+\omega'+\Omega'} + \frac{1}{DQ^2+\omega+\Omega+\omega'+\Omega'} \Big] \tag{5.1.13}$$

To construct the full 2 ladder type-I contribution then we also need to be consider the inequalities

$$\omega, \omega+\Omega > 0 \quad \omega', \omega'-\Omega' < 0 \tag{5.1.14}$$

$$\omega, \omega+\Omega < 0 \quad \omega', \omega'-\Omega' > 0 \tag{5.1.15}$$

which will give the same result as

$$T \sum_{\omega>0} T \sum_{\omega'>0} \frac{1}{DQ^2+\omega+\Omega+\omega'} \frac{1}{DQ^2+\omega+\omega'+\Omega'} \tag{5.1.16}$$

Therefore the full 2 ladder Type-I contribution will be of the form

$$\begin{aligned} K &= 16e^4 D^2 \delta_{\alpha\gamma}\delta_{\beta\delta} \sum_Q \frac{2}{2DQ^2+\Omega+\Omega'} T \sum_{\omega>0} T \sum_{\omega'>0} \Big[\frac{1}{DQ^2+\omega+\omega'} \\ &\quad - \frac{1}{DQ^2+\omega+\Omega+\omega'} - \frac{1}{DQ^2+\omega+\omega'+\Omega'} + \frac{1}{DQ^2+\omega+\Omega+\omega'+\Omega'} \Big] \end{aligned}$$

$$+ \quad 16e^4D^2\delta_{\alpha\delta}\delta_{\beta\gamma}\sum_Q T\sum_{\omega>0} T\sum_{\omega'>0}\frac{2}{DQ^2+\omega+\omega'}\frac{1}{DQ^2+\omega+\Omega+\omega'+\Omega'}$$

$$+ \quad 16e^4D^2\delta_{\alpha\delta}\delta_{\beta\gamma}\sum_Q T\sum_{\omega>0} T\sum_{\omega'>0}\frac{1}{DQ^2+\omega+\Omega+\omega'}\frac{1}{DQ^2+\omega+\omega'+\Omega'} \tag{5.1.17}$$

5.1.2 2 ladder-Type II

The next diagram to calculate is once again shown in figure (5.3) and frequency inequalities will be

$$\omega<0 \quad \omega+\Omega>0 \quad \omega'>0 \quad \omega'+\Omega'>0 \tag{5.1.18}$$

$$\omega<0 \quad \omega+\Omega<0 \quad \omega'>0 \quad \omega'+\Omega'>0 \tag{5.1.19}$$

$$\omega>0 \quad \omega+\Omega>0 \quad \omega'<0 \quad \omega'+\Omega'<0 \tag{5.1.20}$$

$$\omega>0 \quad \omega+\Omega>0 \quad \omega'<0 \quad \omega'+\Omega'>0 \tag{5.1.21}$$

Each of the two Hikami boxes will contribute a factor of $2\pi N(0)\tau^3$ but the correct prefactor must be evaluated for each frequency combination. This is due to the fact that adding an extra impurity line at certain positions will contribute to leading order; the extra Hikami box will contribute an extra factor of $2\pi N(0)\tau$ which will cancel with the impurity line contribution of $1/2\pi N(0)\tau$. To emphasise this point the contribution from the first inequality will be rigorously calculated, and the results for the remaining factors will be stated in sequential order. Integrating out the Green's functions and contracting on the current verticies will give the general

contribution of

$$K = 8\left(\frac{e^4 v_F^4}{d^2}\right)\delta_{\alpha\beta}\delta_{\gamma\delta}(2\pi N(0)\tau^3)^2 \sum_Q T\sum_\omega T\sum_{\omega'}\Gamma(\omega',\omega)\Gamma(\omega',\omega) \quad (5.1.22)$$

The inequality (5.1.18) has leading order contributions with Hikami representation shown in figure 5.5 The overall factor will need to be calculated for each of the

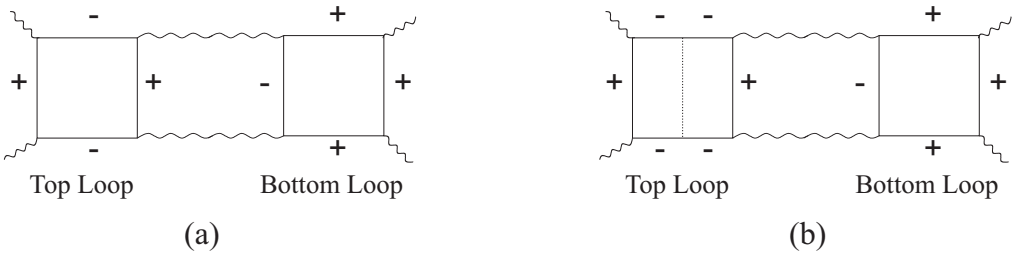

Figure 5.5 – (a) The Hikami representation of the 2 ladder Type-II contribution. (b) includes an additional non-crossing impurity scatterer which will give a diagram of the same order as (a)

two leading order representations using the formula

$$N(0)\int d\xi [G^-]^m [G^+]^n = 2\pi N(0)\tau \begin{pmatrix} m+n-2 \\ m-1 \end{pmatrix} (-i\tau)^{m-1}(i\tau)^{n-1} \quad (5.1.23)$$

The top loop from figure 5.5(a) will give a factor of

$$2\pi N(0)\tau \begin{pmatrix} 2 \\ 1 \end{pmatrix} (-i\tau)(i\tau) = 2 \times [2\pi N(0)\tau^3] \quad (5.1.24)$$

and the bottom loop will give a factor of

$$2\pi N(0)\tau \begin{pmatrix} 2 \\ 0 \end{pmatrix} (-i\tau)^0 (i\tau)^2 = -1 \times [2\pi N(0)\tau^3] \tag{5.1.25}$$

The top loop from figure 5.5(b) is slightly different due to there being two 'seperate' components either side of the single impurity line. Including the factor of $1/2\pi N(0)\tau$ from the single impurity line, this will give a factor of

$$\frac{(2\pi N(0)\tau)^2}{2\pi N(0)\tau} \begin{pmatrix} 1 \\ 1 \end{pmatrix} \begin{pmatrix} 1 \\ 1 \end{pmatrix} (-i\tau)^{1+1} (i\tau)^{0+0} = -1 \times [2\pi N(0)\tau^3] \tag{5.1.26}$$

and the bottom loop is the same as for figure 5.5(a). Therefore the overall factor will be

$$(2-1) \times (-1)[2\pi N(0)\tau^3]^2 \tag{5.1.27}$$

which is

$$-(2\pi N(0)\tau^3)^2 \tag{5.1.28}$$

With the substitution $\omega \to -\omega$ the contribution can be evaluated as

$$-(2\pi N(0)\tau^3)^2 T \sum_{\omega>0} \sum_{\omega'>0} \left[\frac{1}{(DQ^2+\omega+\omega')^2} - \frac{1}{(DQ^2+\omega+\Omega+\omega')^2} \right] \tag{5.1.29}$$

However, the inequality (5.1.19) will give a different contribution from taking the k-summation. The diagram cannot have a single impurity line which means that the Hikami box can only be represented as shown in figure 5.5(a). The overall

factor will therefore be given as

$$+(2\pi N(0)\tau^3)^2 \tag{5.1.30}$$

and will be the same overall factor as for inequality (5.1.20).

The full 2 ladder Type-II contribution, including the contributions from the additional impurity line, is given by

$$\begin{aligned} K &= 8e^4D^2\delta_{\alpha\beta}\delta_{\gamma\delta}\sum_Q T\sum_{\omega>0}T\sum_{\omega'>0}\Big[\frac{1}{(DQ^2+\omega+\omega')^2}-\frac{1}{(DQ^2+\omega+\Omega+\omega')^2} \\ &\quad -\frac{1}{(DQ^2+\omega+\omega'+\Omega')^2}+\frac{1}{(DQ^2+\omega+\Omega+\omega'+\Omega')^2}\Big] \\ &+ 8e^4D^2\delta_{\alpha\beta}\delta_{\gamma\delta}\sum_Q T\sum_{\omega>0}T\sum_{\omega'>0}\Big[\frac{-1}{(DQ^2+\omega+\omega')^2}+\frac{1}{(DQ^2+\omega+\Omega+\omega')^2} \\ &\quad +\frac{1}{(DQ^2+\omega+\omega'+\Omega')^2}+\frac{3}{(DQ^2+\omega+\Omega+\omega'+\Omega')^2}\Big] \end{aligned} \tag{5.1.31}$$

5.1.3 3 ladder calculation

The 3 ladder Type-I contributions will consist of the diagram in figure (5.3). The electromagnetic response function for this diagram will be of the form

$$\begin{aligned} K=\Big(\frac{e}{m}\Big)^4 T\sum_Q\sum_{k,k',k''}\sum_{\omega,\omega'} \quad & (k+Q)_\alpha \quad [G^+(k+Q)]^2G^-(k) \\ & k''_\gamma G^+(k''+q)[G^-(k''+Q)]^2k'_\beta k'_\gamma[G^+(k')G^-(k')]^2 \\ & \Gamma(\omega,\omega')\Gamma(\omega+\Omega,\omega')\Gamma(\omega,\omega'+\Omega) \end{aligned} \tag{5.1.32}$$

The k-summation can be transformed and solved as

$$\begin{aligned}\sum_k (k+Q)_\alpha [G^+(k+Q)]^2 G^-(k) &= \sum_k k_\alpha \left(\frac{-k.Q}{m}\right)[G^+(k)G^-(k)]^2 \\ &= -\frac{ev_F^2}{d} Q_\alpha (4\pi N(0)\tau^3) \end{aligned} \tag{5.1.33}$$

and the k' and k''-summations can be solved with a similar method to give

$$K = \frac{-4e^4 D^2}{d}\delta_{\alpha\gamma}\delta_{\beta\delta}(4\pi N(0)\tau^3)^3 \sum_Q T\sum_\omega T\sum_{\omega'} DQ^2\Gamma(\omega,\omega')\Gamma(\omega+\Omega,\omega')\Gamma(\omega,\omega'+\Omega)$$

Due to the Heaviside functions in the ladder functions Γ there are only 2 possible inequalities to evaluate which are given by

$$\begin{aligned} &\omega > 0 \quad \omega+\Omega > 0 \quad \omega' < 0 \quad \omega'+\Omega' < 0 \\ &\omega < 0 \quad \omega+\Omega < 0 \quad \omega' > 0 \quad \omega'+\Omega' > 0 \end{aligned} \tag{5.1.34}$$

The inequality (5.1.34) will give the form of $\Gamma(\omega,\omega')\Gamma(\omega+\Omega,\omega')\Gamma(\omega,\omega'+\Omega)$ as proportional to

$$T\sum_{\omega>0} T\sum_{\omega'<-\Omega'} \frac{1}{DQ^2+\omega+\Omega-\omega'}\frac{1}{DQ^2+\omega-\omega'}\frac{1}{DQ^2+\omega-\omega'-\Omega'} \tag{5.1.35}$$

and by making the transformation $\omega' \to -(\omega'+\Omega)$ this will give

$$T\sum_{\omega>0} T\sum_{\omega'>0} \frac{1}{DQ^2+\omega+\omega'}\frac{1}{DQ^2+\omega+\omega'+\Omega'}\frac{1}{DQ^2+\omega+\omega'+\Omega+\Omega'} \tag{5.1.36}$$

The remaining inequality (5.1.34) will give $\Gamma(\omega,\omega')\Gamma(\omega+\Omega,\omega')\Gamma(\omega,\omega'+\Omega)$ as proportional to

$$T\sum_{\omega<-\Omega}T\sum_{\omega'>0}\frac{1}{DQ^2-\omega-\Omega+\omega'}\frac{1}{DQ^2-\omega+\omega'}\frac{1}{DQ^2-\omega+\omega'+\Omega'} \quad (5.1.37)$$

and by making the transformation $\omega\to-(\omega+\Omega)$ this will give

$$T\sum_{\omega>0}T\sum_{\omega'>0}\frac{1}{DQ^2+\omega+\omega'}\frac{1}{DQ^2+\omega+\omega'+\Omega}\frac{1}{DQ^2+\omega+\omega'+\Omega+\Omega'} \quad (5.1.38)$$

The remaining contributions will be the 3 diagrams which are 'rotations' of this one and 4 diagrams corresponding to the inequalities corresponding to $\omega'-\Omega'$ which can be calculated using a very similar technique. This will give the overall 3-ladder Type-I contribution as

$$\begin{aligned}&\frac{-128e^4D^2}{d}\delta_{\alpha\gamma}\delta_{\beta\delta}\sum_Q T\sum_{\omega>0}T\sum_{\omega'>0}\left[\frac{DQ^2}{A(\omega,\omega')(A(\omega,\omega')+\Omega)(A(\omega,\omega')+\Omega+\Omega')}+\right.\\&\qquad\left.\frac{DQ^2}{A(\omega,\omega')(A(\omega,\omega')+\Omega')(A(\omega,\omega')+\Omega+\Omega')}\right]\\&\frac{-128e^4D^2}{d}\delta_{\alpha\delta}\delta_{\beta\gamma}\sum_Q T\sum_{\omega>0}T\sum_{\omega'>0}\left[\frac{DQ^2}{A(\omega,\omega')(A(\omega,\omega')+\Omega)(A(\omega,\omega')+\Omega')}+\right.\\&\qquad\left.\frac{DQ^2}{A(\omega,\omega')+\Omega)(A(\omega,\omega')+\Omega')(A(\omega,\omega')+\Omega+\Omega')}\right]\end{aligned} \quad (5.1.39)$$

where

$$A(\omega,\omega')=DQ^2+\omega+\omega' \quad (5.1.40)$$

The 3-ladder Type-II contribution is shown in figure (5.3) and will also consist of 8 diagrams which correspond to 2 rotations each with 4 combinations of $\omega \pm \Omega$ and $\omega \pm \Omega$ to give

$$\frac{-64e^4D^2}{d}\delta_{\alpha\beta}\delta_{\gamma\delta}\sum_Q T\sum_{\omega>0}T\sum_{\omega'>0}\left[\frac{DQ^2}{(A(\omega,\omega')+\Omega+\Omega')^2(A(\omega,\omega')+\Omega)}\right.$$
$$+\frac{DQ^2}{(A(\omega,\omega')+\Omega)^2(A(\omega,\omega')+\Omega+\Omega')}$$
$$+\frac{DQ^2}{(A(\omega,\omega')+\Omega+\Omega')^2(A(\omega,\omega')+\Omega')}$$
$$\left.+\frac{DQ^2}{(A(\omega,\omega')+\Omega')^2(A(\omega,\omega')+\Omega+\Omega')}\right] \quad (5.1.41)$$

5.1.4 4 ladder calculation

The 4 ladder contribution is shown in figure (5.3) and consists of 4 seperate diagrams corresponding to 2 rotations. The contributions will give the electromagnetic response function as

$$\begin{aligned} K &= 8\frac{e^4D^2}{d(d+2)}(\delta_{\alpha\beta}\delta_{\gamma\delta}+\delta_{\alpha\gamma}\delta_{\beta\delta}+\delta_{\alpha\delta}\delta_{\beta\gamma})(4\pi N(0)\tau^3)^4 \\ &\quad \sum_Q T\sum_\omega T\sum_{\omega'}(DQ^2)^2\Gamma(\omega,\omega')\Gamma(\omega+\Omega,\omega')\Gamma(\omega,\omega'+\Omega)\Gamma(\omega+\Omega,\omega'+\Omega) \end{aligned} \quad (5.1.42)$$

In the limit $\omega>0, \omega+\Omega>0, \omega'<0, \omega'+\Omega'<0$ the ladder functions will become

$$T\sum_{\omega>0}T\sum_{\omega'<-\Omega'}\frac{1}{DQ^2+\omega+\Omega-\omega'}\frac{1}{(DQ^2+\omega-\omega')^2}\frac{1}{DQ^2+\omega-\omega'-\Omega'}$$

and by making the transformation $\omega' \to -(\omega' + \Omega')$ this will give the final result as

$$T\sum_{\omega>0} T\sum_{\omega'>0} \frac{1}{DQ^2+\omega+\omega'} \frac{1}{(DQ^2+\omega+\omega'+\Omega')^2} \frac{1}{DQ^2+\omega+\omega'+\Omega+\Omega'}$$

The other 4 ladder diagrams can be calculated using a very similar method to give the final 4 ladder contribution as

$$\begin{aligned}\frac{128e^4D^2}{d(d+2)}\left(\delta_{\alpha\beta}\delta_{\gamma\delta}+\delta_{\alpha\gamma}\delta_{\beta\delta}+\delta_{\alpha\delta}\delta_{\beta\gamma}\right)\sum_Q T\sum_{\omega>0} T\sum_{\omega'>0}\Bigg[&\frac{(DQ^2)^2}{A(\omega,\omega')^2(A(\omega,\omega')+\Omega)(A(\omega,\omega')+\Omega')}\\ &+\frac{(DQ^2)^2}{(A(\omega,\omega')+\Omega+\Omega')^2(A(\omega,\omega')+\Omega)(A(\omega,\omega')+\Omega')}\\ &+\frac{(DQ^2)^2}{A(\omega,\omega')(A(\omega,\omega')+\Omega)^2(A(\omega,\omega')+\Omega+\Omega')}\\ &+\frac{(DQ^2)^2}{A(\omega,\omega')(A(\omega,\omega')+\Omega')^2(A(\omega,\omega')+\Omega+\Omega')}\\ &+\frac{2(DQ^2)^2}{A(\omega,\omega')(A(\omega,\omega')+\Omega)(A(\omega,\omega')+\Omega')(A(\omega,\omega')+\Omega+\Omega')}\Bigg]\end{aligned} \tag{5.1.43}$$

5.2 UCF calculations in the DC limit

The n_s correction to the conductivity due to mesoscopic fluctuations only requires the DC-limit of the UCF calculation. This section will begin with the calculation of the normal state DC fluctuations where it will be shown that a large number of diagrams will cancel. To simplify matters, these diagrams will be denoted as Right and Wrong-sign terms and the cancellations will be explained more thoroughly in the the second subsection of this chapter.

5.2.1 DC calculations

The DC-limit can be calculated by taking the $\mathcal{O}(\Omega\Omega')$ contribution of the AC calculation - noting that the $\mathcal{O}(1)$, $\mathcal{O}(\Omega)$ and $\mathcal{O}(\Omega')$ will give zero contribution in the normal state as this will imply the presence of a superfluid state. To $\mathcal{O}(\Omega\Omega')$ the full 2-ladder contribution can be calculated as

$$16e^4D^2\sum_Q T\sum_{\omega>0}T\sum_{\omega'>0}\left[\frac{1}{DQ^2(DQ^2+\omega+\omega')^3}+\frac{18}{(DQ^2+\omega+\omega')^4}\right] \tag{5.2.1}$$

where the first term comes only from the 2-ladder Type-I diagrams and the second term comes from a combination of the 2-ladder Type-I and Type-II diagrams.

The first term in the square brackets will be evaluated last and the second term can be split up as

$$\frac{3}{(DQ^2+\omega+\omega')^4}+\frac{15}{(DQ^2+\omega+\omega')^4} \tag{5.2.2}$$

the reason for this will become clearer, and will be explained in detail after the integrals of each of the terms in the 3 and 4 ladder will be calculated. The d-dimensional integral identity

$$\int d^dx\frac{(x^2)^\alpha}{(x^2+a^2)^\beta}=\pi^{d/2}a^{d+2\alpha-2\beta}\frac{\Gamma(\alpha+d/2)\Gamma(\beta-\alpha-d/2)}{\Gamma(d/2)\Gamma(\beta)} \tag{5.2.3}$$

where $\Gamma(x)$ is the usual gamma function

$$\Gamma(x)=\int_0^\infty t^{x-1}e^{-t}dt \tag{5.2.4}$$

The second term in (5.2.2) can now be written as

$$240e^4D^2T\sum_{\omega>0}T\sum_{\omega'>0}\pi^{d/2}\left(\frac{\omega+\omega'}{D}\right)^{d/2-4}\frac{\Gamma(4-d/2)}{3!} \tag{5.2.5}$$

where the substitution $\Gamma(4) = 3!$.

To $\mathcal{O}(\Omega\Omega')$ the full 3-ladder contribution can be calculated as

$$\frac{-128e^4D^2}{d}\sum_{Q}T\sum_{\omega>0}T\sum_{\omega'>0}\frac{24DQ^2}{(DQ^2+\omega+\omega')^5} \tag{5.2.6}$$

Using identity (5.2.3) this can be rewritten as

$$\frac{-3072e^4D^2}{d}T\sum_{\omega>0}T\sum_{\omega'>0}\pi^{d/2}\left(\frac{\omega+\omega'}{D}\right)^{d/2-4}\frac{\Gamma(1+d/2)\Gamma(4-d/2)}{\Gamma(d/2)\Gamma(5)} \tag{5.2.7}$$

This looks familiar to the 2-ladder term calculated previously except for $\Gamma(1+d/2)$ term in the numerator which can be simplified using integration by parts

$$\Gamma(1+d/2) = \int_0^\infty t^{d/2}e^{-t}dt = \left.\frac{-t^{d/2}}{e^t}\right|_{t=0}^{t=\infty} + \frac{d}{2}\Gamma(d/2) \tag{5.2.8}$$

It is obvious that the limits involving the first term in this expression will be zero as the term in the denominator grows exponentially larger that of the numerator when $t \to \infty$. This will give the 3-ladder contribution as

$$\frac{-3072e^4D^2}{d}T\sum_{\omega>0}T\sum_{\omega'>0}\pi^{d/2}\left(\frac{\omega+\omega'}{D}\right)^{d/2-4}\frac{d}{2}\frac{\Gamma(4-d/2)}{4!} \tag{5.2.9}$$

To $\mathcal{O}(\Omega\Omega')$ the full 4-ladder contribution can be calculated as

$$\frac{128e^4D^2}{d(d+2)}\sum_Q T\sum_{\omega>0}T\sum_{\omega'>0}\frac{30(DQ^2)^2}{(DQ^2+\omega+\omega')^6} \tag{5.2.10}$$

Using identity (5.2.3 this can be rewritten as

$$\frac{3840e^4D^2}{d(d+2)}T\sum_{\omega>0}T\sum_{\omega'>0}\pi^{d/2}\left(\frac{\omega+\omega'}{D}\right)^{d/2-4}\frac{\Gamma(2+d/2)\Gamma(4-d/2)}{\Gamma(d/2)\Gamma(6)} \tag{5.2.11}$$

which also looks similar to the 2-ladder and 3-ladder contributions. As before, $\Gamma(2+d/2)$ can be simplified using the integration by parts method as

$$\begin{aligned}\Gamma(2+d/2) &= \int_0^\infty t^{1+d/2}e^{-t}dt = \left[\frac{-t^{1+d/2}}{e^t}\right]_0^\infty + (1+d/2)\Gamma(1+d/2)\\ &= (1+d/2)(d/2)\Gamma(d/2)\end{aligned} \tag{5.2.12}$$

where the final line uses the substitution of $\Gamma(1+d/2)$ derived previously together with the use of L'Hopital's rule to evaluate the e^-t term as zero. This will give the final 4-ladder contribution as

$$\frac{3840e^4D^2}{d}T\sum_{\omega>0}T\sum_{\omega'>0}\pi^{d/2}\left(\frac{\omega+\omega'}{D}\right)^{d/2-4}(1+d/2)(d/2)\frac{\Gamma(4-d/2)}{5!} \tag{5.2.13}$$

Combining all of these terms will give

$$\frac{e^4D^2\pi^{d/2}}{\Gamma(4-d/2)}\left(\frac{\omega+\omega'}{D}\right)^{d/2-4}T\sum_{\omega>0}T\sum_{\omega'>0}\left[\frac{240}{3!}-\frac{3072}{2(4!)}+\frac{11520}{4(5!)}\right]=0 \tag{5.2.14}$$

which is valid in all dimensions. This shows that the only contribution in the DC

limit comes from the contributions in the 2-ladder calculation

$$16e^4D^2\sum_Q T\sum_{\omega>0}T\sum_{\omega'>0}\left[\frac{1}{DQ^2(DQ^2+\omega+\omega')^3}+\frac{3}{(DQ^2+\omega+\omega')^4}\right] \quad (5.2.15)$$

The first term can be solved using integration by parts as

$$\int_{-\infty}^{\infty}\frac{1}{DQ^2(DQ^2+\omega+\omega')^3}d^dQ=-\int_{-\infty}^{\infty}\frac{2}{(DQ^2+\omega+\omega')^4}d^dQ \quad (5.2.16)$$

This gives the full contribution as

$$16e^4D^2T\sum_{\omega>0}T\sum_{\omega'>0}\frac{1}{V}\int_{-\infty}^{\infty}\frac{1}{(DQ^2+\omega+\omega')^4}d^dQ \quad (5.2.17)$$

where V is the volume of the system. Using the identity given in (5.2.3) this can be calculated as

$$\frac{16\pi^{d/2}e^4D^2\Gamma(4-d/2)}{3!V(2\pi)^d}T\sum_{\omega>0}T\sum_{\omega'>0}\left(\frac{\omega+\omega'}{D}\right)^{d/2-4} \quad (5.2.18)$$

and the volume of the system will be given by $V=(L/L_\phi)^d$ where $L_\phi=\sqrt{D\tau}$. The summations can be solved in integral form which give

$$\begin{aligned}\delta g^2 &\propto \frac{0.537e^4}{\hbar^2} \quad \text{for} \quad d=1\\ &\propto \frac{0.752e^4}{\hbar^2} \quad \text{for} \quad d=2\\ &\propto \frac{0.909e^4}{\hbar^2} \quad \text{for} \quad d=3\end{aligned} \quad (5.2.19)$$

which proves that the fluctuations $\sqrt{\delta g^2}$ is of order $\frac{e^2}{h}$ at zero temperature.

5.2.2 Right and Wrong-sign contributions

In calculating the full AC calculation there were 4 inequalities in the frequencies to take into account and these will be labelled as follows

$$\left.\begin{array}{cccc} \omega > 0 & \omega + \Omega > 0 & \omega' < 0 & \omega' + \Omega' < 0 \\ \omega < 0 & \omega + \Omega < 0 & \omega' > 0 & \omega' + \Omega' > 0 \end{array}\right\} \quad \text{"Wrong-Sign"} \tag{5.2.20}$$

$$\left.\begin{array}{cccc} \omega > 0 & \omega + \Omega < 0 & \omega' > 0 & \omega' + \Omega' < 0 \\ \omega < 0 & \omega + \Omega > 0 & \omega' < 0 & \omega' + \Omega' > 0 \end{array}\right\} \quad \text{"Right-Sign"} \tag{5.2.21}$$

By using this grouping it can be seen that the terms cancelling each other in (5.2.14) all come from the wrong-sign contributions. This is why the second term in (5.2.1) was split up into 2 contributions which represented the Right and Wrong-sign terms. This is an important result as many research papers state that the AC results can be derived from that of the DC case. This is untrue due to the Wrong-sign cancellations which means that a lot of the AC information is 'lost' when transforming into the DC limit.

Chapter 6

SUPERCONDUCTING UCF

The aim of this calculation is to find the n_s correction due to mesoscopic fluctuations. This requires the UCF diagrams to be calculated with the superconducting Green's functions together with the superconducting ladder , with all its possible combinations. The motivation of this calculation means that the only contribution to be evaluated will be in the limit $Q, \Omega = 0$. The diagrams to be calculated are diagrammatically the same as in the normal case, shown previously in figure 5.3. The set of diagrams have been separated into two types; *Type-I* and *Type-II* which are labelled correspondingly in figure 5.3. A given diagram will then be split up into the corresponding terms representing the different vertex contributions from the superconducting ladder. In the main text, the *Type-I: 2 ladder calculation* will be shown rigorously but the further calculations will only show the main results. Note that the full results will be shown in the appendix.

6.1 2 ladder calculation

6.1.1 2 Ladder calculation - Type-I

The diagram to be calculated is the third diagram shown in figure 5.3 but, due to the superconducting ladder, will have 4 seperate terms corresponding to

$$\tau_3 \otimes \tau_3, \quad \tau_3 \otimes \tilde{\bar{\omega}}, \quad \tilde{\bar{\omega}} \otimes \tau_3 \quad \text{and} \quad \tilde{\bar{\omega}} \otimes \tilde{\bar{\omega}} \tag{6.1.1}$$

where the notation $\tilde{\bar{\omega}} = (i\bar{\omega} - \bar{\Delta}\tau_1)/\overline{W}$. The labeling will start from the uppermost vertex and will sequentially run clockwise. The superconducting ladder was calculated in a previous section but is rewritten for the readers convenience as

$$\Gamma = \frac{1}{4\pi N(0)\tau^2} \frac{1}{DQ^2 + W + W'} \left[\tau_3 \otimes \tau_3 - \frac{(i\bar{\omega}\tau_0 - \bar{\Delta}\tau_1) \otimes (i(\bar{\omega} + \Omega)\tau_0 - \bar{\Delta}\tau_1)}{\overline{WW}'} \right] \tag{6.1.2}$$

Note that the factors of $\frac{1}{4\pi N(0)\tau^2} \frac{1}{DQ^2+W+W'}$ will be initially omitted from the calculations including the factors of 2 that will arise from taking each trace, but will be included in the final result.

- $\tau_3 \otimes \tau_3$ **term**

The full contributon will be a product of the individual traces of the inner and outer loop and so will be calculated independently before the full contribution is constructed.

The outer loop contribution from the the diagram in figure 6.1 can be written

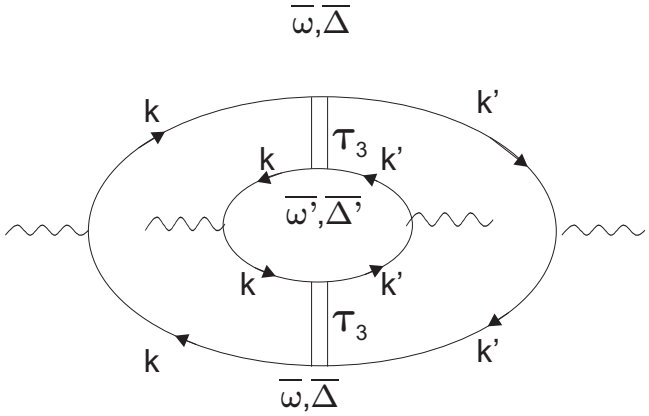

Figure 6.1 – The 2 ladder $\tau \otimes \tau$ contribution to the superconducting UCF calculation.

as

$$G(k,\bar{\omega})\tau_3 G(k',\bar{\omega})G(k',\bar{\omega})\tau_3 G(k,\bar{\omega}) \tag{6.1.3}$$

Using the superconducting Green's function, and making sure to multiply through by the conjugate of the denominator as to remove the matrix contribution in the denominator this leaves

$$\frac{i\bar{\omega}+\xi\tau_3+\bar{\Delta}\tau_1}{\bar{\omega}^2+\xi^2+\bar{\Delta}^2}\tau_3\frac{i\bar{\omega}+\xi'\tau_3+\bar{\Delta}\tau_1}{\bar{\omega}^2+\xi'^2+\bar{\Delta}^2}\frac{i\bar{\omega}+\xi'\tau_3+\bar{\Delta}\tau_1}{\bar{\omega}^2+\xi'^2+\bar{\Delta}^2}\tau_3\frac{i\bar{\omega}+\xi\tau_3+\bar{\Delta}\tau_1}{\bar{\omega}^2+\xi^2+\bar{\Delta}^2} \tag{6.1.4}$$

Next we must commute τ_3 through until it acts upon the other τ_3 to give the identity. This will give us

$$\frac{i\bar{\omega}+\xi\tau_3+\bar{\Delta}\tau_1}{\bar{\omega}^2+\xi^2+\bar{\Delta}^2}\frac{i\bar{\omega}+\xi'\tau_3-\bar{\Delta}\tau_1}{\bar{\omega}^2+\xi'^2+\bar{\Delta}^2}\frac{i\bar{\omega}+\xi'\tau_3-\bar{\Delta}\tau_1}{\bar{\omega}^2+\xi'^2+\bar{\Delta}^2}\frac{i\bar{\omega}+\xi\tau_3+\bar{\Delta}\tau_1}{\bar{\omega}^2+\xi^2+\bar{\Delta}^2} \tag{6.1.5}$$

Multiplying out the numerators and by making the substitution $\overline{W} = \sqrt{\bar{\Delta}^2+\bar{\omega}^2}$

and $\overline{W}' = \sqrt{\bar{\Delta}'^2 + \bar{\omega}'^2}$

$$\frac{\Big([\xi\xi' - \overline{W}^2] - i\Delta\tau_2(\xi+\xi') + i\bar{\omega}\tau_3(\xi+\xi')\Big)\Big([\xi\xi' - \overline{W}^2] + i\Delta\tau_2(\xi+\xi') + i\bar{\omega}\tau_3(\xi+\xi')\Big)}{(\xi^2+\overline{W}^2)^2(\xi'^2+\overline{W}^2)^2}$$
$$= \frac{(\xi\xi' - \overline{W}^2)^2 + (\bar{\Delta}^2 - \bar{\omega}^2)(\xi+\xi')^2 + 2i\bar{\omega}\bar{\Delta}\tau_1(\xi+\xi')^2 + 2i\bar{\omega}\tau_3(\xi+\xi')(\xi\xi' - \overline{W}^2)}{(\xi^2+\overline{W}^2)^2(\xi'^2+\overline{W}^2)^2} \tag{6.1.6}$$

This will lead us to the solution of the outer loop, which we will define as I_1 for later convenience

$$I_1 = \frac{(\xi\xi' - \overline{W}^2)^2 + (\bar{\Delta}^2 - \bar{\omega}^2)(\xi+\xi')^2 + 2i\bar{\omega}\bar{\Delta}\tau_1(\xi+\xi')^2 + 2i\bar{\omega}\tau_3(\xi+\xi')(\xi\xi' - \overline{W}^2)}{(\xi^2+\overline{W}^2)^2(\xi'^2+\overline{W}^2)^2} \tag{6.1.7}$$

Now we must take the trace of the inner and outer loop seperately which will give the overall outer loop contribution of

$$\frac{[\xi\xi' - \overline{W}^2]^2 + (\bar{\Delta}^2 - \bar{\omega}^2)(\xi+\xi')^2}{(\xi^2+\overline{W}^2)^2(\xi'^2+\overline{W}^2)^2} \tag{6.1.8}$$

The next step is to calculate the contribution from the outer loop which can be written as

$$G(k',\bar{\omega}')\tau_3 G(k,\bar{\omega}')G(k,\bar{\omega}')\tau_3 G(k',\bar{\omega}') \tag{6.1.9}$$

Once again, this can be given as

$$\frac{i\bar{\omega}' + \xi'\tau_3 + \bar{\Delta}'\tau_1}{\bar{\omega}'^2 + \xi'^2 + \bar{\Delta}'^2}\tau_3\frac{i\bar{\omega}' + \xi\tau_3 + \bar{\Delta}'\tau_1}{\bar{\omega}'^2 + \xi^2 + \bar{\Delta}'^2}\frac{i\bar{\omega}' + \xi\tau_3 + \bar{\Delta}'\tau_1}{\bar{\omega}'^2 + \xi^2 + \bar{\Delta}'^2}\tau_3\frac{i\bar{\omega}' + \xi'\tau_3 + \bar{\Delta}'\tau_1}{\bar{\omega}'^2 + \xi'^2 + \bar{\Delta}'^2}$$

In a similar way to the outer loop, this can be evaluated to give

$$I_2 = \frac{(\xi\xi' - \overline{W}'^2)^2 + (\bar{\Delta}'^2 - \bar{\omega}'^2)(\xi + \xi')^2 + 2i\bar{\omega}'\bar{\Delta}'\tau_1(\xi + \xi')^2 + 2i\bar{\omega}'\tau_3(\xi + \xi')(\xi\xi' - \overline{W}'^2)}{(\xi^2 + \overline{W}'^2)^2(\xi'^2 + \overline{W}'^2)^2} \tag{6.1.10}$$

which has been denoted as I_2 for later convenience. Taking the trace this will give the overall inner loop solution of

$$\frac{[\xi\xi' - \overline{W}'^2]^2 + (\bar{\Delta}'^2 - \bar{\omega}'^2)(\xi + \xi')^2}{(\xi^2 + \overline{W}'^2)^2(\xi'^2 + \overline{W}'^2)^2} \tag{6.1.11}$$

Now we must calculate the total contribution from the inner and outer loop contribution. It must be noted that we will be integrating with respect to ξ and ξ' which means that only the even terms will give a non-zero integral, but this will be implemented later. The full $\tau_3 \otimes \tau_3$ contribution will be from the product of the inner and outer loop contributions which will give

$$\frac{\left[(\xi\xi' - \overline{W}^2)^2 + (\bar{\Delta}^2 - \bar{\omega}^2)(\xi + \xi')^2\right]\left[(\xi\xi' - \overline{W}'^2)^2 + (\bar{\Delta}'^2 - \bar{\omega}'^2)(\xi + \xi')^2\right]}{(\xi^2 + \overline{W}^2)^2(\xi^2 + \overline{W}'^2)^2(\xi'^2 + \overline{W}^2)^2(\xi'^2 + \overline{W}'^2)^2} \tag{6.1.12}$$

- $\tau_3 \otimes (i\bar{\omega} - \bar{\Delta}\tau_1)$ **term**

The next diagram to calculate is shown in figure 6.2 and, once again, we will be calculating the inner and outer loop seperately before combining the result.

The outer loop contribution is given by

$$G(k, \bar{\omega})\tau_3 G(k', \bar{\omega})G(k', \bar{\omega})\frac{(i\bar{\omega} - \bar{\Delta}\tau_1)}{\overline{W}}G(k, \bar{\omega}) \tag{6.1.13}$$

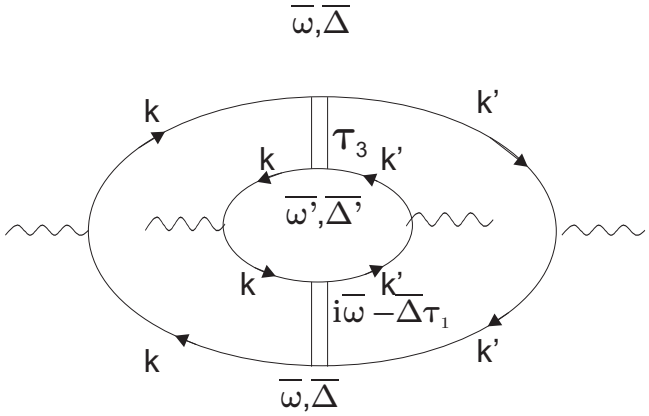

Figure 6.2 – The 2 ladder $\tau \otimes \tilde{\omega}$ contribution to the superconducting UCF calculation.

Substituting the full Green's functions one is given

$$\frac{i\bar{\omega}+\xi\tau_3+\bar{\Delta}\tau_1}{\bar{\omega}^2+\xi^2+\bar{\Delta}^2}\tau_3\frac{i\bar{\omega}+\xi'\tau_3+\bar{\Delta}\tau_1}{\bar{\omega}^2+\xi'^2+\bar{\Delta}^2}\frac{i\bar{\omega}+\xi'\tau_3+\bar{\Delta}\tau_1}{\bar{\omega}^2+\xi'^2+\bar{\Delta}^2}\frac{(i\bar{\omega}-\bar{\Delta}\tau_1)}{\overline{W}}\frac{i\bar{\omega}+\xi\tau_3+\bar{\Delta}\tau_1}{\bar{\omega}^2+\xi^2+\bar{\Delta}^2} \tag{6.1.14}$$

In a previous section we proved that $(i\bar{\omega}-\bar{\Delta}\tau_1)G=\tau_3 G\tau_3(i\bar{\omega}+\bar{\Delta}\tau_1)$. This result can be used to commute $(i\bar{\omega}-\bar{\Delta}\tau_1)$ to passed the Green's function (to the right) which will give

$$\frac{i\bar{\omega}+\xi\tau_3+\bar{\Delta}\tau_1}{\bar{\omega}^2+\xi^2+\bar{\Delta}^2}\tau_3\frac{i\bar{\omega}+\xi'\tau_3+\bar{\Delta}\tau_1}{\bar{\omega}^2+\xi'^2+\bar{\Delta}^2}\frac{i\bar{\omega}+\xi'\tau_3+\bar{\Delta}\tau_1}{\bar{\omega}^2+\xi'^2+\bar{\Delta}^2}\tau_3\frac{i\bar{\omega}+\xi\tau_3+\bar{\Delta}\tau_1}{\bar{\omega}^2+\xi^2+\bar{\Delta}^2}\tau_3\frac{(i\bar{\omega}+\bar{\Delta}\tau_1)}{\overline{W}} \tag{6.1.15}$$

This can now be related back to the function I_1 as

$$I_1\tau_3\frac{(i\bar{\omega}+\bar{\Delta}\tau_1)}{\overline{W}} \tag{6.1.16}$$

Expanding out term by term and taking the trace will give

$$\frac{[-2\bar{\omega}^2(\xi+\xi')(\xi\xi'-\overline{W}^2)]/\overline{W}}{(\xi^2+\overline{W}^2)^2(\xi'^2+\overline{W}^2)^2} \tag{6.1.17}$$

The inner loop contribution will now be calculated as

$$G(k',\bar{\omega}')\tau_3 G(k,\bar{\omega}')G(k,\bar{\omega}')\frac{(i\bar{\omega}'-\bar{\Delta}'\tau_1)}{\overline{W}'}G(k',\bar{\omega}') \tag{6.1.18}$$

Once again, this can be reduced down to the form

$$I_2\tau_3\frac{(i\bar{\omega}'+\bar{\Delta}'\tau_1)}{\overline{W}'} \tag{6.1.19}$$

The trace can be taken which will give

$$\frac{[-2\bar{\omega}'^2(\xi+\xi')(\xi\xi'-\overline{W}'^2)]/\overline{W}'}{(\xi^2+\overline{W}'^2)^2(\xi'^2+\overline{W}'^2)^2} \tag{6.1.20}$$

Combining the inner and outer loop contribution, we are left with

$$\frac{[4\bar{\omega}^2\bar{\omega}'^2(\xi+\xi')^2(\xi\xi'-\overline{W}^2)(\xi\xi'-\overline{W}'^2)/\overline{WW}']}{(\xi^2+\overline{W}^2)^2(\xi^2+\overline{W}'^2)^2(\xi'^2+\overline{W}^2)^2(\xi'^2+\overline{W}'^2)^2} \tag{6.1.21}$$

- $(i\bar{\omega}-\bar{\Delta}\tau_1)\otimes\tau_3$ **term**

The next calulation is the contribution from the $(i\bar{\omega}-\bar{\Delta}\tau_1)\otimes\tau_3$ term in the superconducting ladder, which will give the diagram shown in figure 6.3.

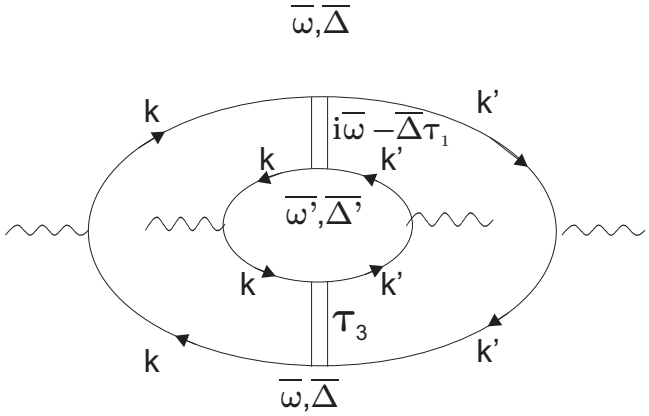

Figure 6.3 – The 2 ladder $\tilde{\omega} \otimes \tau$ contribution to the superconducting UCF calculation.

The outer loop contribution will be

$$G(k,\bar{\omega})\frac{(i\bar{\omega}-\bar{\Delta}\tau_1)}{\overline{W}}G(k',\bar{\omega})G(k',\bar{\omega})\tau_3 G(k,\bar{\omega}) \tag{6.1.22}$$

As for the previous calculation, this can be commuted to give the result

$$\frac{i\bar{\omega}+\Delta\tau_1}{\overline{W}}\tau_3 I_1 \tag{6.1.23}$$

Due to the trace being invariant under cyclic permutations and that I_1 does not contain any τ_2 components; this contribution is equal to the outer loop of the $\tau_3 \otimes (i\bar{\omega}-\bar{\Delta}\tau_1)$ term, given as

$$\frac{[-2\bar{\omega}^2(\xi+\xi')(\xi\xi'-\overline{W}^2)]/\overline{W}}{(\xi^2+\overline{W}^2)^2(\xi'^2+\overline{W}^2)^2} \tag{6.1.24}$$

Now, the inner loop must be considered, and is written as

$$G(k',\bar{\omega}')\frac{(i\bar{\omega}'-\bar{\Delta}'\tau_1)}{\overline{W}'}G(k,\bar{\omega}')G(k,\bar{\omega}')\tau_3 G(k',\bar{\omega}') \tag{6.1.25}$$

Commuting through, this can be related back to the expression I_2 as

$$\frac{i\bar{\omega}'+\Delta'\tau_1}{\overline{W}'}\tau_3 I_2 \tag{6.1.26}$$

This will also given the same result as that of the inner loop from the $\tau_3\otimes(i\bar{\omega}-\bar{\Delta}\tau_1)$ term. Therefore, the full contribution will become

$$\frac{[4\bar{\omega}^2\bar{\omega}'^2(\xi+\xi')^2(\xi\xi'-\overline{W}^2)(\xi\xi'-\overline{W}'^2)/\overline{W}\overline{W}']}{(\xi^2+\overline{W}^2)^2(\xi^2+\overline{W}'^2)^2(\xi'^2+\overline{W}^2)^2(\xi'^2+\overline{W}'^2)^2} \tag{6.1.27}$$

- $(i\bar{\omega}-\bar{\Delta}\tau_1)\otimes(i\bar{\omega}-\bar{\Delta}\tau_1)$ **term**

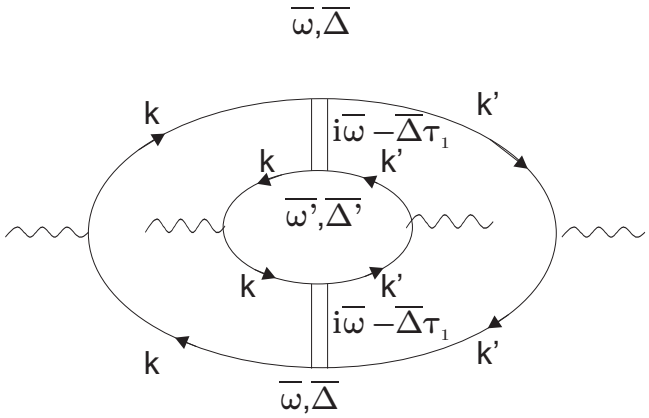

Figure 6.4 – The 2 ladder $\tilde{\omega}\otimes\tilde{\omega}$ contribution to the superconducting UCF calculation.

The final contribution can be evaluated using the diagram in figure 6.4 which

will give

$$G(k,\bar{\omega})\frac{(i\bar{\omega}-\bar{\Delta}\tau_1)}{\overline{W}}G(k',\bar{\omega})G(k',\bar{\omega})\frac{(i\bar{\omega}-\bar{\Delta}\tau_1)}{\overline{W}}G(k,\bar{\omega}) \tag{6.1.28}$$

Using the commutation rules this can be simplified as

$$\frac{(i\bar{\omega}+\bar{\Delta}\tau_1)}{\overline{W}}\tau_3 I_1 \tau_3 \frac{(i\bar{\omega}+\bar{\Delta}\tau_1)}{\overline{W}} \tag{6.1.29}$$

Cyclically permuting terms and also commuting τ_3 will give

$$I_1 \frac{(i\bar{\omega}-\bar{\Delta}\tau_1)}{\overline{W}}\frac{(i\bar{\omega}-\bar{\Delta}\tau_1)}{\overline{W}} \tag{6.1.30}$$

which will equate to

$$\frac{\Big[(\bar{\Delta}^2-\bar{\omega}^2)(\xi\xi'-\overline{W}^2)^2+(\bar{\Delta}^2-\bar{\omega}^2)^2(\xi+\xi')^2+4\bar{\omega}^2\bar{\Delta}^2(\xi+\xi')^2\Big]/\overline{W}^2}{(\xi^2+\overline{W}^2)^2(\xi'^2+\overline{W}^2)^2} \tag{6.1.31}$$

The next step is the inner loop contribution which can be expressed as

$$G(k',\bar{\omega}')\frac{(i\bar{\omega}'-\bar{\Delta}'\tau_1)}{\overline{W}'}G(k,\bar{\omega}')G(k,\bar{\omega}')\frac{(i\bar{\omega}'-\bar{\Delta}'\tau_1)}{\overline{W}'}G(k',\bar{\omega}') \tag{6.1.32}$$

Once again, this can be expressed in terms of I_2 as

$$\frac{(i\bar{\omega}'+\bar{\Delta}'\tau_1)}{\overline{W}'}\tau_3 I_2 \tau_3 \frac{(i\bar{\omega}'+\bar{\Delta}'\tau_1)}{\overline{W}'} = I_2 \frac{(i\bar{\omega}'-\bar{\Delta}'\tau_1)}{\overline{W}'}\frac{(i\bar{\omega}'-\bar{\Delta}'\tau_1)}{\overline{W}'} \tag{6.1.33}$$

which equates to

$$\frac{\Big[(\bar{\Delta}'^2-\bar{\omega}'^2)(\xi\xi'-\overline{W}'^2)^2+(\bar{\Delta}'^2-\bar{\omega}'^2)^2(\xi+\xi')^2+4\bar{\omega}'^2\bar{\Delta}'^2(\xi+\xi')^2\Big]/\overline{W}'^2}{(\xi^2+\overline{W}'^2)^2(\xi'^2+\overline{W}'^2)^2}$$

(6.1.34)

The full contribution will become

$$\frac{\Big[(\bar{\Delta}^2-\bar{\omega}^2)(\xi\xi'-\overline{W}^2)^2+(\bar{\Delta}^2-\bar{\omega}^2)^2(\xi+\xi')^2+4\bar{\omega}^2\bar{\Delta}^2(\xi+\xi')^2\Big]/\overline{W}^2}{(\xi^2+\overline{W}^2)^2(\xi'^2+\overline{W}^2)^2}$$
$$\times\frac{\Big[(\bar{\Delta}'^2-\bar{\omega}'^2)(\xi\xi'-\overline{W}'^2)^2+(\bar{\Delta}'^2-\bar{\omega}'^2)^2(\xi+\xi')^2+4\bar{\omega}'^2\bar{\Delta}'^2(\xi+\xi')^2\Big]/\overline{W}'^2}{(\xi^2+\overline{W}'^2)^2(\xi'^2+\overline{W}'^2)^2}$$

- **Reversed inner loop direction**

Due to the fact that each of the inner loop contributions are symmetric in ξ and ξ' means that the overall contribution with the reversed inner loop is identical to that of the calculations done previously. Therefore this will merely add an overall coefficient of 2 to the final solution, which will be added in later together with the factors of 2 from taking each individual trace.

- **Overall contribution**

Expanding out the numerator from each term and simplifying will give

$$(\xi\xi'-\overline{W}^2)(\xi\xi'-\overline{W}'^2)\Big[\frac{2(\bar{\Delta}^2\bar{\Delta}'^2+\bar{\omega}^2\bar{\omega}'^2)}{\overline{W}^2\overline{W}'^2}\Big]$$

$$+(\xi+\xi')^2(\xi\xi'-\overline{W}^2)^2\Big[\frac{2(\bar{\Delta}^2\bar{\Delta}'^2-\bar{\omega}^2\bar{\omega}'^2)}{\overline{W}^2}\Big]$$

$$+(\xi+\xi')^2(\xi\xi'-\overline{W}'^2)^2\Big[\frac{2(\bar{\Delta}^2\bar{\Delta}'^2-\bar{\omega}^2\bar{\omega}'^2)}{\overline{W}'^2}\Big]$$

$$-(\xi+\xi')^2(\xi\xi'-\overline{W}^2)(\xi\xi'-\overline{W}'^2)\Big[8\frac{\bar{\omega}^2\bar{\omega}'^2}{\overline{W}\overline{W}'}\Big]$$

$$+(\xi+\xi')^4\Big[2(\bar{\Delta}^2\bar{\Delta}'^2+\bar{\omega}^2\bar{\omega}'^2)\Big] \tag{6.1.35}$$

Now we must evaluate the integrals with respect to ξ and ξ'. Note that since the limits of our integrals are $\pm\infty$ then the only contributions will come from terms even in ξ and ξ'. This will reduce the problem to only 4 integrals denoted as A_n where $n = 1, ..., 4$ given in the appendix. Recall that the main contribution comes from electrons near the Fermi surface which causes $\sum_k \to N(0)\int d\xi_k$. Taking the integrals will give

$$\frac{2(N(0))^2\bar{\Delta}^2\bar{\Delta}'^2(\overline{W}+\overline{W}')^4}{\overline{W}^4\overline{W}'^4(\overline{W}+\overline{W}')^6} \tag{6.1.36}$$

Including the factors from the superconducting ladders, the factor of 2 for each of the traces taken, a factor of $\left(\frac{ek_F}{m}\right)^2\delta_{\alpha\beta}$ and a factor of 2 from the reversed inner loop will give a final soulution of

$$\left(\frac{ek_F}{\pi m\tau}\right)^4\delta_{\alpha\beta}\sum_Q\sum_{\omega,\omega'}\frac{\bar{\Delta}^2\bar{\Delta}'^2}{\overline{W}^4\overline{W}'^4}\frac{1}{(\overline{W}+\overline{W}')^2}\frac{1}{(DQ^2+W+W')^2} \tag{6.1.37}$$

6.1.2 Type-II diagrams

The next diagram to calculate is the 2 ladder Type-II contribution which is shown in figure 6.5. The inner and outer loop contribution for each configuration is given in the table below. Note that a new annotation of even-$\tilde{\bar{\omega}}$ (and odd-$\tilde{\bar{\omega}}$) will be included which corresponds to an even (odd) number of $\tilde{\bar{\omega}}$ terms on the ladders. This annotation will prove to be very useful as the separate traces in the even (or odd) contributions will simplify amongst themselves, as will be shown in the further calculations.

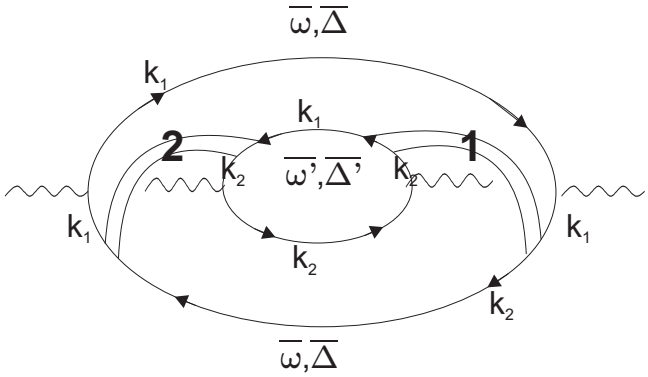

Figure 6.5 – The 2 ladder Type-II UCF diagram. The numbers on the superconducting ladders indicate the order for which the labels process

Configuration	Outer Loop	Inner Loop
$\tau_3\tau_3$ and $\tilde{\bar{\omega}}\tilde{\bar{\omega}}$	$\mathcal{A}^O$	$\mathcal{A}^I$
$\tau_3\tilde{\bar{\omega}}$ and $\tilde{\bar{\omega}}\tau_3$	$\mathcal{A}^O\tau_3\frac{(i\bar{\omega}+\bar{\Delta}\tau_1)}{\overline{W}}$	$\mathcal{A}^I\tau_3\frac{(i\bar{\omega}'+\bar{\Delta}'\tau_1)}{\overline{W}'}$

where $\mathcal{A}^O = G(k_1,\bar{\omega})G(k_1,\bar{\omega})\tau_3 G(k_2,\bar{\omega})\tau_3 G(k_1,\bar{\omega})$ and $\mathcal{A}^I = G(k_2,\bar{\omega}')G(k_2,\bar{\omega}')\tau_3 G(k_1,\bar{\omega}')\tau_3 G(k_2,\bar{\omega}')$ The odd-$\tilde{\bar{\omega}}$ will be calculated by solving

$$\mathrm{Tr}\{G(k_1,\bar{\omega})G(k_1,\bar{\omega})\tau_3 G(k_2,\bar{\omega})\tau_3 G(k_1,\bar{\omega})\tau_3\frac{(i\bar{\omega}+\bar{\Delta}\tau_1)}{\overline{W}}\}$$
$$\times\,\mathrm{Tr}\{G(k_2,\bar{\omega}')G(k_2,\bar{\omega}')\tau_3 G(k_1,\bar{\omega}')\tau_3 G(k_2,\bar{\omega}')\tau_3\frac{(i\bar{\omega}'+\bar{\Delta}'\tau_1)}{\overline{W}'}\}$$

and the even-$\tilde{\bar{\omega}}$ will be calculated by solving

$$\mathrm{Tr}\{G(k_1,\bar{\omega})G(k_1,\bar{\omega})\tau_3 G(k_2,\bar{\omega})\tau_3 G(k_1,\bar{\omega})\}$$
$$\times\,\mathrm{Tr}\{G(k_2,\bar{\omega}')G(k_2,\bar{\omega}')\tau_3 G(k_1,\bar{\omega}')\tau_3 G(k_2,\bar{\omega}')\}$$

Taking the traces and integrating with respect to ξ_1 and ξ_2 will give the final result as

$$\frac{2\bar{\Delta}^2\bar{\Delta}'^2}{\overline{W}^4\overline{W}'^4(\overline{W}+\overline{W}')^2} \tag{6.1.38}$$

6.1.3 Type-II with additional impurity

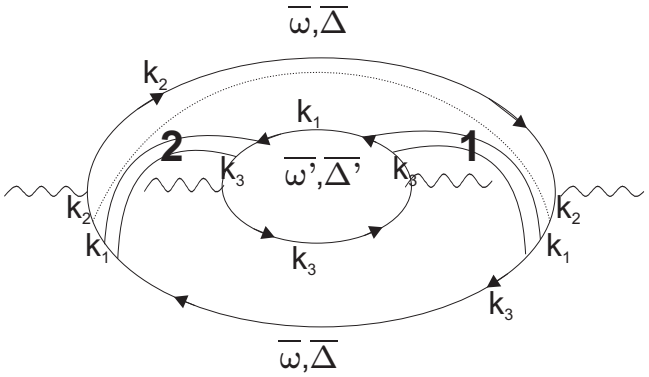

Figure 6.6 – The 2 ladder Type-II diagram with the additional impurity line, which gives the same order contribution as the ordinary 2 ladder Type-II diagram, for the superconducting UCF calculation.

The next 2 ladder diagram will be that shown in figure 6.6 as the additional impurity line does not cross any external lines. The inner and outer loop contributions corresponding to each configuration is shown in the table below.

Configuration	Outer Loop	Inner Loop
$\tau_3\tau_3$ and $\tilde{\bar{\omega}}\tilde{\bar{\omega}}$	$\mathcal{F}_2^O$	$\mathcal{F}_2^I$
$\tau_3\tilde{\bar{\omega}}$ and $\tilde{\bar{\omega}}\tau_3$	$\mathcal{F}_2^O\tau_3\frac{(i\bar{\omega}-\bar{\Delta}\tau_1)}{\overline{W}}$	$\mathcal{F}_2^I\tau_3\frac{(i\bar{\omega}'-\bar{\Delta}'\tau_1)}{\overline{W}'}$

where $\mathcal{F}_2^O = G(k_2,\bar{\omega})G(k_2,\bar{\omega})\tau_3G(k_1,\bar{\omega})\tau_3G(k_3,\bar{\omega})\tau_3G(k_1,\bar{\omega})\tau_3G(k_2,\bar{\omega})$ and $\mathcal{F}_2^I = G(k_3,\bar{\omega}')G(k_3,\bar{\omega}')\tau_3G(k_1,\bar{\omega}')\tau_3G(k_3,\bar{\omega})$

- Odd-$\tilde{\bar{\omega}}$ terms

The odd-$\tilde{\bar{\omega}}$ will be calculated by solving

$$\mathrm{Tr}\{\mathcal{F}_2^O\tau_3\frac{(i\bar{\omega}-\bar{\Delta}\tau_1)}{\overline{W}}\}\mathrm{Tr}\{\mathcal{F}_2^I\tau_3\frac{(i\bar{\omega}'-\bar{\Delta}'\tau_1)}{\overline{W}'}\} \tag{6.1.39}$$

The first trace term will become

$$\begin{aligned}
&-\overline{W}^2(\xi_2+\overline{W}^2)(\xi_1+\xi_2)(\xi_1\xi_3-\overline{W}^2)-\overline{W}^2(\xi_2+\overline{W}^2)(\xi_1+\xi_3)(\xi_1\xi_2-\overline{W}^2)\\
&\quad-2\bar{\omega}^2\xi_2(\xi_1\xi_2-\overline{W}^2)(\xi_1\xi_3-\overline{W}^2)+2\bar{\omega}^2\overline{W}^2\xi_2(\xi_1+\xi_2)(\xi_1+\xi_3)\\
&\quad+2\bar{\omega}^2\overline{W}^2(\xi_1+\xi_2)(\xi_1\xi_3-\overline{W}^2)+2\bar{\omega}^2\overline{W}^2(\xi_1+\xi_3)(\xi_1\xi_2-\overline{W}^2)
\end{aligned}$$

and the second trace becomes

$$-\overline{W}'^2(\xi_3+\overline{W}'^2)(\xi_1+\xi_3)-2\bar{\omega}'^2\xi_3(\xi_1\xi_3-\overline{W}'^2)+2\bar{\omega}'^2\overline{W}'^2(\xi_1+\xi_3) \tag{6.1.40}$$

Integrating with respect to ξ_i (where $i=1,2,3$) gives

$$\frac{\big[-\bar{\Delta}^2\bar{\Delta}'^2(\overline{W}^2+4\overline{W}\overline{W}'+3\overline{W}'^2)+4\bar{\Delta}^2\bar{\omega}'^2\overline{W}'^2\big]\pi^3}{4\overline{W}^4\overline{W}'^4(\overline{W}+\overline{W}')^5} \tag{6.1.41}$$

- Even-$\tilde{\bar{\omega}}$ terms

The Even-$\tilde{\bar{\omega}}$ will be calculated by solving

$$\mathrm{Tr}\{\mathcal{F}_2^O\}\mathrm{Tr}\{\mathcal{F}_2^I\} \tag{6.1.42}$$

The first trace term will become

$$\begin{aligned}(\xi_2+\overline{W}^2)(\xi_1\xi_2-\overline{W}^2)(\xi_1\xi_3-\overline{W}^2)-\overline{W}^2(\xi_2+\overline{W}^2)(\xi_1+\xi_2)(\xi_1+\xi_3)\\ -2\bar{\omega}^2(\xi_1\xi_2-\overline{W}^2)+2\bar{\omega}^2\overline{W}^2(\xi_1+\xi_2)(\xi_1+\xi_3)\\ -2\bar{\omega}\xi_2(\xi_1+\xi_2)(\xi_1\xi_3-\overline{W}^2)-2\bar{\omega}^2\xi_2(\xi_1+\xi_3)(\xi_1\xi_2-\overline{W}^2)\end{aligned}$$

and the second trace becomes

$$(\xi_3+\overline{W}'^2)(\xi_1\xi_3-\overline{W}'^2)-2\bar{\omega}'^2(\xi_1\xi_3-\overline{W}'^2)-2\bar{\omega}'^2\xi_3(\xi_1+\xi_3) \quad (6.1.43)$$

Integrating with respect to ξ_i (where $i=1,2,3$) gives

$$\frac{\big[-\bar{\Delta}^2\bar{\Delta}'^2(\overline{W}^2+4\overline{W}\overline{W}'+3\overline{W}'^2)+4\bar{\Delta}^2\bar{\omega}'^2\overline{W}'^2\big]\pi^3}{4\overline{W}^4\overline{W}'^4(\overline{W}+\overline{W}')^5} \quad (6.1.44)$$

The contributions from the even and odd-$\tilde{\omega}$ terms are the same, however, the odd-$\tilde{\omega}$ terms will have an extra minus sign due to the minus sign in the superconducting ladder. This means that the overall contribution will be zero.

6.1.4 The full 2-ladder contribution

The full 2 ladder contribution will come from the Type-I and Type-II diagrams as

$$3\left(\frac{ek_F}{\pi m\tau}\right)^4\delta_{\alpha\beta}\sum_Q\sum_{\omega,\omega'}\frac{\bar{\Delta}^2\bar{\Delta}'^2}{\overline{W}^4\overline{W}'^4}\frac{1}{(\overline{W}+\overline{W}')^2}\frac{1}{(DQ^2+W+W')^2} \quad (6.1.45)$$

6.2 3 ladder calculation

6.2.1 Type-I diagrams

The 3 ladder Type-I diagram is represented in figure 6.7 and will have 8 seperate contributions due to the different vertex combinations of the superconducting ladder. As in the previous section, the even and odd-$\tilde{\bar{\omega}}$ contributions will be taken seperately.

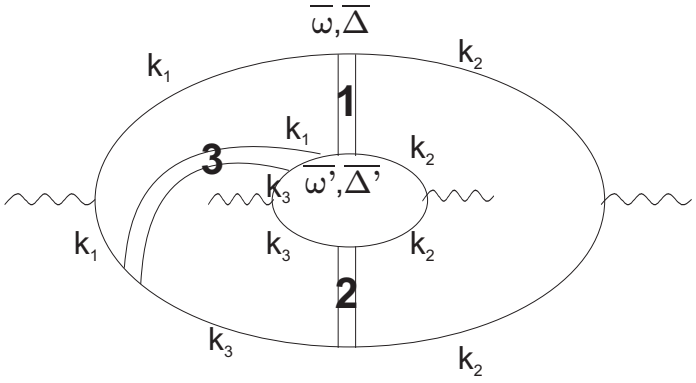

Figure 6.7

Before the constructing the inner and outer loop contributions it must be realised that the Green's functions $G(k_3{+}Q, \bar{\omega})$ and $G(k_1{+}Q, \bar{\omega}')$ must be expanded to second order. This will give

$$G(k_3 + Q, \bar{\omega}) \rightarrow \left(\frac{kV_F}{m}\right) G(k_3, \bar{\omega})\tau_3 G(k_3, \bar{\omega}) = \tilde{G}(k_3, \bar{\omega}) \tag{6.2.1}$$

and the same form for $G(k_1 + Q, \bar{\omega}')$. Each of the 4 diagrams for the odd-$\tilde{\bar{\omega}}$ contribution can be calculated and simplified to give

$$\frac{-4\bar{\omega}\bar{\omega}'}{\overline{WW'}}\mathrm{Tr}\{I_{1,2}\tau_3\tilde{G}(k_3, \bar{\omega})\tau_3\}\mathrm{Tr}\{I'_{2,3}\tau_3\tilde{G}(k_1, \bar{\omega}')\tau_3\} \tag{6.2.2}$$

where $I_{1,2}$ has been calculated in a previous section. The full even-$\tilde{\bar{\omega}}$ contribution can be simplified to give

$$\frac{4\bar{\omega}\bar{\omega}'}{\overline{W}^2\overline{W}'^2}\mathrm{Tr}\{I_{1,2}\tau_3\tilde{G}(k_3,\bar{\omega})(i\bar{\omega} - \bar{\Delta}\tau_1)\}\mathrm{Tr}\{I_{2,3}\tau_3\tilde{G}(k_1,\bar{\omega}')(i\bar{\omega}' - \bar{\Delta}'\tau_1)\} \quad (6.2.3)$$

Integrating the odd and even-$\tilde{\bar{\omega}}$ terms with respect to ξ_i (where $i = 1, 2, 3$) will give

$$(-1)\left(\frac{kV_F}{m}\right)^2 \frac{128\bar{\omega}^2\bar{\omega}'^2}{\overline{W}^2\overline{W}'^2(\overline{W}+\overline{W}')^9} + \left(\frac{kV_F}{m}\right)^2 \frac{128\bar{\omega}^2\bar{\omega}'^2}{\overline{W}^2\overline{W}'^2(\overline{W}+\overline{W}')^9} \quad (6.2.4)$$

where the $\left(\frac{kV_F}{m}\right)^2$ coefficient comes from the expansion of $G(k_3+Q,\bar{\omega})$ Both terms cancel to give the full 3 ladder Type-I contribution as zero.

6.2.2 Type-II diagrams

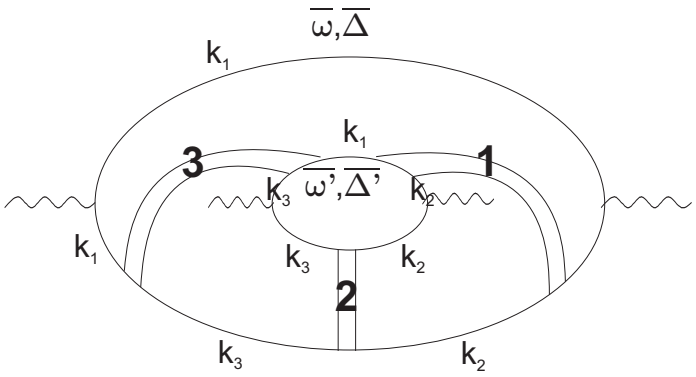

Figure 6.8

The 4 odd-$\tilde{\bar{\omega}}$ terms can be factorised to give

$$\frac{4i\bar{\omega}'}{\overline{W}'}\mathrm{Trace}\{\mathcal{F}_3^O\tau_3\frac{i\bar{\omega}+\bar{\Delta}\tau_1}{\overline{W}}\} \times \mathrm{Trace}\{\mathcal{F}_3^I\tau_3\} \quad (6.2.5)$$

and the 4 even-$\tilde{\bar{\omega}}$ terms can be simplified to give

$$\frac{-4\bar{\omega}'}{\overline{W}'^2}\text{Trace}\{\mathcal{F}_3^O\}\text{Trace}\{\mathcal{F}_3^I(\bar{\omega}' - i\bar{\Delta}\tau_1)\} \tag{6.2.6}$$

where $\mathcal{F}_3^O = \tau_3 G(k_1,\bar{\omega})G(k_1,\bar{\omega})G(k_1,\bar{\omega})\tau_3\tilde{G}(k_2,\bar{\omega})\tau_3\tilde{G}(k_3,\bar{\omega})$ and $\mathcal{F}_3^I = G(k_3,\bar{\omega}')\tau_3 G(k_2,\bar{\omega}')G(k_2,\bar{\omega}')\tau_3 G(k_1,\bar{\omega}')G(k_3,\bar{\omega}')$. As in the 3 ladder Type-I calculation, the even and odd-$\tilde{\bar{\omega}}$ terms give the same result after integrating with respect to $\xi_{1,2,3}$, with a minus sign difference.

This gives the full 3 ladder Type-II as having zero contribution.

6.2.3 Type-II with additional impurity line

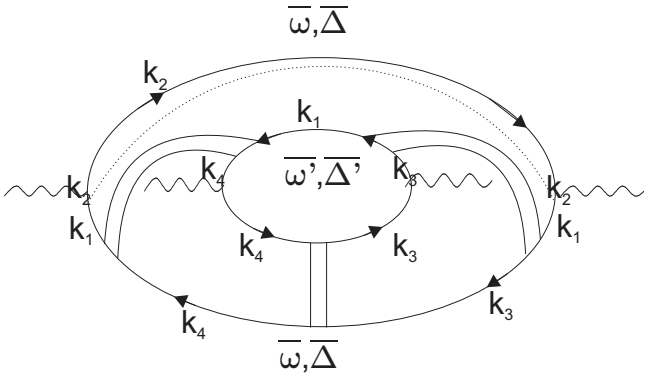

Figure 6.9

The 4 odd-$\tilde{\bar{\omega}}$ diagrams can be simplified to give

$$\frac{-2i\bar{\omega}'}{\overline{WW}'}\text{Trace}\{\mathcal{F}_{3i}^O\tau_3(i\bar{\omega} + \bar{\Delta}\tau_1)\}\text{Trace}\{\mathcal{F}_{3i}^I\tau_3\} \tag{6.2.7}$$

where $\mathcal{F}_{3i}^O = \tau_3 G(k_2,\bar{\omega})G(k_2,\bar{\omega})G(k_2,\bar{\omega})\tau_3 G(k_1,\bar{\omega})\tau_3\tilde{G}(k_3,\bar{\omega})\tau_3\tilde{G}(k_4,\bar{\omega})\tau_3 G(k_1,\bar{\omega})$

and $\mathcal{F}^I_{3i} = G(k_3,\bar{\omega}')\tau_3 G(k_4,\bar{\omega}')G(k_4,\bar{\omega}')\tau_3 G(k_1,\bar{\omega}')\tau_3 G(k_3,\bar{\omega}')$. This gives a zero contribution when the integral with respect to $\xi_{1,2,3}$ is taken. and the 4 even-$\tilde{\omega}$ diagrams can be factorised to give

$$\frac{-2i\bar{\omega}'}{\overline{W}'^2}\text{Trace}\{\mathcal{F}^O_{3i}\}\text{Trace}\{\mathcal{F}^I_{3i}(\bar{\omega}' - i\bar{\Delta}\tau_1)\} \tag{6.2.8}$$

which also gives a zero contribution after taking the integral.

6.2.4 The full 3-ladder contribution

The full 3 ladder contribution is zero.

6.3 4 ladder calculation

6.3.1 Type-I diagrams

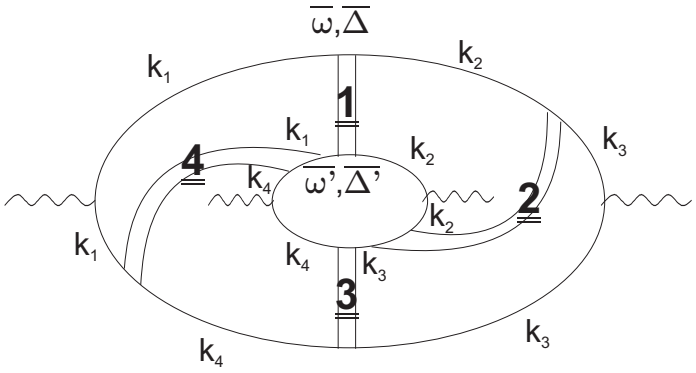

Figure 6.10

The 8 even-$\tilde{\bar{\omega}}$ terms can be cancelled and simplified into the form

$$\frac{-4\bar{\omega}^2\bar{\omega}'^2}{\overline{W}^2\overline{W}'^2}\Big[\mathrm{Trace}\{\tilde{G}(k_2,\bar{\omega})\tau_3 I_{1,3}\tau_3\tilde{G}(k_4,\bar{\omega})(i\bar{\omega}-\bar{\Delta}\tau_1)\Big] \times\Big[\mathrm{Trace}\{\tilde{G}(k_3,\bar{\omega}')\tau_3 I_{2,4}\tau_3\tilde{G}(k_1,\bar{\omega}')(i\bar{\omega}'-\bar{\Delta}'\tau_1)\Big] \tag{6.3.1}$$

and the 8 odd-$\tilde{\bar{\omega}}$ terms can be written as

$$\frac{-4\bar{\omega}\bar{\omega}'}{\overline{W}\overline{W}'}\mathrm{Trace}\{\tilde{G}(k_2,\bar{\omega})\tau_3 I_{1,3}\tau_3\tilde{G}(k_4,\bar{\omega})\tau_3\}\mathrm{Trace}\{\tilde{G}(k_3,\bar{\omega}')\tau_3 I_{2,4}\tau_3\tilde{G}(k_1,\bar{\omega}')\tau_3\} \tag{6.3.2}$$

Taking the integrals with respect to $\xi_{1,2,3,4}$ will give the final 4 ladder contribution as

$$\frac{-512\bar{\omega}^2\bar{\omega}'^2\pi^4}{\overline{W}^2\overline{W}'^2(\overline{W}+\overline{W}')^{12}}+\frac{512\bar{\omega}^2\bar{\omega}'^2\pi^4}{\overline{W}^2\overline{W}'^2(\overline{W}+\overline{W}')^{12}} \tag{6.3.3}$$

which both cancel to give zero.

6.3.2 Type-II diagrams

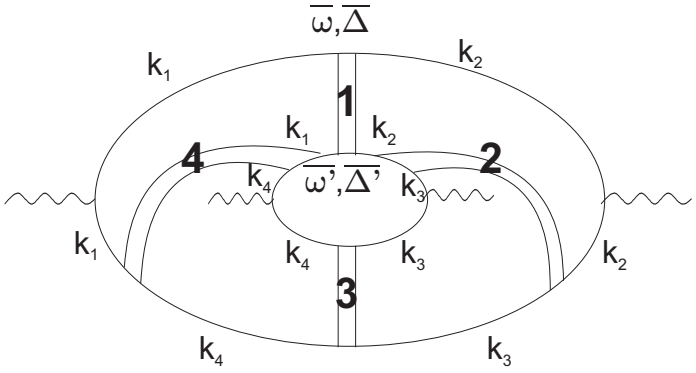

Figure 6.11

The even-$\tilde{\bar{\omega}}$ terms can be simplified to give

$$\frac{-4\bar{\omega}\bar{\omega}'}{\overline{W}^2\overline{W}'^2}\text{Trace}\{I_{1,2}\tau_3\tilde{G}(k_3,\bar{\omega})\tau_3\tilde{G}(k_4,\bar{\omega})(i\bar{\omega}-\bar{\Delta}\tau_1)\}$$
$$\times\text{Trace}\{I_{3,4}\tau_3\tilde{G}(k_1,\bar{\omega}')\tau_3\tilde{G}(k_2,\bar{\omega}')(i\bar{\omega}-\bar{\Delta}\tau_1)\} \tag{6.3.4}$$

and the odd-$\tilde{\bar{\omega}}$ terms can be simplified to give

$$\frac{-4\bar{\omega}\bar{\omega}'}{\overline{W}\overline{W}'}\text{Trace}\{\tau_3 I_{1,2}\tau_3\tilde{G}(k_3,\bar{\omega})\tau_3\tilde{G}(k_4,\bar{\omega})\}\text{Trace}\{\tau_3 I_{3,4}\tau_3\tilde{G}(k_1,\bar{\omega}')\tau_3\tilde{G}(k_2,\bar{\omega}')\} \tag{6.3.5}$$

Integrating both components will give

$$\frac{512\pi^4\bar{\omega}^2\bar{\omega}'^2}{\overline{W}^2\overline{W}'^2(\overline{W}+\overline{W}')^{12}}+\frac{-512\pi^4\bar{\omega}^2\bar{\omega}'^2}{\overline{W}^2\overline{W}'^2(\overline{W}+\overline{W}')^{12}} \tag{6.3.6}$$

Which both cancel to give zero.

6.3.3 The full 4-ladder contribution

The full 4 ladder contribution is zero.

6.4 Full Superconducting UCF contribution

The previous sections have shown that the only contribution to the full superconducting fluctuations will come from the 2-ladder Type-I and 2-ladder Type-II calculations. Recall that the only contribution in the normal-state DC limit is also the 2-ladder Type-I and II diagrams (right sign contributions). This possesses the question whether the results of the normal-state diagrams can give any insight into the superconducting contributions, which will briefly be discussed in chapter

7.2

The full superconducting contribution is given as

$$3\left(\frac{ek_F}{m\tau}\right)^4 \delta_{\alpha\beta} \sum_Q \sum_{\omega,\omega'} \frac{\bar{\Delta}^2 \bar{\Delta}'^2}{W^4 W'^4} \frac{1}{(W+W')^2} \frac{1}{(DQ^2+W+W')^2} \tag{6.4.1}$$

The next step is to transform $\bar{\omega}, \bar{\Delta} \to \omega, \Delta$ so that the integrals can be evaluated. In chapter 4.3 it was shown that $\bar{\Delta}/\bar{\omega} = \Delta/\omega$ and that in the limit $\overline{W} + \overline{W} \approx 1/\tau$ and $1/\overline{W} \approx 1/\tau$ and $1/\overline{W}' \approx 1/\tau$. Transforming and taking these limits the response function can be written as

$$\left(\frac{ek_F}{\pi m\tau}\right)^4 \sum_Q \sum_{\omega,\omega'} \frac{\Delta^2 \Delta'^2}{W^2 W'^2} \frac{1}{(DQ^2+W+W')^2} \tag{6.4.2}$$

The Q integral can be taken in d-dimensions using the identity (5.2.3) to give

$$\sum_Q \frac{1}{(DQ^2+W+W')^2} = \frac{\pi\Gamma(2-d/2)}{D^{d/2}} (W+W')^{d/2-2} \tag{6.4.3}$$

This will give the response function as

$$\left(\frac{ek_F}{m}\right)^4 \left(\frac{1}{4\pi N(0)\tau^2}\right)^2 N(0)^2 \tau^6 \frac{\pi\Gamma(2-d/2)}{D^{d/2}} \times \sum_{\omega,\omega'} \frac{\Delta^2 \Delta'^2}{(\Delta^2+\omega^2)(\Delta'^2+\omega'^2)} \frac{1}{(\sqrt{\Delta^2+\omega^2}+\sqrt{\Delta'^2+\omega'^2})^{2-d/2}} \tag{6.4.4}$$

In 2-dimensions one can make the substitution $\omega = \Delta x$ and $\omega' = \Delta' y$ and this can

then be simplified to solving the equation

$$\int\int_{-\infty}^{\infty} \frac{1}{(x^2+1)(y^2+1)} \frac{\Delta\Delta'}{\Delta\sqrt{x^2+1}+\Delta'\sqrt{y^2+1}} dxdy \tag{6.4.5}$$

By using the substitutions $x = \tan\theta$ and $y = \tan\phi$ can be simplified to

$$\int\int_{0}^{\pi/2} \frac{\Delta\Delta'}{\Delta\sec\theta+\Delta'\sec\phi} d\theta d\phi = \int\int_{0}^{\pi/2} \frac{\Delta\cos\theta\cos\phi}{\cos\theta+\frac{\Delta}{\Delta'}\cos\phi} d\theta d\phi \tag{6.4.6}$$

Solving the θ integral first and for ease of annotation will denote $a = \frac{\Delta}{\Delta'}\cos\phi$ to give

$$\int_{0}^{\pi/2} \frac{a\Delta'\cos\theta}{\cos\theta+a} d\theta = \frac{\pi\Delta' a}{2} - \int_{0}^{\pi/2} \frac{a^2}{\cos\theta+a} d\theta \tag{6.4.7}$$

The second term above can be simplified by using the substitution $t = \tan\theta/2$ and by using the identity $\cos\theta = \frac{1-t^2}{1+t^2}$ to give

$$\frac{\pi\Delta' a}{2} - \Delta' \int_{0}^{1} \frac{2a^2}{(a+1)+(a-1)t^2} dt \tag{6.4.8}$$

Separating into partial fractions, integrating each term and simplifying will give

$$\frac{\pi\Delta' a}{2} - \frac{\Delta' a^2}{\sqrt{a^2-1}} \ln\left[\frac{1+\frac{\sqrt{a+1}}{\sqrt{a-1}}}{1-\frac{\sqrt{a+1}}{\sqrt{a-1}}}\right] \tag{6.4.9}$$

The next step is to complete the ϕ integral which will be of the form

$$\int_{0}^{\pi/2} \frac{\pi\Delta\cos\phi}{2} - \frac{\frac{\Delta^2}{\Delta'}\cos^2\phi}{\sqrt{1-\frac{\Delta}{\Delta'}\cos^2\phi}} \ln\left[\frac{1+\frac{\sqrt{1+\frac{\Delta}{\Delta'}\cos\phi}}{\sqrt{1-\frac{\Delta}{\Delta'}\cos\phi}}}{1-\frac{\sqrt{1+\frac{\Delta}{\Delta'}\cos\phi}}{\sqrt{1-\frac{\Delta}{\Delta'}\cos\phi}}}\right] d\phi \tag{6.4.10}$$

By making the substitution $\frac{\Delta}{\Delta'}\cos\phi = \cos m$ then this becomes

$$\int_0^{\pi/2} \frac{\pi\Delta\cos\phi}{2} d\phi - \int_0^{\pi/2} \frac{\Delta\cos^2 m}{\sin m} \ln\left[\frac{1+\tan\frac{m}{2}}{1-\tan\frac{m}{2}}\right] dm \tag{6.4.11}$$

The first term will give $\pi/2$ and the second term can be manipulated into the form

$$\int_0^{\pi/2} \frac{\Delta\cos^2 m}{2\sin m} \ln\left[\frac{(\cos(m/2)+\sin(m/2))^2}{(\cos(m/2)-\sin(m/2))^2}\right] dm = \int_0^{\pi/2} \frac{\Delta\cos^2 m}{2\sin m} \ln\left[\frac{1+\sin m}{1-\sin m}\right] dm \tag{6.4.12}$$

and expanded out to give

$$\int_0^{\pi/2} \cos^2 m \left[1 + \frac{\sin^2 m}{3} + \frac{\sin^4 m}{5} + ...\right] dm = \mathcal{I}_0 + \frac{\mathcal{I}_1}{3} + \frac{\mathcal{I}_2}{5} + ... \tag{6.4.13}$$

where

$$\mathcal{I}_n = \int_0^{\pi/2} \cos^2 m \sin^{2n} m dm \tag{6.4.14}$$

By using integration by parts this will give the solution as

$$\frac{\pi}{2}\left[\frac{1}{2} + \frac{1}{2\times 3\times 4} + \frac{1\times 3}{2\times 4\times 5\times 6} + \frac{1\times 3\times 5}{2\times 4\times 6\times 7\times 8} + ...\right] \tag{6.4.15}$$

The infinite series can be evaluated by using the expansion

$$\frac{1}{\sqrt{1-x^2}} = 1 + \frac{1}{2}x^2 + \frac{1\times 3}{2\times 4}x^4 + ... \tag{6.4.16}$$

and

$$\int\int \frac{1}{\sqrt{1-x^2}} = \left[\frac{1}{2}x^2 + \frac{1}{2\times 3\times 4}x^4 + \frac{1\times 3}{2\times 4\times 5\times 6}x^6 + \frac{1\times 3\times 5}{2\times 4\times 6\times 7\times 8}x^8 + ...\right]$$

$$= x\sin^{-1}x + \sqrt{1-x^2} \tag{6.4.17}$$

Evaluating between $x = 0$ and $x = 1$ will give the this integral as

$$\frac{\pi}{2}\left(\frac{\pi}{2} - 1\right) \tag{6.4.18}$$

This will give the full solution in 2-dimensions as

$$\frac{\pi\Delta}{2} - \frac{\Delta\pi}{4}(-2+\pi) = \Delta\left(\pi - \frac{\pi^2}{4}\right) \tag{6.4.19}$$

which gives the final result in 2 dimensions as

$$\left(\frac{ek_F}{m}\right)^4 \left(\frac{1}{4\pi N(0)\tau^2}\right)^2 N(0)^2\tau^6 \frac{1}{D}\Delta\left(\pi - \frac{\pi^2}{4}\right) \tag{6.4.20}$$

which, when simplified, will give

$$\langle(\delta n_s)^2\rangle \left(\frac{e^2}{m}\right)^2 = A\frac{e^4k_F^4\tau^2}{m^4}\frac{\Delta}{D} \tag{6.4.21}$$

where $A = (1-\pi/4)/4\pi$. However, it must be realised that a factor of $Volume^{-1}$ has not been included in the Q-integral. In previous calculations this was not needed as the factor V cancels throughout the calculation, but in the UCF calculation it must be included as there is no cancellation [4]. This can be explained

by using the argument that

$$\int \frac{d^d Q}{(DQ^2)^2} \to Q^{d-4} \to L^{d-4} \tag{6.4.22}$$

which would imply that $(\delta\sigma)^2 \sim L^{4-d}$ and therefore $(\delta g)^2 \sim L^d$. We know that $(\delta g)^2$ should be $O(1)$ which implies that the result should be divided by a factor of the volume, V. This will give $V = L^d$ where L is the size of the system, and in 2-dimensions this will give

$$\delta n_s^2 = A \frac{k_F^4 \tau^2}{m^2} \frac{\hbar}{\zeta(0)^2 L^2} \tag{6.4.23}$$

where $\zeta(0) = \sqrt{D\hbar/\Delta}$ and is the length scale at which the fluctuations of δn_s will become independent.

6.4.1 Superfluid density calculation

In the superconducting case the contribution from the Drude conductivity will give the electromagnetic function as

$$K(Q = 0, 0) = \frac{n_s e^2}{m} = \frac{\pi n e^2 \tau}{m} T \sum_{\omega} \frac{\Delta^2}{\Delta^2 + \omega^2} \tag{6.4.24}$$

Transforming the summation into an integral and evaluating will give

$$\langle n_s \rangle = \pi \Delta n \tau \tag{6.4.25}$$

which is the average superfluid density of the system. By using the substitution

$$n = \frac{2\pi k_F^2}{(2\pi)^2} = \frac{k_F^2}{2\pi} \qquad \text{for} \qquad d = 2 \tag{6.4.26}$$

this can be written as

$$n_s = \frac{\Delta k_F^2 \tau}{4} \tag{6.4.27}$$

The fluctuations were calculated in the previous subsection and evaluating will give

$$\delta n_s = A \frac{k_F^4 \tau^2}{m^2} \frac{\hbar}{\zeta(0)^2 L^2} = A \frac{D^2}{\zeta(0)^2 L^2} \tag{6.4.28}$$

A negative superfluid density may be plausible when the fluctuations in n_s become comparable to the average value, which can be evaluated by the fluctuations δn_s divided by the average $\langle n_s \rangle$, given as

$$\left\langle \frac{(\delta n_s)^2}{(n_s)^2} \right\rangle = \frac{4AD^2}{\Delta^2 \tau^2} \frac{1}{\zeta(0)^2 L^2 k_F^4} = \frac{e^4 D^2}{\Delta^2} \frac{1}{\langle G \rangle^2} \frac{1}{\zeta(0)^2 L^2 p_F^4} \tag{6.4.29}$$

where $\langle G \rangle$ is the conductance of a normal metal.

Chapter 7

CONCLUSION

7.1 Conclusion

The results of chapter 5 show that there are significant cancellations in calculating the DC limit from the AC results of the normal state UCF diagrams. This shows that one cannot simply derive the AC results from the DC diagrams.

The results in chapter 6 were calculated using exact methods of superconducting Green's function on all diagrammatic UCF diagrams. This has reproduced the assumptions of Spivak and Zyuzin which were quoted in their 1988 research paper [7]. The agreement between the results show that the fluctuations in n_s can become comparable to the mean value which gives rise to the possibility of regions of negative superfluid densities. This implies that at the SIT transition there may exist islands of a local negative superfluid density which will result in Aharonov-Bohm oscillations of $h/4e$ and a reversal of the Josephson current.

It must also be noted that the contributing diagrams in the wrong sign cancellations also cancel one another in the superconducting UCF calculations. Many research papers have questioned the idea of deriving any superconducting diagrams purely from the AC normal state results. However, this thesis shows that there

may exist a link between the DC normal state diagrams and the superconducting contributions. Although this may just be a coincidence in the calculations of this thesis it is a possibility of further study; and in the next subsection the relation between the AC normal state and the superconducting diagrams will be shown for possible further study for the reader.

7.2 Further Study

A method known as the Exact Eigenstates Method was originally proposed in 1989 by Ramakrishnan [35] which uses a mathematical model to construct the results of the superconducting diagrams from the normal state AC diagrams. This method has not be used in this thesis as the derivation from the AC UCF diagrams will be more complex than evaluating the results deriving them from basic principles. However, throughout this thesis it has been shown that the only diagrams which contribute in the normal state DC diagrams are also the only diagrams which contribute in the superconducting regime. This may imply that the superconducting diagrammatic contributions can be derived directly from the normal state DC diagrams. This is a possible area for further study. As finalization, the calculation of the reduction formula, which relates the normal state AC rsults to the superconducting results, will be derived for the Drude conductivity bubble.

7.2.1 Calculating the reduction formula using Kubo Diagrammatics

The *Exact Eigenstates Method* (EEM) is a mathematical formula which relates the superconducting-state electromagnetic response function in terms of the normal-

state electromagnetic response function. This can then be related to the correction in the superconducting number density. From previous sections, we have ruthlessly calculated the superconducting response function for weak localisation and found it to be a very long and rigorous calculation. The EEM will give the reader a much easier way to calculate such a diagram - as, essentially, all that is calculated is the normal-state diagram and the superconducting representation is given for 'free'. The equation relating the superconducting representation to the normal-state representation will be denoted as the *Reduction Formula*

This method has a major assumption that the order parameter, Δ, is position independent.

Normal-state

The easiest way to derive the *Reduction Formula* will be to use the full Green's function on the simplest model - in this case the conductivity bubble.

Before proceeding one must realise that the Green's function is now the full, non-averaged Green's function which takes the form

$$G(\mathbf{r},\mathbf{r}';i\omega_l)=\sum_m \frac{\phi_m(\mathbf{r})\phi_m(\mathbf{r}')}{i\omega-\epsilon_m} \tag{7.2.1}$$

where $\phi_m(\mathbf{r})$ corresponds to the eigenstates of the system.

Substituting the full Green's function into the Kubo formula will give

$$K_{\alpha\beta}(\mathbf{r},\mathbf{r}';i\Omega)=\left(\frac{e}{2m}\right)^2 T\sum_\omega\sum_{m,n}\frac{1}{i\omega-\xi_m}\frac{1}{i\omega+i\Omega-\xi_n}p_{nm\alpha}(\mathbf{r})p_{nm\beta}(\mathbf{r}') \tag{7.2.2}$$

where

$$p_{nm\alpha}(\mathbf{r}) = \phi_n(\mathbf{r})\frac{\partial}{\partial r_\alpha}\phi_m(\mathbf{r}) - \phi_m(\mathbf{r})\frac{\partial}{\partial r_\alpha}\phi_n(\mathbf{r}) \tag{7.2.3}$$

are the current matrix elements. Fistly, change variables to $\xi_n = \xi$ and $\xi_m = \xi' + \xi$ and then approximate the energy levels by a continuous spectrum, $\sum_n = 2N(0)\int d\xi$ to give

$$K_{\alpha\beta}(\mathbf{r},\mathbf{r}';i\Omega) = \frac{N(0)e^2}{2m^2}T\sum_\omega\sum_m\int d\xi\frac{1}{i\omega-\xi-\xi'}\frac{1}{i\omega+i\Omega-\xi}p_{nm\alpha}(\mathbf{r})p_{nm\beta}(\mathbf{r}') \tag{7.2.4}$$

The integral contains two poles, $\xi = i\varepsilon - \xi'$ and $\xi = i\varepsilon + i\Omega$. The only contribution will be when there is a pole either side of the real axis which implies that ε and $\varepsilon + \Omega$ must have opposite sign. This condition will be satisfied by introducing the heaviside function, Θ, which will be added at the end of the calculation. Using the residue theorem and closing the contour in the UHP

$$\begin{aligned} Res(f, i\xi + i\Omega) &= 2\pi i\frac{(\xi - i\omega - i\Omega)}{(i\omega-\xi-\xi')[-(\xi-i\omega-i\Omega)]} \\ &= \left[\frac{-2\pi i}{i\omega-\xi-\xi'}\right]_{\xi=i\omega+i\Omega} \\ &= \frac{2\pi i}{i\Omega+\xi'} \end{aligned} \tag{7.2.5}$$

The full electromagnetic response will become

$$K_{\alpha\beta}(\mathbf{r},\mathbf{r}';i\Omega) = \frac{\pi i N(0)e^2}{2m^2}T\sum_\omega\sum_m\frac{2\pi i}{i\Omega+\xi'}\Theta(-\omega)\Theta(\omega+\Omega)p_{nm\alpha}(\mathbf{r})p_{nm\beta}(\mathbf{r}') \tag{7.2.6}$$

We know that $\sum_\omega \Theta(-\omega)\Theta(\omega+\Omega) = \frac{\Omega}{2\pi}$ and $\sigma(i\Omega) = K(i\Omega)/\Omega$ we get

$$\sigma_{\alpha\beta}(\mathbf{r},\mathbf{r}';i\Omega) = \frac{iN(0)e^2}{2m^2}\sum_m \frac{1}{i\Omega+\xi_m-\xi_n} p_{nm\alpha}(\mathbf{r})p_{nm\beta}(\mathbf{r}') \tag{7.2.7}$$

This gives us the normal-state conductivity for the conduction bubble using the full Green's function. The next step is to calculate the superconducting representation and then try to relate it to the normal conductivity that has just been derived.

Superconducting-state

In the superconducting case one must introduce the *Pauli Matricies*, $\tau_{1,2,3}$, together with the identity, τ_0, to obtain

$$K_{\alpha\beta}(\mathbf{r},\mathbf{r}';i\Omega) = \left(\frac{e}{2m}\right)^2 T\sum_\omega\sum_{m,n} Tr\left[\frac{1}{i\omega-\xi_m\tau_3-\Delta\tau_1}\frac{1}{i\omega+i\Omega-\xi_n\tau_3-\Delta\tau_1}\right] p_{nm\alpha}(\mathbf{r})p_{nm\beta}(\mathbf{r}') \tag{7.2.}$$

This can be simplified using the identity $\tau_\alpha\tau_\beta = i\omega_{\alpha\beta\gamma}\tau_\gamma$ (ie $\varepsilon_{123}=1$, $\varepsilon_{213}=-1$ etc) to give

$$\frac{1}{i\omega-\xi_m\tau_3-\Delta\tau_1}\frac{1}{\omega+i\Omega-\xi_n\tau_3-\Delta\tau_1} = \frac{-\omega(\omega+\Omega)+(\xi+\xi')\xi+\Delta^2}{[(\xi+\xi')^2+\Delta^2+\omega^2][\xi^2+\Delta^2+(\omega+\Omega)^2]} \tag{7.2.9}$$

Using the usual substitution $\sum_n = 2N(0)\int d\xi$ then the electromagnetic response becomes

$$\left(\frac{e}{2m}\right)^2 2N(0)T\sum_\omega\sum_m \int d\xi \frac{-\omega(\omega+\Omega)+(\xi+\xi')\xi+\Delta^2}{[(\xi+\xi')^2+\Delta^2+\omega^2][\xi^2+\Delta^2+(\omega+\Omega)^2]} p_{nm\alpha}(\mathbf{r})p_{nm\beta}(\mathbf{r}')$$

The integral can now be solved using the residue theorem as

$$\int d\xi \frac{-\omega(\omega+\Omega)+(\xi+\xi')\xi+\Delta^2}{(\xi+\xi'-iW)(\xi+\xi'+iW)(\xi+iW')(\xi-iW')}$$

where $W=\sqrt{\Delta^2+\omega^2}$ and $W'=\sqrt{\Delta^2+(\omega+\Omega)^2}$. Closing the contour in the UHP will enclose the poles $\xi=iW'$ and $\xi=iW-\xi'$ giving the residues as

$$\sum_{\xi^*} Res(f,\xi^*)=\frac{1}{2iWW'}\left[(A+WW')\frac{(W+W')}{(\xi'^2+(W+W')^2)}\right]$$

where $A=\Delta^2-\omega(\omega+\Omega)$.

Doing partial fractions will give

$$\sum_{\xi^*} Res(f,\xi^*) = \frac{(A+WW')}{2iWW'}\left[\frac{1}{(\xi'+i(W+W'))}-\frac{1}{(\xi'-i(W+W'))}\right]$$

Notice that the final two terms will give the same result when summed over all ξ and so this finally reduces down to

$$K_{\alpha\beta}(\mathbf{r},\mathbf{r}';i\Omega) = \frac{N(0)e^2 i}{2m^2}\pi T\sum_{\omega}\sum_{m}\left[1+\frac{\Delta^2-\omega(\omega+\Omega)}{WW'}\right] \frac{1}{iW+iW'+\xi_m-\xi_n}p_{nm\alpha}(\mathbf{r})p_{nm\beta}(\mathbf{r}') \tag{7.2.10}$$

This formula can be compared to the normal-state EEM formula and the reduction formula will be given as

$$K(0,i\Omega)=\pi T\sum_{\omega}\left[1+\frac{\Delta^2-\omega(\omega+\Omega)}{WW'}\right]\sigma(iW+iW') \tag{7.2.11}$$

where $K(0,i\Omega)$ is the electromagnetic response function in the superconducting

regime and σ is the conductivity in the normal state AC regime. Therefore, this shows that by replacing Ω with $iW + iW'$ in the normal state regime and by adding a prefactor of $\left[1 + \frac{\Delta^2 - \omega(\omega+\Omega)}{WW'}\right]$ then this will give the full superconducting electromagnetic response function.

Appendix A

MULTIPLY GREEN'S FUNCTION INTEGRAL

A.1 Green's functions identity

Throughout the normal state UCF calculation the assumption has been used that

$$N(0)\int d\xi[G^-]^m[G^+]^n = 2\pi N(0)\tau \begin{pmatrix} m+n-2 \\ m-1 \end{pmatrix} (-i\tau)^{m-1}(i\tau)^{n-1} \quad \text{(A.1.1)}$$

This result will be rigorously proved using Cauchy's Residue theorem together with complex contour integration in this section.

Recalling the form of the retarded and advanced Green's function, we can write

$$\int d\xi[G^-]^m[G^+]^n = \int d\xi \frac{1}{(i\omega - \xi - \frac{i}{2\tau})^m} \frac{1}{(i\omega - \xi + \frac{i}{2\tau})^n} \quad \text{(A.1.2)}$$

This integral can be performed as the sum of residues in the upper and lower-half

plane as

$$2\pi i \frac{d}{d\xi^{n-1}} \left[\frac{1}{(i\omega - \xi - \frac{i}{2\tau})^m} \right]_{\xi \to i\omega + i/2\tau} + 2\pi i \frac{d}{d\xi^{m-1}} \left[\frac{1}{(i\omega - \xi + \frac{i}{2\tau})^m} \right]_{\xi \to i\omega + i/2\tau} \tag{A.1.3}$$

Taking the differential and substituting the poles will give

$$2\pi i(-1)^{n-1}(-i\tau)^{m+n-1}[m(m+1)(m+2)...(m+n-1)] + 2\pi i(-1)^{m-1}(i\tau)^{m+n-1}[n(n+1)(n+2)...(m+n-1)] \tag{A.1.4}$$

By factorising out a factor of $i\tau$ and then substituting $(i\tau)^{m+n-2} = (i\tau)^{m-1}(i\tau)^{n-1}$ one can write this as

$$2\pi\tau(-i\tau)^{m-1}(i\tau)^{n-1}\left[m(m+1)(m+2)...(m+n-1) - n(n-1)(n-2)...(m+n-1)\right]$$

which can finally be simplified into the form

$$2\pi\tau \begin{pmatrix} m+n-2 \\ m-1 \end{pmatrix} (-i\tau)^{m-1}(i\tau)^{n-1} \tag{A.1.5}$$

This proves the result given at the beginning of this section which is used in chapters 3 and 5.

Appendix B

SUPERCONDUCTING UCF

B.1 2 ladder superconducting UCF calculation

B.1.1 Type-II

The odd-$\tilde{\bar{\omega}}$ will be calculated by solving

$$\mathrm{Tr}\{G(k_1,\bar{\omega})G(k_1,\bar{\omega})\tau_3 G(k_2,\bar{\omega})\tau_3 G(k_1,\bar{\omega})\tau_3\frac{(i\bar{\omega}+\bar{\Delta}\tau_1)}{W}\}$$
$$\times\,\mathrm{Tr}\{G(k_2,\bar{\omega}')G(k_2,\bar{\omega}')\tau_3 G(k_1,\bar{\omega}')\tau_3 G(k_2,\bar{\omega}')\tau_3\frac{(i\bar{\omega}'+\bar{\Delta}'\tau_1)}{W'}\}$$

which will give the numerator

$$\Big[-W^2(\xi_1^2+W^2)(\xi_1+\xi_2)+2\bar{\omega}^2W^2(\xi_1+\xi_2)-2\bar{\omega}^2\xi_1(\xi_1\xi_2-W^2)\Big]$$
$$\times\Big[-W'^2(\xi_2^2+W'^2)(\xi_1+\xi_2)+2\bar{\omega}'^2W'^2(\xi_1+\xi_2)-2\bar{\omega}'^2\xi_2(\xi_1\xi_2-W'^2)\Big]$$

The even-$\tilde{\bar{\omega}}$ will be calculated by solving

$$\mathrm{Tr}\{G(k_1,\bar{\omega})G(k_1,\bar{\omega})\tau_3 G(k_2,\bar{\omega})\tau_3 G(k_1,\bar{\omega})\}\mathrm{Tr}\{G(k_2,\bar{\omega}')G(k_2,\bar{\omega}')\tau_3 G(k_1,\bar{\omega}')\tau_3 G(k_2,\bar{\omega}')\}$$

(B.1.1)

which will give the numerator

$$\frac{1}{WW'}\Big[(\xi_1^2+W^2)(\xi_1\xi_2-W^2)-2\bar{\omega}^2(\xi_1\xi_2-W^2)-2\bar{\omega}^2\xi_1(\xi_1+\xi_2)\Big]$$
$$\times\Big[(\xi_2^2+W'^2)(\xi_1\xi_2-W'^2)-2\bar{\omega}'^2(\xi_1\xi_2-W'^2)-2\bar{\omega}'^2\xi_2(\xi_1+\xi_2)\Big]$$

with both even and odd contributions having a denominator

$$(\xi_1^2+W^2)^3(\xi_1^2+W'^2)(\xi_2^2+W^2)(\xi_2^2+W'^2)^3 \tag{B.1.2}$$

B.1.2 Type-II additional impurity line

Odd-$\tilde{\bar{\omega}}$ contribution

The odd-$\tilde{\bar{\omega}}$ term is given by

$$\mathrm{Tr}\{\mathcal{F}^O\tau_3\frac{(i\bar{\omega}-\bar{\Delta}\tau_1)}{W}\}\mathrm{Tr}\{\mathcal{F}^I\tau_3\frac{(i\bar{\omega}'-\bar{\Delta}'\tau_1)}{W'}\} \tag{B.1.3}$$

the first trace term can be calculated to give

$$-W^2(\xi_2+W^2)(\xi_1+\xi_2)(\xi_1\xi_3-W^2)-W^2(\xi_2+W^2)(\xi_1+\xi_3)(\xi_1\xi_2-W^2)$$
$$-2\bar{\omega}^2\xi_2(\xi_1\xi_2-W^2)(\xi_1\xi_3-W^2)+2\bar{\omega}^2W^2\xi_2(\xi_1+\xi_2)(\xi_1+\xi_3)$$
$$+2\bar{\omega}^2W^2(\xi_1+\xi_2)(\xi_1\xi_3-W^2)+2\bar{\omega}^2W^2(\xi_1+\xi_3)(\xi_1\xi_2-W^2)$$

and the second trace term can be calculated to give

$$- W'^2(\xi_3 + W'^2)(\xi_1 + \xi_3) - 2\bar{\omega}'^2\xi_3(\xi_1\xi_3 - W'^2) + 2\bar{\omega}'^2W'^2(\xi_1 + \xi_3) \quad \text{(B.1.4)}$$

Multiplying both of the trace terms together and integrating with respect to ξ_i (where $i = 1, 2, 3$) gives the final odd-$\tilde{\bar{\omega}}$ as

$$(-1)\frac{\big[-\bar{\Delta}^2\bar{\Delta}'^2(W^2 + 4WW' + 3W'^2) + 4\bar{\Delta}^2\bar{\omega}'^2W'^2\big]\pi^3}{4W^4W'^4(W + W')^5} \quad \text{(B.1.5)}$$

The (-1) coefficient is due to the minus sign in the superconducting ladder.

Even-$\tilde{\bar{\omega}}$ contribution

The Even-$\tilde{\bar{\omega}}$ will be calculated by solving

$$\mathrm{Tr}\{\mathcal{F}^O\}\mathrm{Tr}\{\mathcal{F}^I\} \quad \text{(B.1.6)}$$

The first trace term will become

$$\begin{aligned}(\xi_2 + W^2)(\xi_1\xi_2 - W^2)(\xi_1\xi_3 - W^2) - W^2(\xi_2 + W^2)(\xi_1 + \xi_2)(\xi_1 + \xi_3)\\ - 2\bar{\omega}^2(\xi_1\xi_2 - W^2) + 2\bar{\omega}^2W^2(\xi_1 + \xi_2)(\xi_1 + \xi_3)\\ - 2\bar{\omega}\xi_2(\xi_1 + \xi_2)(\xi_1\xi_3 - W^2) - 2\bar{\omega}^2\xi_2(\xi_1 + \xi_3)(\xi_1\xi_2 - W^2)\end{aligned}$$

and the second trace becomes

$$(\xi_3 + W'^2)(\xi_1\xi_3 - W'^2) - 2\bar{\omega}'^2(\xi_1\xi_3 - W'^2) - 2\bar{\omega}'^2\xi_3(\xi_1 + \xi_3) \quad \text{(B.1.7)}$$

Integrating with respect to ξ_i (where $i = 1, 2, 3$) gives

$$\frac{\big[-\bar{\Delta}^2\bar{\Delta}'^2(W^2+4WW'+3W'^2)+4\bar{\Delta}^2\bar{\omega}'^2W'^2\big]\pi^3}{4W^4W'^4(W+W')^5} \tag{B.1.8}$$

The contributions from the even and odd-$\tilde{\bar{\omega}}$ terms are the same, however, the odd-$\tilde{\bar{\omega}}$ terms will have an extra minus sign due to the minus sign in the superconducting ladder. This means that the overall contribution will be zero.

B.2 3 ladder Superconducting UCF calculation

B.2.1 Type-I

Odd-$\tilde{\bar{\omega}}$ terms

The inner and outer loop contributions, after commuting into an appropriate form, are given here below.

Configuration	Outer Loop	Inner Loop
$\tau_3\tau_3\tilde{\bar{\omega}}$	$I_{1,2}\tau_3\tilde{G}(k_3,\bar{\omega})\tau_3\frac{i\bar{\omega}+\bar{\Delta}\tau_1}{W}$	$I_{2,3}\tau_3\tilde{G}(k_1,\bar{\omega}')\tau_3\frac{i\bar{\omega}'+\bar{\Delta}'\tau_1}{W'}$
$\tau_3\tilde{\bar{\omega}}\tau_3$	$I_{1,2}\tau_3\tilde{G}(k_3,\bar{\omega})\tau_3\frac{i\bar{\omega}+\bar{\Delta}\tau_1}{W}$	$I_{2,3}\tau_3\tilde{G}(k_1,\bar{\omega}')\tau_3\frac{i\bar{\omega}'-\bar{\Delta}'\tau_1}{W'}$
$\tilde{\bar{\omega}}\tau_3\tau_3$	$I_{1,2}\tau_3\tilde{G}(k_3,\bar{\omega})\tau_3\frac{i\bar{\omega}-\bar{\Delta}\tau_1}{W}$	$I_{2,3}\tau_3\tilde{G}(k_1,\bar{\omega}')\tau_3\frac{i\bar{\omega}'+\bar{\Delta}'\tau_1}{W'}$
$\tilde{\bar{\omega}}\tilde{\bar{\omega}}\tilde{\bar{\omega}}$	$-I_{1,2}\tau_3\tilde{G}(k_3,\bar{\omega})\tau_3\frac{i\bar{\omega}-\bar{\Delta}\tau_1}{W}$	$-I_{2,3}\tau_3\tilde{G}(k_1,\bar{\omega}')\tau_3\frac{i\bar{\omega}'-\bar{\Delta}'\tau_1}{W'}$

These different contributions can be factorised and simplified to give the full odd-$\tilde{\bar{\omega}}$ solution as

$$\frac{-4\bar{\omega}\bar{\omega}'}{WW'}\mathrm{Tr}\{I_{1,2}\tau_3 G(k_3,\bar{\omega})\tau_3 G(k_3,\bar{\omega})\tau_3\}\mathrm{Tr}\{I_{2,3}\tau_3 G(k_1,\bar{\omega}')\tau_3 G(k_1,\bar{\omega}')\tau_3\} \quad \text{(B.2.1)}$$

The full contribution becomes

$$\frac{16\bar{\omega}^2\bar{\omega}'^2}{WW'}\Big[\frac{\xi_3(\xi_1\xi_2-W^2)^2-W^2\xi_3(\xi_1+\xi_2)^2+(\xi_3^2-W^2)(\xi_1+\xi_2)(\xi_1\xi_2-W^2)}{(\xi_1^2+W^2)^2(\xi_2^2+W^2)^2(\xi_3^2+W^2)^2}\Big]$$
$$\times\Big[\frac{\xi_1(\xi_2\xi_3-W'^2)^2-W'^2\xi_1(\xi_2+\xi_3)^2+(\xi_1^2-W'^2)(\xi_2+\xi_3)(\xi_2\xi_3-W'^2)}{(\xi_1^2+W'^2)^2(\xi_2^2+W'^2)^2(\xi_3^2+W'^2)^2}\Big]$$

Taking the integral with respect to ξ_1, ξ_2 and ξ_3, and recalling that a factor of $\frac{kV_F}{m}$ should be included from the expansion of each $G(k+Q)$ term together with

a minus sign due to the odd number of $\tilde{\bar{\omega}}$ terms, will give the final solution as

$$-\left(\frac{kV_F}{m}\right)^2 \frac{128\bar{\omega}^2\bar{\omega}'^2}{W^2W'^2(W+W')^9} \tag{B.2.2}$$

Even-$\tilde{\bar{\omega}}$ terms

The inner and outer loop contribution, after commuting into an appropriate form, is given as

Configuration	Outer Loop	Inner Loop
$\tau_3\tau_3\tau_3$	$I_{1,2}\tau_3\tilde{G}(k_3,\bar{\omega})$	$I_{2,3}\tau_3\tilde{G}(k_1,\bar{\omega}')$
$\tau_3\tilde{\bar{\omega}}\tilde{\bar{\omega}}$	$-I_{1,2}\tau_3\tilde{G}(k_3,\bar{\omega})$	$I_{2,3}\tau_3\tilde{G}(k_1,\bar{\omega}')\frac{i\bar{\omega}'-\bar{\Delta}'\tau_1}{W'}\frac{i\bar{\omega}'-\bar{\Delta}'\tau_1}{W'}$
$\tilde{\bar{\omega}}\tau_3\tilde{\bar{\omega}}$	$I_{1,2}\tau_3\tilde{G}(k_3,\bar{\omega})\frac{i\bar{\omega}-\bar{\Delta}\tau_1}{W}\frac{i\bar{\omega}-\bar{\Delta}\tau_1}{W}$	$-I_{2,3}\tau_3\tilde{G}(k_1,\bar{\omega}')$
$\tilde{\bar{\omega}}\tilde{\bar{\omega}}\tau_3$	$I_{1,2}\tau_3\tilde{G}(k_3,\bar{\omega})\frac{i\bar{\omega}-\bar{\Delta}\tau_1}{W}\frac{i\bar{\omega}-\bar{\Delta}\tau_1}{W}$	$I_{2,3}\tau_3\tilde{G}(k_1,\bar{\omega}')\frac{i\bar{\omega}'-\bar{\Delta}'\tau_1}{W'}\frac{i\bar{\omega}'-\bar{\Delta}'\tau_1}{W'}$

Combining and factorising will give the full 3 ladder even-$\tilde{\bar{\omega}}$ contribution as

$$\left[\frac{2\bar{\omega}^2}{W^2}\mathrm{Tr}\{I_{1,2}\tau_3\tilde{G}(k_3,\bar{\omega})\}+\frac{2i\bar{\omega}\bar{\Delta}}{W^2}\mathrm{Tr}\{I_{1,2}\tau_3\tilde{G}(k_3,\bar{\omega}')\tau_1\}\right] \times\left[\frac{2\bar{\omega}'^2}{W'^2}\mathrm{Tr}\{I_{2,3}\tau_3\tilde{G}(k_1,\bar{\omega}')\}+\frac{2i\bar{\omega}'\bar{\Delta}'}{W'^2}\mathrm{Tr}\{I_{2,3}\tau_3\tilde{G}(k_1,\bar{\omega}')\tau_1\}\right]$$

which can be simplified into the form

$$\frac{-4\bar{\omega}\bar{\omega}'}{W^2W'^2}\mathrm{Tr}\{I_{1,2}\tau_3\tilde{G}(k_3,\bar{\omega})(i\bar{\omega}\ -\ \bar{\Delta}\tau_1)\}\mathrm{Tr}\{I_{2,3}\tau_3\tilde{G}(k_1,\bar{\omega}')(i\bar{\omega}'\ -\ \bar{\Delta}'\tau_1)\} \tag{B.2.3}$$

Integrating through by ξ_1, ξ_2 and ξ_3 will give the final solution as

$$\left(\frac{kV_F}{m}\right)^2 \frac{128\bar{\omega}^2\bar{\omega}'^2}{W^2W'^2(W+W')^9} \tag{B.2.4}$$

B.2.2 Type-II

Odd-$\tilde{\bar{\omega}}$ terms

Configuration	Outer Loop	Inner Loop
$\tau_3\tau_3\tilde{\bar{\omega}}$	$A^O\tau_3\frac{i\bar{\omega}+\bar{\Delta}\tau_1}{W}$	$A^I\tau_3\frac{i\bar{\omega}'-\bar{\Delta}'\tau_1}{W'}$
$\tau_3\tilde{\bar{\omega}}\tau_3$	$A^O\tau_3\frac{i\bar{\omega}+\bar{\Delta}\tau_1}{W}$	$A^I\tau_3\frac{i\bar{\omega}'-\bar{\Delta}'\tau_1}{W'}$
$\tilde{\bar{\omega}}\tau_3\tau_3$	$A^O\tau_3\frac{i\bar{\omega}+\bar{\Delta}\tau_1}{W}$	$A^I\tau_3\frac{i\bar{\omega}'+\bar{\Delta}'\tau_1}{W'}$
$\tilde{\bar{\omega}}\tilde{\bar{\omega}}\tilde{\bar{\omega}}$	$-A^O\tau_3\frac{i\bar{\omega}+\bar{\Delta}\tau_1}{W}$	$-A^I\tau_3\frac{i\bar{\omega}'-\bar{\Delta}'\tau_1}{W'}$

where $A^O = \tau_3 G(k_1,\bar{\omega})G(k_1,\bar{\omega})G(k_1,\bar{\omega})\tau_3\tilde{G}(k_2,\bar{\omega})\tau_3\tilde{G}(k_3,\bar{\omega})$ and $A^I = G(k_3,\bar{\omega}')\tau_3 G(k_2,\bar{\omega}')G(k_2,\bar{\omega}')\tau_3 G(k_1,\bar{\omega}')G(k_3,\bar{\omega}')$. The inner and outer loop contributions can be factorised to give

$$\frac{4i\bar{\omega}'}{W'}\text{Trace}\{A^O\tau_3\frac{i\bar{\omega}+\bar{\Delta}\tau_1}{W}\}\times\text{Trace}\{A^I\tau_3\} \tag{B.2.5}$$

The numerator can be calculated and taking the trace will give

$$\begin{aligned}\frac{-4\bar{\omega}\bar{\omega}'}{WW'}\Big[&-W^2\xi_1(\xi_1+\xi_3)(\xi_1\xi_2-W^2)(\xi_2\xi_3-W^2)-W^2\xi_1(\xi_2+\xi_3)(\xi_1\xi_2-W^2)(\xi_1\xi_3-W^2)\\&+W^4\xi_1(\xi_1+\xi_3)(\xi_2+\xi_3)(\xi_1+\xi_2)-W^2\xi_1(\xi_1+\xi_2)(\xi_1\xi_3-W^2)(\xi_2\xi_3-W^2)\\&-W^2(\bar{\Delta}^2-\bar{\omega}^2)(\xi_1+\xi_2)(\xi_1+\xi_3)(\xi_2\xi_3-W^2)-W^2(\bar{\Delta}^2-\bar{\omega}^2)(\xi_1+\xi_2)(\xi_2+\xi_3)(\xi_1\xi_3-W^2)\\&-W^2(\bar{\Delta}^2-\bar{\omega}^2)(\xi_1+\xi_3)(\xi_2+\xi_3)(\xi_1\xi_2-W^2)+(\bar{\Delta}^2-\bar{\omega}^2)(\xi_1\xi_2-W^2)(\xi_1\xi_3-W^2)(\xi_2\xi_3-W^2)\Big]\\&\times\Big[\xi_3(\xi_1+\xi_2)(\xi_2\xi_3-W'^2)-W'^2(\xi_1+\xi_2)(\xi_2+\xi_3)\\&+(\xi_1\xi_2-W'^2)(\xi_2\xi_3-W'^2)+\xi_3(\xi_2+\xi_3)(\xi_1\xi_2-W'^2)\Big]\end{aligned} \tag{B.2.}$$

Even-$\tilde{\bar{\omega}}$ terms

Configuration	Outer Loop	Inner Loop
$\tau_3\tau_3\tau_3$	A^O	A^I
$\tilde{\bar{\omega}}\tau_3\tilde{\bar{\omega}}$	$-A^O$	$A^I \frac{i\bar{\omega}'-\bar{\Delta}'\tau_1}{W'} \frac{i\bar{\omega}'-\bar{\Delta}'\tau_1}{W'}$
$\tilde{\bar{\omega}}\tilde{\bar{\omega}}\tau_3$	$-A^O$	$-A^I$
$\tau_3\tilde{\bar{\omega}}\tilde{\bar{\omega}}$	$-A^O$	$A^I \frac{i\bar{\omega}'-\bar{\Delta}'\tau_1}{W'} \frac{i\bar{\omega}'-\bar{\Delta}'\tau_1}{W'}$

This can be simplified to

$$\frac{-4\bar{\omega}'}{W'^2}\text{Trace}\{A^O\}\text{Trace}\{A^I(\bar{\omega}' - i\bar{\Delta}\tau_1)\} \tag{B.2.7}$$

This can be calculated as

$$\begin{aligned}
&\frac{2\bar{\omega}'}{W'^2}\Big[-W^2\xi_1(\xi_1+\xi_2)(\xi_2+\xi_3)(\xi_1\xi_3-W^2)+\xi_1(\xi_1\xi_2-W^2)(\xi_1\xi_3-W^2)(\xi_2\xi_3-W^2)\\
&\quad -W^2\xi_1(\xi_1+\xi_2)(\xi_1+\xi_3)(\xi_2\xi_3-W^2)-W^2\xi_1(\xi_1+\xi_3)(\xi_2+\xi_3)(\xi_1\xi_2-W^2)\\
&-W^2(\bar{\Delta}^2-\bar{\omega}^2)(\xi_1+\xi_2)(\xi_1+\xi_3)(\xi_2+\xi_3)+(\bar{\Delta}^2-\bar{\omega}^2)(\xi_1+\xi_3)(\xi_1\xi_2-W^2)(\xi_2\xi_3-W^2)\\
&+(\bar{\Delta}^2-\bar{\omega}^2)(\xi_1+\xi_2)(\xi_1\xi_3-W^2)(\xi_2\xi_3-W^2)+(\bar{\Delta}^2-\bar{\omega}^2)(\xi_2+\xi_3)(\xi_1\xi_2-W^2)(\xi_1\xi_3-W^2)\Big]\\
&\Big[-\bar{\omega}'W'^2\xi_3(\xi_1+\xi_2)(\xi_2+\xi_3)+\bar{\omega}'\xi_3(\xi_1\xi_2-W'^2)(\xi_2\xi_3-W'^2)\\
&\quad +\bar{\omega}'W'^2(\xi_1+\xi_2)(\xi_2\xi_3-W'^2)+\bar{\omega}'W'^2(\xi_2+\xi_3)(\xi_1\xi_2-W'^2)\Big]
\end{aligned}$$

B.2.3 Type-II additional impurity line

Odd-$\tilde{\bar{\omega}}$ terms

Configuration	Outer Loop	Inner Loop
$\tau_3\tau_3\tilde{\bar{\omega}}$ and $\tilde{\bar{\omega}}\tau_3\tau_3$	$B^O\tau_3\frac{i\bar{\omega}+\bar{\Delta}\tau_1}{W}$	$B^I\tau_3\frac{i\bar{\omega}'+\bar{\Delta}'\tau_1}{W'}$
$\tau_3\tilde{\bar{\omega}}\tau_3$ and $\tilde{\bar{\omega}}\tilde{\bar{\omega}}\tilde{\bar{\omega}}$	$B^O\tau_3\frac{i\bar{\omega}+\bar{\Delta}\tau_1}{W}$	$B^I\tau_3\frac{i\bar{\omega}'-\bar{\Delta}'\tau_1}{W'}$

This can be simplified to

$$\frac{-2i\bar{\omega}'}{WW'}\text{Trace}\{B^O\tau_3(i\bar{\omega}+\bar{\Delta}\tau_1)\}\text{Trace}\{B^I\tau_3\} \tag{B.2.8}$$

and calculated as

$$\begin{aligned}
\text{Trace}\{B^O\tau_3(i\bar{\omega}+\bar{\Delta}\tau_1)\} &= i\bar{\omega}\big[\xi_2(\xi_1\xi_2-W^2)^2(\xi_3\xi_4-W^2)^2 \\
&-2W^2\xi_2(\xi_1+\xi_2)(\xi_3+\xi_4)(\xi_1\xi_2-W^2)(\xi_3\xi_4-W^2)+W^4\xi_2(\xi_1+\xi_2)^2(\xi_3+\xi_4)^2 \\
&+2W^2(\xi_1+\xi_2)(\xi_1\xi_2-W^2)(\xi_3\xi_4-W^2)^2-2W^4(\xi_1+\xi_2)^2(\xi_3+\xi_4)(\xi_3\xi_4-W^2) \\
&+2W^2(\xi_3+\xi_4)(\xi_1\xi_2-W^2)^2(\xi_3\xi_4-W^2)-2W^4(\xi_1+\xi_2)(\xi_3+\xi_4)^2(\xi_1\xi_2-W^2) \\
&+4\bar{\omega}(\bar{\Delta}^2-\bar{\omega}^2)(\xi_1+\xi_2)(\xi_1\xi_2-W^2)(\xi_3\xi_4-W^2)^2-4\bar{\omega}(\bar{\Delta}^2-\bar{\omega}^2)W^2(\xi_1+\xi_2)^2(\xi_3+\xi_4)(\xi_1\xi_2-W^2) \\
&+4\bar{\omega}(\bar{\Delta}^2-\bar{\omega}^2)(\xi_3+\xi_4)(\xi_1\xi_2-W^2)^2(\xi_3\xi_4-W^2)-4\bar{\omega}(\bar{\Delta}^2-\bar{\omega}^2)W^2(\xi_1+\xi_2)(\xi_3+\xi_4)^2(\xi_1\xi_2-W^2)\big]
\end{aligned}$$

$$\begin{aligned}
\text{Trace}\{B^I\tau_3\} = i\bar{\omega}'\big[&(\xi_3\xi_4-W'^2)^2-W'^2(\xi_3+\xi_4)^2 \\
&+2\xi_1(\xi_3+\xi_4)(\xi_3\xi_4-W'^2)\big]
\end{aligned} \tag{B.2.9}$$

Integrating with respect to ξ_i (where $i=1,2,3,4$) we are left with a zero contribution.

Even-$\tilde{\bar{\omega}}$ terms

Configuration	Outer Loop	Inner Loop
$\tau_3\tau_3\tau_3$ and $\tilde{\bar{\omega}}\tau_3\tilde{\bar{\omega}}$	B^O	B^I
$\tau_3\tilde{\bar{\omega}}\tilde{\bar{\omega}}$ and $\tilde{\bar{\omega}}\tilde{\bar{\omega}}\tau_3$	$-B^O$	$B^I\frac{i\bar{\omega}'-\bar{\Delta}'\tau_1}{W'}\frac{i\bar{\omega}'-\bar{\Delta}'\tau_1}{W'}$

This can be simplified to

$$\frac{-2i\bar{\omega}'}{W'^2}\text{Trace}\{B^O\}\text{Trace}\{B^I(\bar{\omega}' - i\bar{\Delta}\tau_1)\} \tag{B.2.10}$$

This can be calculated as

$$\begin{aligned}
\text{Trace}\{B^O\} &= \xi_2(\xi_1\xi_2 - W^2)^2(\xi_3\xi_4 - W^2)^2 + W^4\xi_2(\xi_1+\xi_2)^2(\xi_3+\xi_4)^2 \\
&- W^2\xi_2(\xi_1+\xi_2)^2(\xi_3\xi_4 - W^2)^2 - 4W^2\xi_2(\xi_1+\xi_2)(\xi_3+\xi_4)(\xi_1\xi_2 - W^2)(\xi_3\xi_4 - W^2) \\
&- W^2\xi_2(\xi_3+\xi_4)^2(\xi_1\xi_2 - W^2)^2 \\
&+ 2(\bar{\omega}^2 - \bar{\Delta}^2)(\xi_1+\xi_2)(\xi_3\xi_4 - W^2)^2 - 2(\bar{\omega}^2 - \bar{\Delta}^2)W^2(\xi_1+\xi_2)^2(\xi_3+\xi_4)(\xi_3\xi_4 - W^2) \\
&+ 2(\bar{\omega}^2 - \bar{\Delta}^2)(\xi_3+\xi_4)(\xi_1\xi_2 - W^2)^2(\xi_3\xi_4 - W^2) - 2(\bar{\omega}^2 - \bar{\Delta}^2)W^2(\xi_1+\xi_2)(\xi_3+\xi_4)^2(\xi_1\xi_2 - W^2)
\end{aligned}$$

and

$$\begin{aligned}
\text{Trace}\{B^I(\bar{\omega}' - i\bar{\Delta}'\tau_1)\} &= -W'^2(\xi_3\xi_4 - W'^2)^2 - W'^4(\xi_3+\xi_4)^2 \\
&+ 2\bar{\omega}'^2W'^2(\xi_3+\xi_4) - 2\bar{\omega}'^2\xi_1(\xi_3+\xi_4)(\xi_3\xi_4 - W'^2)
\end{aligned}$$

Combining the two terms and integrating with respect to ξ_i (where $i = 1, 2, 3, 4$) we are left with a zero contribution.

B.3 4 ladder Superconducting UCF calculation

B.3.1 Type-I

Odd-$\tilde{\bar{\omega}}$ terms

Config.	Outer Loop	Inner Loop
$\tau_3\tau_3\tau_3\tilde{\bar{\omega}}$	$\tilde{G}(k_2,\bar{\omega})\tau_3 I_{1,3}\tau_3\tilde{G}(k_4,\bar{\omega})\tau_3(i\bar{\omega}+\bar{\Delta}\tau_1)$	$\tilde{G}(k_3,\bar{\omega}')\tau_3 I_{2,4}\tau_3\tilde{G}(k_1,\bar{\omega}')\tau_3(i\bar{\omega}'+\bar{\Delta}'\tau_1)$
$\tau_3\tilde{\bar{\omega}}\tau_3\tau_3$	$\tilde{G}(k_2,\bar{\omega})\tau_3 I_{1,3}\tau_3\tilde{G}(k_4,\bar{\omega})\tau_3(i\bar{\omega}-\bar{\Delta}\tau_1)$	$\tilde{G}(k_3,\bar{\omega}')\tau_3 I_{2,4}\tau_3\tilde{G}(k_1,\bar{\omega}')\tau_3(i\bar{\omega}'-\bar{\Delta}'\tau_1)$
$\tau_3\tau_3\tilde{\bar{\omega}}\tau_3$	$\tilde{G}(k_2,\bar{\omega})\tau_3 I_{1,3}\tau_3\tilde{G}(k_4,\bar{\omega})\tau_3(i\bar{\omega}+\bar{\Delta}\tau_1)$	$\tilde{G}(k_3,\bar{\omega}')\tau_3 I_{2,4}\tau_3\tilde{G}(k_1,\bar{\omega}')\tau_3(i\bar{\omega}-\bar{\Delta}\tau_1)$
$\tilde{\bar{\omega}}\tau_3\tau_3\tau_3$	$\tilde{G}(k_2,\bar{\omega})\tau_3 I_{1,3}\tau_3\tilde{G}(k_4,\bar{\omega})\tau_3(i\bar{\omega}-\bar{\Delta}\tau_1)$	$\tilde{G}(k_3,\bar{\omega}')\tau_3 I_{2,4}\tau_3\tilde{G}(k_1,\bar{\omega}')\tau_3(i\bar{\omega}+\bar{\Delta}\tau_1)$
$\tau_3\tilde{\bar{\omega}}\tilde{\bar{\omega}}\tilde{\bar{\omega}}$	$-\tilde{G}(k_2,\bar{\omega})\tau_3 I_{1,3}\tau_3\tilde{G}(k_4,\bar{\omega})\tau_3(i\bar{\omega}-\bar{\Delta}\tau_1)$	$-\tilde{G}(k_3,\bar{\omega}')\tau_3 I_{2,4}\tau_3\tilde{G}(k_1,\bar{\omega}')\tau_3(i\bar{\omega}'+\bar{\Delta}'\tau_1)$
$\tilde{\bar{\omega}}\tilde{\bar{\omega}}\tau_3\tilde{\bar{\omega}}$	$-\tilde{G}(k_2,\bar{\omega})\tau_3 I_{1,3}\tau_3\tilde{G}(k_4,\bar{\omega})\tau_3(i\bar{\omega}+\bar{\Delta}\tau_1)$	$-\tilde{G}(k_3,\bar{\omega}')\tau_3 I_{2,4}\tau_3\tilde{G}(k_1,\bar{\omega}')\tau_3(i\bar{\omega}'-\bar{\Delta}'\tau_1)$
$\tilde{\bar{\omega}}\tilde{\bar{\omega}}\tilde{\bar{\omega}}\tau_3$	$-\tilde{G}(k_2,\bar{\omega})\tau_3 I_{1,3}\tau_3\tilde{G}(k_4,\bar{\omega})\tau_3(i\bar{\omega}+\bar{\Delta}\tau_1)$	$-\tilde{G}(k_3,\bar{\omega}')\tau_3 I_{2,4}\tau_3\tilde{G}(k_1,\bar{\omega}')\tau_3(i\bar{\omega}'+\bar{\Delta}\tau_1)$
$\tilde{\bar{\omega}}\tau_3\tilde{\bar{\omega}}\tilde{\bar{\omega}}$	$-\tilde{G}(k_2,\bar{\omega})\tau_3 I_{1,3}\tau_3\tilde{G}(k_4,\bar{\omega})\tau_3(i\bar{\omega}-\bar{\Delta}\tau_1)$	$-\tilde{G}(k_3,\bar{\omega}')\tau_3 I_{2,4}\tau_3\tilde{G}(k_1,\bar{\omega}')\tau_3(i\bar{\omega}'-\bar{\Delta}\tau_1)$

By factorising and simplifying we are left with

$$\frac{-4\bar{\omega}\bar{\omega}'}{WW'}\text{Trace}\{\tilde{G}(k_2,\bar{\omega})\tau_3 I_{1,3}\tau_3\tilde{G}(k_4,\bar{\omega})\tau_3\}\text{Trace}\{\tilde{G}(k_3,\bar{\omega}')\tau_3 I_{2,4}\tau_3\tilde{G}(k_1,\bar{\omega}')\tau_3\} \tag{B.3.1}$$

$$\begin{aligned}
&\frac{16\bar{\omega}^2\bar{\omega}'^2}{WW'}\Big[(\xi_2+\xi_4)(\xi_1\xi_3-W^2)^2(\xi_2\xi_4-W^2)-W^2(\xi_1+\xi_3)^2(\xi_2+\xi_4)(\xi_2\xi_4-W^2)\\
&\quad+(\xi_1+\xi_3)(\xi_1\xi_3-W^2)(\xi_2\xi_4-W^2)^2-W^2(\xi_1+\xi_3)(\xi_2+\xi_4)^2(\xi_1\xi_3-W^2)\Big]\\
&\times\Big[(\xi_2+\xi_4)(\xi_1\xi_3-W'^2)^2(\xi_2\xi_4-W'^2)-W'^2(\xi_1+\xi_3)^2(\xi_2+\xi_4)(\xi_2\xi_4-W'^2)\\
&\quad+(\xi_1+\xi_3)(\xi_1\xi_3-W'^2)(\xi_2\xi_4-W'^2)^2-W^2(\xi_1+\xi_3)(\xi_2+\xi_4)^2(\xi_1\xi_3-W'^2)\Big]
\end{aligned}$$

Integrating with respect to $\xi_{1,2,3,4}$, and including the minus sign due to it being

and odd contribution, will give the full odd-$\tilde{\bar{\omega}}$ contribution as

$$\frac{-512\pi^4\bar{\omega}^2\bar{\omega}'^2}{W^2W'^2(W+W')^{12}} \tag{B.3.2}$$

Even-$\tilde{\bar{\omega}}$ terms

Configuration	Outer Loop	Inner Loop
$\tau_3\tau_3\tau_3\tau_3$, $\tilde{\bar{\omega}}\tilde{\bar{\omega}}\tilde{\bar{\omega}}\tilde{\bar{\omega}}$	$\tilde{G}(k_2,\bar{\omega})\tau_3 I_{1,3}\tau_3\tilde{G}(k_4,\bar{\omega})$	$\tilde{G}(k_3,\bar{\omega}')\tau_3 I_{2,4}\tau_3\tilde{G}(k_1,\bar{\omega}')$
$\tau_3\tau_3\tilde{\bar{\omega}}\tilde{\bar{\omega}}$, $\tilde{\bar{\omega}}\tilde{\bar{\omega}}\tau_3\tau_3$	$-\tilde{G}(k_2,\bar{\omega})\tau_3 I_{1,3}\tau_3\tilde{G}(k_4,\bar{\omega})$	$\tilde{G}(k_3,\bar{\omega}')\tau_3 I_{2,4}\tau_3\tilde{G}(k_1,\bar{\omega}')\frac{i\bar{\omega}'-\bar{\Delta}'\tau_1}{W'}\frac{i\bar{\omega}'-\bar{\Delta}'\tau}$
$\tau_3\tilde{\bar{\omega}}\tau_3\tilde{\bar{\omega}}$, $\tilde{\bar{\omega}}\tau_3\tilde{\bar{\omega}}\tau_3$	$\tilde{G}(k_2,\bar{\omega})\tau_3 I_{1,3}\tau_3\tilde{G}(k_4,\bar{\omega})\frac{i\bar{\omega}-\bar{\Delta}\tau_1}{W}\frac{i\bar{\omega}-\bar{\Delta}\tau_1}{W}$	$\tilde{G}(k_3,\bar{\omega}')\tau_3 I_{2,4}\tau_3\tilde{G}(k_1,\bar{\omega}')\frac{i\bar{\omega}'-\bar{\Delta}'\tau_1}{W'}\frac{i\bar{\omega}'-\bar{\Delta}'\tau}$
$\tilde{\bar{\omega}}\tau_3\tau_3\tilde{\bar{\omega}}$, $\tau_3\tilde{\bar{\omega}}\tilde{\bar{\omega}}\tau_3$	$\tau_3 I_{1,3}\tau_3\tilde{G}(k_4,\bar{\omega})\tilde{G}(k_2,\bar{\omega})\frac{i\bar{\omega}\bar{\Delta}\tau_1}{W}\frac{i\bar{\omega}-\bar{\Delta}\tau_1}{W}$	$-\tilde{G}(k_3,\bar{\omega}')\tau_3 I_{2,4}\tau_3\tilde{G}(k_1,\bar{\omega}')$

By factorising and simplifying we can write the overall contribution as

$$\begin{aligned}\frac{-4\bar{\omega}^2\bar{\omega}'^2}{W^2W'^2}&\Big[\text{Trace}\{\tilde{G}(k_2,\bar{\omega})\tau_3 I_{1,3}\tau_3\tilde{G}(k_4,\bar{\omega})(i\bar{\omega}-\bar{\Delta}\tau_1)\Big]\\ &\times\Big[\text{Trace}\{\tilde{G}(k_3,\bar{\omega}')\tau_3 I_{2,4}\tau_3\tilde{G}(k_1,\bar{\omega}')(i\bar{\omega}'-\bar{\Delta}'\tau_1)\Big]\end{aligned} \tag{B.3.3}$$

Calculating the traces will give

$$\begin{aligned}&\frac{-4\bar{\omega}^2\bar{\omega}'^2}{W^2W'^2}\Big[-4i\bar{\omega}W^2\xi_2\xi_4(\xi_1\xi_3-W^2)^2+4i\bar{\omega}W^4\xi_2\xi_4(\xi_1+\xi_3)^2\\ &-4i\bar{\omega}W^2\xi_4(\xi_1+\xi_2)(\xi_2^2-W^2)(\xi_1\xi_3-W^2)+i\bar{\omega}(\xi_2^2-W^2)(\xi_4-W^2)(\xi_1\xi_3-W^2)^2\\ &-i\bar{\omega}W^2(\xi_1+\xi_3)^2(\xi_2^2-W^2)(\xi_4^2-W^2)-4i\bar{\omega}W^2\xi_2(\xi_1+\xi_3)(\xi_4^2-W^2)(\xi_1\xi_3-W^2)\Big]\\ &\times\Big[-4i\bar{\omega}'W'^2\xi_1\xi_3(\xi_2\xi_4-W'^2)^2+4i\bar{\omega}'W'^4\xi_1\xi_3(\xi_2+\xi_4)^2\\ &-4i\bar{\omega}'W'^2\xi_1(\xi_2+\xi_3)(\xi_3^2-W'^2)(\xi_2\xi_4-W'^2)+i\bar{\omega}'(\xi_3^2-W'^2)(\xi_1-W'^2)(\xi_2\xi_4-W'^2)^2\\ &-i\bar{\omega}'W'^2(\xi_2+\xi_4)^2(\xi_3^2-W'^2)(\xi_1^2-W'^2)-4i\bar{\omega}'W'^2\xi_3(\xi_2+\xi_4)(\xi_1^2-W'^2)(\xi_2\xi_4-W'^2)\Big]\end{aligned}$$

Taking the integral with respect to $\xi_{1,2,3,4}$ will give the final 4 ladder Even-$\tilde{\bar{\omega}}$

contribution as

$$\frac{512\bar{\omega}^2\bar{\omega}'^2\pi^4}{W^2W'^2(W+W')^{12}} \tag{B.3.4}$$

B.3.2 Type-II

Even-$\tilde{\bar{\omega}}$ terms

Configuration	Outer Loop	Inner Loop
$\tau_3\tau_3\tau_3\tau_3$, $\tau_3\tilde{\bar{\omega}}\tau_3\tilde{\bar{\omega}}$	$I_{1,2}\tau_3\tilde{G}(k_3,\bar{\omega})\tau_3\tilde{G}(k_4,\bar{\omega})$	$I_{3,4}\tau_3\tilde{G}(k_1,\bar{\omega}')\tau_3\tilde{G}(k_2,\bar{\omega}')$
$\tau_3\tau_3\tilde{\bar{\omega}}\tilde{\bar{\omega}}$, $\tau_3\tilde{\bar{\omega}}\tilde{\bar{\omega}}\tau_3$	$-I_{1,2}\tau_3\tilde{G}(k_3,\bar{\omega})\tau_3\tilde{G}(k_4,\bar{\omega})$	$I_{3,4}\tau_3\tilde{G}(k_1,\bar{\omega}')\tau_3\tilde{G}(k_2,\bar{\omega}')\frac{i\bar{\omega}'-\bar{\Delta}'\tau_1}{W'}\frac{i\bar{\omega}'-\bar{\Delta}'}{W'}$
$\tilde{\bar{\omega}}\tau_3\tilde{\bar{\omega}}\tau_3$, $\tilde{\bar{\omega}}\tilde{\bar{\omega}}\tilde{\bar{\omega}}\tilde{\bar{\omega}}$	$I_{1,2}\tau_3\tilde{G}(k_3,\bar{\omega})\tau_3\tilde{G}(k_4,\bar{\omega})\frac{i\bar{\omega}-\bar{\Delta}\tau_1}{W}\frac{i\bar{\omega}-\bar{\Delta}\tau_1}{W}$	$I_{3,4}\tau_3\tilde{G}(k_1,\bar{\omega}')\tau_3\tilde{G}(k_2,\bar{\omega}')\frac{i\bar{\omega}'-\bar{\Delta}'\tau_1}{W'}\frac{i\bar{\omega}'-\bar{\Delta}'}{W'}$
$\tilde{\bar{\omega}}\tau_3\tau_3\tilde{\bar{\omega}}$, $\tilde{\bar{\omega}}\tilde{\bar{\omega}}\tau_3\tau_3$	$I_{1,2}\tau_3\tilde{G}(k_3,\bar{\omega})\tau_3\tilde{G}(k_4,\bar{\omega})\frac{i\bar{\omega}\bar{\Delta}\tau_1}{W}\frac{i\bar{\omega}-\bar{\Delta}\tau_1}{W}$	$-I_{3,4}\tau_3\tilde{G}(k_1,\bar{\omega}')\tau_3\tilde{G}(k_2,\bar{\omega}')$

Simplifying will give

$$\frac{-4\bar{\omega}\bar{\omega}'}{W^2W'^2}\mathrm{Tr}\{I_{1,2}\tau_3\tilde{G}(k_3,\bar{\omega})\tau_3\tilde{G}(k_4,\bar{\omega})(i\bar{\omega}-\bar{\Delta}\tau_1)\}\mathrm{Tr}\{I_{3,4}\tau_3\tilde{G}(k_1,\bar{\omega}')\tau_3\tilde{G}(k_2,\bar{\omega}')(i\bar{\omega}-\bar{\Delta}\tau_1)\} \tag{B.3.5}$$

and the outer loop expansion

$$\begin{aligned}
&\mathrm{Tr}\{I_{1,2}\tau_3\tilde{G}(k_3,\bar{\omega})\tau_3\tilde{G}(k_4,\bar{\omega})(i\bar{\omega}-\bar{\Delta}\tau_1)\}\\
&\quad= i\bar{\omega}\Big[(\xi_1\xi_2-W^2)^2(\xi_3\xi_4-W^2)^2-W^2(\xi_1+\xi_2)^2(\xi_3\xi_4-W^2)^2-W^2(\xi_3+\xi_4)^2(\xi_1\xi_2-W^2)^2\\
&\qquad+W^4(\xi_1+\xi_2)^2(\xi_3+\xi_4)^2-4W^2(\xi_1+\xi_2)(\xi_3+\xi_4)(\xi_1\xi_2-W^2)(\xi_3\xi_4-W^2)\Big]
\end{aligned} \tag{B.3.6}$$

Integrating the product of the inner and outer loops will give the final result as

$$\frac{512\pi^4\bar{\omega}^2\bar{\omega}'^2}{W^2W'^2(W+W')^{12}} \tag{B.3.7}$$

Odd-$\tilde{\bar{\omega}}$ terms

Configuration	Outer Loop	Inner Loop
$\tau_3\tau_3\tau_3\tilde{\bar{\omega}}$ and $\tau_3\tilde{\bar{\omega}}\tau_3\tau_3$	$I_{1,2}\tau_3\tilde{G}(k_3,\bar{\omega})\tau_3\tilde{G}(k_4,\bar{\omega})\tau_3\frac{i\bar{\omega}+\bar{\Delta}\tau_1}{W}$	$I_{3,4}\tau_3\tilde{G}(k_1,\bar{\omega}')\tau_3\tilde{G}(k_2,\bar{\omega}')\tau_3\frac{i\bar{\omega}'+\bar{\Delta}'\tau_1}{W'}$
$\tilde{\bar{\omega}}\tau_3\tau_3\tau_3$ and $\tilde{\bar{\omega}}\tilde{\bar{\omega}}\tau_3\tilde{\bar{\omega}}$	$I_{1,2}\tau_3\tilde{G}(k_3,\bar{\omega})\tau_3\tilde{G}(k_4,\bar{\omega})\tau_3\frac{i\bar{\omega}-\bar{\Delta}\tau_1}{W}$	$I_{3,4}\tau_3\tilde{G}(k_1,\bar{\omega}')\tau_3\tilde{G}(k_2,\bar{\omega}')\tau_3\frac{i\bar{\omega}'+\bar{\Delta}'\tau_1}{W'}$
$\tau_3\tau_3\tilde{\bar{\omega}}\tau_3$ and $\tau_3\tilde{\bar{\omega}}\tilde{\bar{\omega}}\tilde{\bar{\omega}}$	$I_{1,2}\tau_3\tilde{G}(k_3,\bar{\omega})\tau_3\tilde{G}(k_4,\bar{\omega})\tau_3\frac{i\bar{\omega}+\bar{\Delta}\tau_1}{W}$	$I_{3,4}\tau_3\tilde{G}(k_1,\bar{\omega}')\tau_3\tilde{G}(k_2,\bar{\omega}')\tau_3\frac{i\bar{\omega}'-\bar{\Delta}'\tau_1}{W'}$
$\tilde{\bar{\omega}}\tau_3\tilde{\bar{\omega}}\tilde{\bar{\omega}}$ and $\tilde{\bar{\omega}}\tilde{\bar{\omega}}\tilde{\bar{\omega}}\tau_3$	$I_{1,2}\tau_3\tilde{G}(k_3,\bar{\omega})\tau_3\tilde{G}(k_4,\bar{\omega})\tau_3\frac{i\bar{\omega}-\bar{\Delta}\tau_1}{W}$	$I_{3,4}\tau_3\tilde{G}(k_1,\bar{\omega}')\tau_3\tilde{G}(k_2,\bar{\omega}')\tau_3\frac{i\bar{\omega}'-\bar{\Delta}'\tau_1}{W'}$

The entire odd-$\tilde{\bar{\omega}}$ contribution cancels down to

$$\frac{-4\bar{\omega}\bar{\omega}'}{WW'}\text{Trace}\{\tau_3 I_{1,2}\tau_3\tilde{G}(k_3,\bar{\omega})\tau_3\tilde{G}(k_4,\bar{\omega})\}\text{Trace}\{\tau_3 I_{3,4}\tau_3\tilde{G}(k_1,\bar{\omega}')\tau_3\tilde{G}(k_2,\bar{\omega}')\} \tag{B.3.8}$$

Expanding out the outer loop contribution will give

$$\begin{aligned}
&\text{Trace}\{\tau_3 I_{1,2}\tau_3\tilde{G}(k_3,\bar{\omega})\tau_3\tilde{G}(k_4,\bar{\omega})\}\\
&= 2i\bar{\omega}\Big[(\xi_3+\xi_4)(\xi_1\xi_2-W^2)^2(\xi_3\xi_4-W^2)+(\xi_1+\xi_2)(\xi_1\xi_2-W^2)(\xi_3\xi_4-W^2)^2\\
&\quad -W^2(\xi_1+\xi_2)^2(\xi_3+\xi_4)(\xi_3\xi_4-W^2)-W^2(\xi_1+\xi_2)(\xi_3+\xi_4)^2(\xi_1\xi_2-W^2)\Big]
\end{aligned}$$

Integrating the product of the inner and outer loop and recalling that the Odd-$\tilde{\bar{\omega}}$ terms will give an additional minus sign will give the final result as

$$\frac{-512\pi^4\bar{\omega}^2\bar{\omega}'^2}{W^2W'^2(W+W')^{12}} \tag{B.3.9}$$

List of references

[1] A.Altland, B.D.Simons, and D.Taras-Semchuk. *arXiv:cond-mat*, (9807371), 1998.

[2] A.D.Stone and Y.Imry. *Phys. Rev Lett*, 56(2), 1986.

[3] B.I.Spivak and S.A.Kivelson. *Phys. Rev. B*, 43(4), 1990.

[4] B.L.Al'tshuler and D.E.Kmel'nitskii. *JETP Lett.*, 42(7), 1985.

[5] B.Spivak and F.Zhou. *Phys. Rev. Lett.*, 74(14), 1994.

[6] L. N. Bulaevskii, V. V. Kuzii, and A. A. Sobyanin. *Pis'ma ZH. Eksp. Teor. Fiz*, 25(7), 1990.

[7] B.Z.Spivak and A.Y.Zyuzin. *Pis'ma Zh. Eksp. Teor. Fiz*, 47(4), 1988.

[8] D.J.Quinn and W.B.Ittner. *J. Appl. Phys*, 33(748), 1962.

[9] Y. Dubi, Y. Meir, and Y. Avishai. *Phys. Rev. B*, 73(054509), 2006.

[10] D.Y.Sharvin and Y.V.Sharvin. *Pis'ma Zh. Eksp. Teor. Fiz*, 34(5), 1981.

[11] A. V. Herzog et. al. *Phys. Rev. Lett.*, 76(4), 1996.

[12] D. A. Bonn et. al. *J. Phys. Chem. Solids*, 56(12), 1995.

[13] D. S. Hopkins et. al. *Phys. Rev. B*, 76(220506), 2007.

[14] D. Tulimeieri et. al. *Phys. Rev. Lett.*, 80(20), 1998.

[15] K. Hashimoto et. al. *Phys. Rev. Lett.*, 102(207001, year=).

[16] R. W. Crane et. al. *Phys. Rev. B*, 75(094506), 2007.

[17] F.Mandl and G.Shaw. *Quantum Field Theory*. Wiley, 1984.

[18] F.Zhou and B.Spivak. *Phys. Rev. Lett.*, 80(25), 1997.

[19] H.Frolich. *Phys. Rev.*, 79(845), 1950.

[20] M. Houzet and M. Skvortsov. *Phys. Rev. B*, 77(024525), 2008.

[21] J.Bardeen, L.N.Cooper, and J.R.Schrieffer. *Phys. Rev.*, 108(1175), 1957.

[22] J.W.Negele and H.Orland. *Quantum Many-Particle Systems.* Addison-Wesley, 1988.

[23] K.A.Parendo, L.M.Hernandez, A.Bhattacharya, and A.M.Goldman. *Phys. Rev. B*, 70(212510), 2004.

[24] J. M. Kosterlitz and D. J. Thouless. *J. Phys. C*, 6(1181), 1973.

[25] A. Levchenko. *Phys. Rev. B*, 79(212511), 2009.

[26] A. V. Lopatin, N. Shah, and V. M. Vinokur. *Phys. Rev. Lett.*, 94(037003), 2005.

[27] M.Tinkham. *Introduction to Superconductivity: Second Edition.* Dover, 1975.

[28] H. Kamerlingh Onnes. *Leiden Comm.*, 120b, 122b, 124c, 1911.

[29] P.A.Lee and A.D.Stone. *Phys. Rev. Lett*, 55(15), 1985.

[30] P.W.Brouwer and C.W.J.Beenakker. *Phys. Rev. B*, 52(23), 1995.

[31] R.A.Webb, S.Washburn, C.P.Umbach, and R.B.Laibowitz. *Phys. Rev. Lett.*, 54(25), 1985.

[32] R.D.Parks. *Supercondctivity Volume 1.* MArcel Dekker, 1969.

[33] S.A.Kivelson and B.I.Spivak. *Phys. Rev. B*, 45(18), 1991.

[34] M. Titov, Ph. Jacquod, and C. W. J. Beenakker. *Phys. Rev. B*, 65(012504), 2001.

[35] T.V.Ramakrishnan. *Phys.Scr. T*, 27(24), 1989.

[36] V.Chandrasekhar, M.J.Rooks, S.Wind, and D.E.Prober. *Phys. Rev. Lett.*, 55(15), 1985.

[37] Y.Imry. *Introduction to Mesoscopic Physics.* Oxford University Press Inc., 1997.